Adsorptive precipitation of vitamin D_3 and vitamin E on gum arabic and sodium alginate using supercritical carbon dioxide

by

Andrea Carolina Vilchez Athanasopulos

A thesis submitted in partial fulfillment of the requirements for the degree of

Master of Science

in

Food Science and Technology

Department of Agricultural, Food and Nutritional Science
University of Alberta

Abstract

Functional food products are formulated with added ingredients that provide health benefits beyond basic nutrition function. However, there are different challenges in the manufacturing of these products with fat-soluble vitamins, such as, vitamin D_3 ($VitD_3$), an essential nutrient responsible for increasing intestinal absorption of calcium and phosphorus, and vitamin E (VitE), a powerful antioxidant that plays an important role in the prevention of many disorders. Some challenges are their high tendency to be degraded or oxidized by heat, light and presence of oxygen, and also their hydrophobic nature limits their further use in aqueous-based products. To overcome these limitations, water-soluble biopolymers can be used as delivery systems. The polysaccharides, gum arabic (GA), and sodium alginate (SA), were dried using the Pressurized Gas eXpanded (PGX) liquid technology, a drying method for high molecular weight water-soluble biopolymers to produce unique morphologies of micro- or nano-sized particles. Then, adsorptive precipitation, an environmentally friendly technology to load hydrophobic bioactives homogeneously onto the biopolymers without the use of any organic solvents, was used to develop novel delivery systems. The objectives of this MSc thesis research were to investigate the effect of adsorptive precipitation process parameters on the loading of fat-soluble bioactive compounds ($VitD_3$ and VitE) on water-soluble biopolymers (GA and SA), and to characterize the powders obtained to ultimately increase the application of these hydrophobic compounds in aqueous-based products. The $VitD_3$ and VitE loaded PGX-GA and PGX-SA particles obtained by adsorptive precipitation under different recirculation flow rates and times were investigated in terms of the vitamin loading content, particle morphology, molecular interactions, thermal behavior, storage stability, and release kinetics. In addition, adsorption kinetics were evaluated for VitE.

The higher loading of $VitD_3$ on the biopolymers was achieved at the recirculation flow rate of 190 mL/min as 10.1 ± 0.2% for GA and 250 mL/min as 13.7 ± 0.1% for SA at 45 min of recirculation time. Uniform coating of $VitD_3$ on the surface of biopolymers was demonstrated by helium ion microscopy (HiM). $VitD_3$ retained some crystalline form on the loaded gum arabic (L-GA). Over 60 days of refrigerated storage, after an initial decrease, the loading of samples stabilized after 21 days for L-SA at 82% and after 28 days L-GA at 80% of the original $VitD_3$ levels. Sustained release of $VitD_3$ was demonstrated for L-GA sample in the simulated intestinal fluid.

For VitE, the highest loading was achieved at the same processing conditions (135 mL/min and 45 min) for both biopolymers with maximum values of 14.95 ± 0.2% for GA, and 22.35 ± 0.1% for SA. Homogeneous coating of VitE on the biopolymers' surface was displayed by HIM images. Loaded samples were quite stable over storage for 28 days with a drop of VitE loading to 91% for GA and 96% for SA of the initial loading. Adsorption kinetics results showed a difference in the rate of the concentration increase up to 50 min for both biopolymers, indicating differences in the surface areas of the biopolymers as well as the interactions between VitE and biopolymers.

The findings on adsorptive precipitation of $VitD_3$ and VitE on the PGX-processed gum arabic and sodium alginate powders demonstrated the great potential of this technology and these food biopolymers for use as delivery systems of fat-soluble vitamins, targeting subsequent aqueous-based product applications.

Preface

This thesis research is an original work by Andrea Carolina Vilchez Athanasopulos under the supervision of Dr. Feral Temelli at the Department of Agricultural, Food and Nutritional Science (AFNS), University of Alberta. The research was financially supported by the Collaborative Research and Development (CRD) grant offered to Dr. Feral Temelli by Natural Sciences and Engineering Research Council of Canada (NSERC) and Ceapro Inc.

All work presented in Chapters 3 and 4 was conducted at the University of Alberta. Five chapters are included this thesis: background information and thesis research objectives in Chapter 1; literature review based on the topics of the two research studies in Chapter 2; Adsorptive precipitation of vitamin D_3 on gum arabic and alginate dried using Pressurized Gas eXpanded (PGX) liquid technology in Chapter 3; Adsorptive precipitation of vitamin E on gum arabic and alginate dried using PGX technology; and overall conclusions and recommendations for future work in Chapter 5. The literature review (Chapter 2), experimental work and data analysis (Chapters 3 and 4) and concluding analysis (Chapter 5) are my original work carried out under the supervision of Dr. Temelli.

Manuscripts based on Chapters 3 and 4 are in preparation for submission to peer-reviewed journals.

Acknowledgements

I would like to thank God for blessing me with accomplishing this research and putting on my way my supervisor. Thank you Dr. Feral Temelli, for all your support, knowledge, dedication, patience not only during my research but also in the difficult moments of my life. Thank you for motivating me every day to give my best in what I love, and I highly appreciate that I had the best mentor during these years; without you it would not have been possible to complete my research and thesis.

Thank you, Dr. Jonathan Curtis, for being my supervisory committee member and providing advice, support and valuable guidance. Also, I would like to thank Dr. Roopesh Mohandas Symaladevi to be an examining committee member and to give me great advice and feedback on my thesis.

Thanks for the financial support of this research project provided by Natural Science and Engineering Research Council of Canada (NSERC), and Ceapro Inc. I would like to express my gratitude to Dr. Paul Moquin, Dr. Bernhard Seifried, Dr. Byron Yépez, and Emily Wong from Ceapro Inc. for providing the PGX-processed gum arabic and sodium alginate samples and their suggestions. Besides, I am grateful for all the support of Dr. Ricardo Do Couto for his help, training and advice during almost my all research. Thanks to Ereddad Kharraz to help me with the DSC analysis and giving me feedback.

Furthermore, I would like to thank my lab family colleagues, Eileen Santos, Carla Valdivieso, Brasathe Jeganathan, Yanzhao Ren, Sule Keskin Ulug, Yonas Gebrehiwot (special thanks for HiM and XRD analysis), Zixiang Liu, and Dr. David Villanueva for their help and support in many aspects during the past years.

Finally, I would like to thank my husband, without him I would not have achieved this goal; thanks for always being by my side, motivating, pushing, and for your infinite love. Last but not least, I want to thank my family for the strong support and love, specially to my sister Adriana. Thank you for being part of my journey.

Table of contents

List of tables

List of figures

List of Abbreviations

ANOVA	Analysis of variance
CO_2	Carbon dioxide
CoQ10	Coenzyme Q10
DSC	Differential scanning calorimetry
DRIs	Dietary reference intakes
EtOH	Ethanol
FTIR	Fourier transform infrared spectrophotometry
G	α-L-guluronate
GA	Gum arabic
HIM	Helium ion microscopy
IOM	U.S. Institute of medicine
IU	International units
L-GA	Bioactive-loaded PGX-GA
L-SA	Bioactive-loaded PGX-SA
M	β-D-mannuronate
PGX	Pressurized gas expanded liquid
PM	Physical mixture
PGX-GA	PGX-processed gum arabic
PGX-SA	PGX-processed sodium alginate
RDA	Recommended daily allowance
SA	Sodium alginate
SCF	Supercritical fluid
SC-CO_2	Supercritical carbon dioxide
SIF	Simulated intestinal fluid
UV	Ultraviolet light
V	Valve
VitD_3	Vitamin D_3
VitE	Vitamin E
XRD	X-Ray diffraction

Chapter 1. Introduction and objectives

Functional food products contain value-added ingredients that can positively benefit human health, and therefore the main goal of consuming functional foods is to achieve optimal health and to reduce the risk of disease. Vitamins are added to multiple products to enhance their nutritional value. However, to manufacture these products in large scale, there are several challenges associated with the addition of vitamins, where the lack of knowledge of the vitamin's physicochemical properties in different mixtures limits ensuring their maximal functionality. Different types of vitamins have been added to food products, exhibiting different physicochemical properties, which depend on their chemical structure, dictating whether they are water-soluble or fat-soluble. The fat-soluble vitamins were chosen as the bioactive compounds to investigate in this MSc thesis research due to their impact on human health and the challenges associated with their addition to aqueous-based products.

Vitamin D_3 ($VitD_3$) is an important nutrient for the human body, responsible for increasing intestinal absorption of calcium and phosphorus. Some benefits related with the consumption of $VitD_3$ are the regulation of calcium and phosphorus homeostasis, reducing the risk of developing heart disease and improving the cardiovascular system, as well as reducing the risk of cancer and autoimmune disorders (Health Canada, 2010). Health Canada is recommending for people 1-70 years of age, a daily dose of 600 IU (15 μg). Moreover, vitamin E (VitE) is a powerful antioxidant through its ability to remove lipoperoxyl radicals and thus plays a decisive role in the prevention of many disorders. However, the main challenge for these vitamins is their high tendency to be degraded or oxidized by heat, light and presence of oxygen. As well, their hydrophobic nature limits their further use in aqueous-based products.

Different delivery systems have been developed for fat-soluble vitamins to overcome some of the formulation challenges. To investigate a novel approach, two water-soluble biopolymers were chosen as carriers in this research. Gum arabic (GA) is a natural, high-molecular-weight biopolymer derived from the exudate of mature *Acacia senegal* and *Acacia seyal* trees, found in the African Sahel district in Sudan. Sodium alginate (SA) is a long-chain, high-molecular-weight polysaccharide derived from brown algae, which can solubilize in water to form highly viscous solutions.

An application of supercritical carbon dioxide (SC-CO_2) technology was implemented in this research to dry these biopolymers. CO_2 under pressure and temperature conditions beyond its critical point (31.1 °C, 73.8 bar) is referred to as SC-CO_2 and can be used as a "green" solvent because it is inert, non-toxic, non-flammable and environmentally friendly. The main properties of SC-CO_2 are its high diffusivity like a gas, combined with high density like a liquid. For decades, based on these properties, SC-CO_2 has been applied in many processes such as, extraction, fractionation, reactions, encapsulation, particle formation and others. Pressurized Gas eXpanded (PGX) liquid technology is a recently developed application of SC-CO_2 invented by Temelli and Seifried (2016), which is a drying method for high molecular weight water-soluble biopolymers in order to produce unique morphologies of micro- or nano-sized particles that cannot be achieved by conventional methods. PGX-dried biopolymers have low bulk densities and very high surface areas, which allow them to be loaded with bioactives as delivery systems.

Another application of SC-CO_2 is adsorptive precipitation, which is an environmentally friendly technology to load hydrophobic bioactives homogeneously onto biopolymers without the use of any organic solvent, and this approach can be used to develop novel delivery systems. In order to improve the dispersion of $VitD_3$ and VitE in aqueous systems, the use of GA and SA

biopolymers as a carrier through the adsorptive precipitation process represent a potential improvement to incorporate fat-soluble vitamins into various food products. Even though conventional techniques have been used for the encapsulation of fat-soluble vitamins as delivery systems (Wagner, 2004; Anandharamakrishnan et al., 2010; Huang, et al., 2010; Piorkowski and McClements, 2014; Goncalves et al., 2015; Maurya and Aggarwal, 2019), the use of PGX-dried biopolymers as carrier and their loading with vitamins using the adsorptive precipitation process have not been reported previously. Such an approach shows great potential in terms of enhanced functionality. Therefore, it is hypothesized that the adsorptive precipitation process can be used to homogeneously load the $VitD_3$ and VitE onto the PGX-processed GA and SA particles with improved functionality, which ultimately can increase their applications in aqueous-based products. In order to test this hypothesis, it is important to understand the effect of different processing parameters to demonstrate the performance of the adsorptive precipitation process in the preparation of the targeted delivery systems.

Therefore, the overall objective of this MSc thesis research was to investigate the effect of adsorptive precipitation process parameters on the loading of fat-soluble bioactive compounds ($VitD_3$ and VitE) on water-soluble biopolymers (GA and SA) that were used as carriers, and to characterize the powders obtained in an effort to ultimately increase the application of the hydrophobic compounds in aqueous-based products. To achieve this, the specific objectives were:

i. To investigate the effect of recirculation time and recirculation flow rate applied during the adsorptive precipitation of $VitD_3$ on GA and SA in terms of $VitD_3$ loading, particle morphology, molecular interactions, thermal behavior, storage stability, and release kinetics of the particles obtained (Chapter 3), and

ii. To determine the effects of recirculation time and recirculation flow rate applied during adsorptive precipitation of VitE on GA and SA in terms of VitE loading, particle morphology, molecular interactions, thermal behavior, storage stability, release kinetics, and adsorption kinetics of the particles obtained (Chapter 4).

Chapter 2. Literature review

Vitamins (Vitamin A, D, E, and K) are considered essential nutrients because they perform many functions in the body. There are many applications where fat-soluble vitamins are required to be incorporated into aqueous media such as foods, health care, and pharmaceutical products. This literature review describes two vitamins (vitamin D_3 and vitamin E) and their health benefits, as well as two biopolymers (gum arabic and sodium alginate) that can be used in delivery systems and processes used to prepare delivery systems.

2.1. Fat-soluble vitamins

2.1.1. Vitamin D_3

Vitamin D_3 ($VitD_3$) is a fat-soluble vitamin as shown in Figure 2.1, and its composition is mainly based on two chemical forms that include vitamin D_2 ($VitD_2$, ergocalciferol) and vitamin D_3 ($VitD_3$, cholecalciferol) (Luo et al., 2012). $VitD_2$ can be synthesized by the plants, while $VitD_3$ can be synthesized in the human skin upon exposure to ultra-violet light to form 7-dehydrocholesterol. Then, in the liver, 7-dehydrocholesterol can be converted to cholecalciferol (inactive form) and 25-hydroxycholesterol, and in the kidney, the cholecalciferol can be converted to 25-hydrocholecalciferol (calcidiol, 25-OH-D_3), and finally to the bioactive compound 1,25-hydrocholecalciferol (calcitriol, 1,25-$(OH)_2$-D_3) (active form) (Maurya et al., 2020).

$VitD_3$ is an essential nutrient for the human body to control the absorption of calcium and phosphorus (Gonnet et al., 2010). $VitD_3$ degrades easily when exposed to light, acid and oxygen, which results in the loss of its functional benefits (Ballard et al., 2007a).

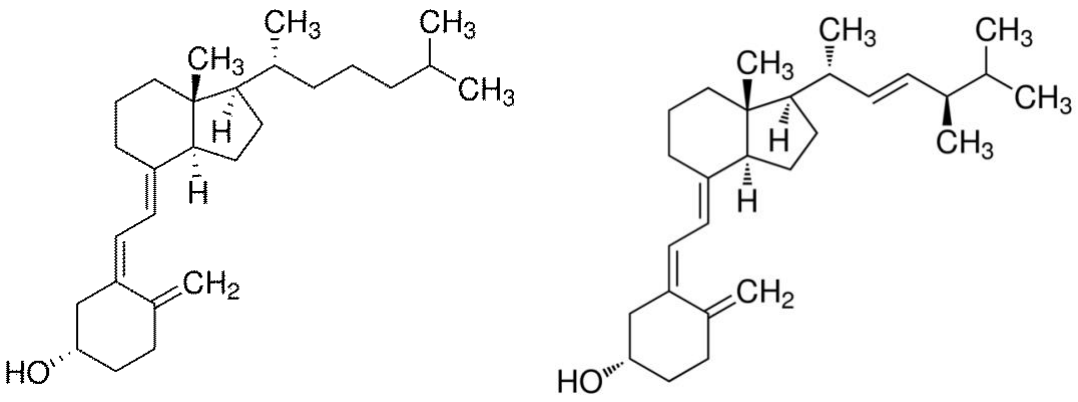

Figure 2. 1. Chemical structure of VitD3 (Cholecalciferol) and VitD2 (ergocalciferol).

2.1.1.1. Benefits

As reviewed by Combs and McClung (2017a), VitD3 is considered beneficial in the prevention of type 2 diabetes and overweight or obesity. In addition, epidemiological cardiovascular health studies have determined that low circulation levels of 25-OH-D3, and factors known to affect the status of VitD3 are associated with the prevalence of coronary risk factors and cardiovascular disease mortality (Combs and McClung, 2017a).

VitD3 and its antiproliferative effects have led to research on its potential use as a combination drug in cancer treatment. VitD3 signaling pathways involves its role as an antiproliferative agent, the actuation of the apoptotic pathways to remove cancer cells and their prevention of angiogenesis (Deeb et al., 2007). Some studies showed that VitD3 provides protective status to lower the risk of cancer. A review of 63 publications (breast (13), prostate (26), ovary (7) and colon (30) cancer) showed numerous cases where VitD3 levels were linked to the association of vitamin D receptor genotype with cancer risk (Garland et al., 2006). VitD3 may also play a role in protecting against leukemia since treatment with 1,25-(OH)2-D3 could suppress cell division. Case and control studies have provided strong evidence of vitamin VitD3 status related with the risk of non-Hodgkin's lymphoma (Combs and McClung, 2017a).

$VitD_3$ is known in bone health as a calcium homeostasis regulator, which helps to prevent osteoporosis and osteomalacia through adequate absorption of calcium from the intestine to strengthen or reshape the bones (Lips and Van Schoor, 2011).

2.1.1.2. Dosage according to Health Canada

Dietary reference intakes (DRIs) for $VitD_3$ were first published in 1997. Since then, a significant amount of information about $VitD_3$ requirements, and the association of $VitD_3$ with chronic diseases and conditions has been published. Due to the availability of sufficient new and relevant scientific research to ensure a reassessment of existing values, Health Canada, the Public Health Agency of Canada and several US government agencies co-sponsored a review of DRIs for $VitD_3$. The decision to commission the U.S. Institute of Medicine (IOM) review reflects the government's objective of ensuring that Canadians benefit from the most current nutritional and health advice. The IOM published its report on the investigation of DRIs for $VitD_3$ on November 30, 2010. The report states that there is no additional health benefit associated with $VitD_3$ intake above the level of the new recommended daily allowance (RDA) of 600 international units (IU) equivalent to 15 μg for people of 1-70 years of age.

$VitD_3$ is a nutrient that helps the body use calcium and phosphorous to build and maintain strong bones and teeth. However, high levels of $VitD_3$ can be related with excess levels of calcium being deposited in the body, which can lead to calcification of the kidney and other soft tissues, including the heart, lungs and blood vessels. The DRIs for $VitD_3$ (Table 2.1) are based on assuming minimal sun exposure and keeping healthy bones (Health Canada, 2010).

Table 2. 1. The RDA and tolerable upper intake level for $VitD_3$ per day (Source: Health Canada (2010)).

Age group	Recommended Dietary Allowance (RDA) per day	Tolerable upper intake level (UL) per day
Infants 0-6 months	400 IU (10 μg)	1000 IU (25 μg)
Infants 7-12 months	400 IU (10 μg)	1500 IU (38 μg)
Infants 1-3 years	600 IU (15 μg)	2500 IU (63 μg)
Infants 4-8 years	600 IU (15 μg)	3000 IU (75 μg)
Children and Adults 9 -70 years	600 IU (15 μg)	4000 IU (100 μg)
Adults >70 years	800 IU (20 μg)	4000 IU (100 μg)
Pregnancy & lactation	600 IU (15 μg)	4000 IU (100 μg)

IU: international units

2.1.1.3. Deficiency and reasons

$VitD_3$ deficiency may result from inadequate skin irradiation, poor dietary intake or deterioration in vitamin metabolic activation. Although exposure to sunlight can improve the biosynthesis of $VitD_3$, it is well documented, especially at extreme latitudes during the winter months that people do not receive enough solar radiation to maintain the proper state of $VitD_3$. Some people in sunnier climates may not produce adequate $VitD_3$, if their lifestyle or health status is affected by indoor activities, or factors such as air pollution or clothing reducing their exposure to sunlight (Combs and McClung, 2017a).

Currently, $VitD_3$ deficiency affects more than one billion adults and children worldwide, and therefore the impact of $VitD_3$ deficiency can be very severe in terms of public health and

should not be minimized (Holick, 2017). Generally, low levels of $VitD_3$ affect bone and skeletal health, mineral homeostasis and can lead to damage in other tissues (Holick, 2010). Similarly, $VitD_3$ is suitable for regulating pathways essential for brain development, mature brain function and homeostasis (Krisanova et al., 2019). In addition, recent studies have shown evidence of $VitD_3$ deficiency in non-skeletal abnormalities, such as cardiovascular disease, cancer and metabolic disorders (Eyles et al., 2013).

Most people have strong seasonal variations in the plasma concentration of 25-OH-D_3; for some, this may be associated with considerable periods of time of suboptimal status of $VitD_3$ if not corrected by dietary sources of the vitamin. Until the practice of food enrichment with $VitD_3$ became widespread, at least in the technologically developed countries, it was difficult to obtain an adequate amount of $VitD_3$ from the diet, because most foods only contained small amounts. Therefore, $VitD_3$ deficiency can have primary and secondary causes: the primary causes involve an inadequate supply of $VitD_3$, inadequate exposure to sunlight, insufficient consumption of foods containing $VitD_3$ and secondary causes relate to altered absorption and metabolism due to gastrointestinal diseases (e.g. small bowel disease, gastrectomy, pancreatitis), involving malabsorption of vitamins (Combs and McClung, 2017a).

2.1.1.4. Challenges in formulation

$VitD_3$ is classified as a fat-soluble vitamin and its solubility in water is negligible (Pike, 1991). Therefore, insolubility is the main problem for the development of various aqueous–based formulations incorporating $VitD_3$ (Delgado et al., 2016; Almarri et al., 2017). In addition, $VitD_3$ is easily oxidized and degraded when exposed to light, oxygen and acid, which results in the loss of its functionality and physiological benefits (Ballard et al., 2007).

$VitD_3$ has been incorporated into dairy products, such as milk and cheese, to improve retention and stability in order to enhance its bioavailability (Yeh et al., 2017). The most commonly used methods are described below. In general, $VitD_3$ is first dissolved in an organic solvent (food grade) such as ethanol, and then mixed with butter oil, and finally with the food matrix to achieve a homogeneous mixture and to ensure uniform distribution. However, some heat application is required in the following step to remove the ethanol, which can lead to vitamin degradation. A major challenge is the loss of $VitD_3$ stability in the food matrix leads to $VitD_3$ degradation that happens with the packaging materials, such as polypacks or tetrapacks (Maurya et al., 2020). The emulsion method in oil phase can be applied to milk, cheese, bread and other food materials, where $VitD_3$ is first dissolved in oil, then the oil is dispersed in water as fine drops to form the emulsion, which is then mixed with the food material. A major challenge is the limitation of food-grade products to form a stable emulsion to ensure $VitD_3$ homogenization in the food matrix (Maurya et al., 2020). However, large amounts of $VitD_3$ are used in the form of powder, emulsion or oil to fortify milk or cheese, compared to the initial concentration incorporated into the batch of milk used (Tippetts et al., 2012; Wagner et al., 2008). This implies large loss of profits for the industry, given the fact that, to date, cheese fortification does not improve the bioavailability of $VitD_3$ compared to supplements (Wagner et al., 2008). To improve the stability and bioavailability of nutrients, encapsulation is a desirable method, where proteins and polysaccharides are often used as a coating material due to their non-toxicity and biodegradability (Luo et al., 2013).

2.1.2. Vitamin E

Vitamin E (VitE) is available in a number of foods and plants, ranging from edible oils to nuts, including wheat, rice bran, barley, oat, coconut, palm, and annatto (Kannappan et al., 2012; Sheppard et al., 1993). Other sources of VitE include rye, amaranth, walnut, hazelnut, poppy seeds,

safflower, maize, and the seeds of grape and pumpkins. In addition, VitE derivatives have also been detected in human milk (Kanno et al., 1999) and palm date (*Phoenix canariensis*) (Nehdi et al., 2010).

VitE is defined as the collective of tocopherols and tocotrienols, which are fat-soluble vitamins and show a powerful antioxidant activity through their lipoperoxyl radical removal properties. VitE consists of eight lipophilic molecules, including alpha-, beta-, gamma- and delta-isomers of tocopherols and tocotrienols (Combs and McClung, 2017b) as shown in Figure 2.2.

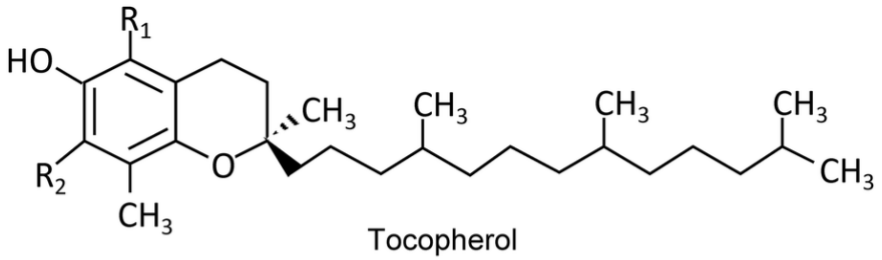

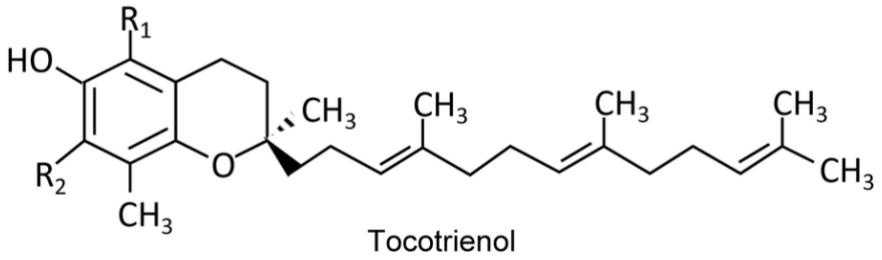

	α	β	γ	δ
R_1	CH_3	CH_3	H	H
R_2	CH_3	H	CH_3	H

Figure 2. 2. Chemical structures of the VitE group (Source: Niki and Abe (2019)).

Tocopherols contain saturated phytyl side chain in the four forms. Three chiral carbons are present in tocopherols at C2 (chromanol ring), and C4' and C8' located in the phytyl side chain (Niki and Abe, 2019). The synthetic α-tocopherol is called all-*rac*-α-tocopherol. Although the use

of phytol from natural sources (with the R-configuration at both the C4' and C8' positions) produces a root product at only the 2nd position, commercial synthesis of VitE now mainly uses a fully synthetic side chain, which produces a mixture of the eight possible stereoisomers, i.e. 2-RS, 4'-RS, and 8'-RS compounds. This mixture is designated with the prefix all-*rac*- (e.g. all-*rac*---tocopherol, all-*rac*---tocopheryl acetate). VitE acetate esters are used in human nutritional supplements and animal feed, while non-esterified forms are used as antioxidants in foods and pharmaceuticals (Combs and McClung, 2017b). On the other hand, tocotrienols contain an unsaturated phytyl side chain with three double bonds at C3', C7' and C11'. *Trans*-configuration can be present on the double bonds at C3' and C7' in the side chain (Niki and Abe, 2019).

VitE oxidizes easily in the presence of heat, light and alkaline conditions; however, esters are less vulnerable to oxidation and have been used in food, cosmetic and pharmaceutical applications more than the free form (Niki and Abe, 2019).

2.1.2.1. Benefits

The effects of VitE on fertility, and on the development of tissues and organs have been well documented. Some of these functions have been confirmed in humans, while others must be evaluated. An important role of VitE focuses on its antioxidant properties (Zingg, 2007).

Oxidative stress underlies many diseases, such as cancer, cardiovascular disease and inflammation. VitE was shown to play a decisive role in the prevention of these disorders, not only as an antioxidant, but also as a modulator of signal transduction and a regulator of gene expression (Zingg, 2007). A review of the literature has indicated that VitE has a positive impact on numerous diseases, including immune system disorders (Mocchegiani et al., 2014; Peh et al., 2016; Szymańska et al., 2017), cardiovascular diseases (Mocchegiani et al., 2014; Galli et al., 2017;

Szymańska et al., 2017), cancer (Mocchegiani et al., 2014; Yan et al., 2015; Szymańska et al., 2017), and neurodegenerative disorders (Aslam et al., 2004; Peh et al., 2016).

The complex metabolic processes compromise intestinal absorption of VitE due to its hydrophobicity, and also regulating its bioavailability prevent its accumulation in lipid-rich tissue cells. At high levels, this vitamin can be absorbed by passive diffusion mechanisms (Goncalves et al., 2015). Current studies suggest that at the lowest doses found in the diet and body, their transport and distribution are selective and regulated, implying specific recognition by transporting proteins, transporters, receptors, and possibly facilitated, by intracellular metabolic capture, and by enzymatic modification as with fatty acids (Traber, 2013; Henry and Kathryn, 2014).

The extra and intracellular carriers are designed to overcome the inherent insolubility of VitE in water and possibly also to protect it from oxidative and metabolic destruction. These proteins regulate absorption and transport, distribution to tissues, cells and subcellular sites of the body, as well as its metabolism to various water-soluble VitE metabolites in urine, such as carboxyethylhydroxychromanes that have the specific role of removing too much VitE from the body (Birringer, 2010; Zhao et al., 2010).

VitE is a lipophilic bioactive compound that has been shown to have potential health benefits. However, its application is limited in food systems, because it degrades rapidly in the presence of oxygen and oxidative processes by free radicals (Anandharamakrishnan and Ishwarya, 2015). As mentioned above, VitE has low solubility in water, which limits its absorption into the gastrointestinal tract and reduces general bioavailability (Abuasal et al., 2012).

2.1.2.2. Dosage according to Health Canada

According to Health Canada, the recommended dietary allowance (RDA) of VitE for people aged 14 years and older, including pregnant women is 15 mg per day of α-tocopherol. This

is equivalent to 22 IU of natural source VitE per day, or 33 IU from synthetic sources. The RDA for breastfeeding women is 28 IU for natural and 42 IU for synthetic VitE. The tolerable upper intake level for adults is 1,000 mg per day of any form of VitE supplements.

In general, an intake of VitE (for example, as part of a multivitamin supplement) of up to 40 IU is considered a "normal" dose. Supplements are available that provide 1.5 IU to 1,500 IU per day. Those that provide 400 IU per day or more are considered "high dose" or "mega dose". Health Canada is developing guidelines for VitE that will recommend precautionary measures for people 55 years of age and older who have heart disease or diabetes, and for people who have or previously had cancer. These people are advised to consult their doctor before taking VitE doses of 400 IU or more. In addition, people who take blood thinners, or who have been diagnosed with a bleeding disorder and/or a vitamin K deficiency should consult their doctor before taking VitE (Health Canada, 2006).

2.1.2.3. Deficiency and reasons

VitE plays a key role in the normal metabolism of all cells. Therefore, its deficiency can affect several different organ systems. Lack of VitE can have primary and secondary causes. The primary causes involve an inadequate supply of vitamin, considering them as diets with an unfavorable dose of VitE. Moreover, the secondary causes are related to absorption, metabolism or vitamin metabolic function and lipid malabsorption, as well as high intake of polyunsaturated fatty acids, which increases the need for VitE (Combs and McClung, 2017b).

Deficiency of VitE has some manifestations, such as progressive neurological disorders, including ataxia, hemolytic anemia, dementia, retinopathy, and anemia in premature infants (Marcel, 2017). As well, VitE at low concentrations can cause children to be more vulnerable to infectious conditions and recurrent infections, and it could also affect their growth (Lobo et al.,

2019). VitE could be related to muscle deterioration when this vitamin is lacking in the body for long periods of time (Lobo et al., 2019).

2.2. Biopolymers as delivery systems

2.2.1. Gum arabic

Gum arabic (GA) is an edible biopolymer derived from the exudates of mature trees, *Acacia senegal* and *Acacia seyal*, found in the African Sahel district in Sudan. The exudate is a thick liquid, rich in fiber that its emanation spreads from the stems and branches under stress conditions, for example, dry season, poor soil fertility and injuries (Phillips and Williams, 2000). GA is mainly composed of 1,3-linked β-D-galactopyranosyl units (Fig. 2.3) and has a high molecular weight of around 250,000 g/mol with a high degree of branching (Sanchez et al., 2018).

GA has unique properties based on its structure. It is a neutral or slightly acidic hydrocolloid (its solution has a pH of 4.5 to 5.0) that contains calcium, magnesium, potassium and sometimes other cations. GA contains three fractions comprised of different types of high molecular-weight biopolymers (BeMiller, 2019). The first fraction, which makes up about 70% to 90% is composed of polysaccharide molecules. Another part includes higher molecular weight molecules that possess a hydrophobic protein as part of their structures. This part constitutes less than 10% of the total hydrocolloid, but it is the part that provides the most beneficial functionality of GA. The polysaccharide structures in this part are covalently bound to a hydrophobic protein by hydroxyproline and, perhaps, units of serine and/or threonine. The total protein content of GA is about 2% by weight, but this fraction can contain up to 25% by weight of protein. These GA components are classified as proteins-polysaccharides and are responsible for the emulsifying properties of GA. The third fraction, which is the smallest portion and represents only about 1% of the total gum, is a glycoprotein (containing 20% to 50% of proteins) (BeMiller, 2019).

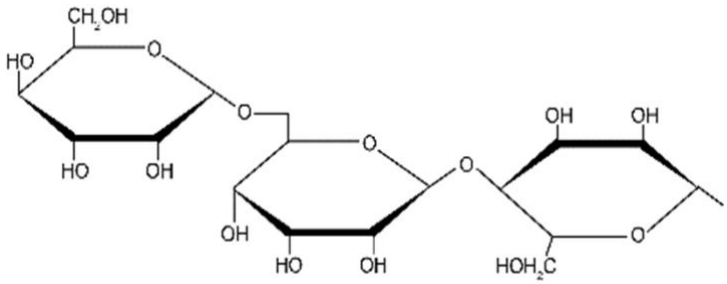

Figure 2. 3. Molecular structure of gum arabic (Source: Korkmaz et al. (2016)).

2.2.1.1 Benefits

GA is widely used in the pharmaceutical industry as a drug carrier, because it is considered a physiologically harmless substance. Also, recent studies have highlighted the antioxidant properties of GA as well as its part in the digestion of lipids and its positive effects when used as a part of treatments for various degenerative diseases, for example, kidney failure and cardiovascular and gastrointestinal diseases (Glover et al., 2009; Montenegro et al., 2012). In addition to its sensory and texturizing properties, GA has the ability to eliminate targeted radicals (Montenegro et al., 2012). There is growing research that its antioxidant function is due to its protein portion, primarily due to specific amino acid residues, for example, histidine, tyrosine and lysine, which, for the most part, are considered as antioxidant molecules (Park et al., 2005).

Previous studies have shown that high dietary fiber ingestion, containing GA, is related to beneficial effects on fat metabolism (Slavin, 2003; Ali et al., 2009). GA has a wide range of potential health benefits (Phillips and Phillips, 2011). These benefits include anti-obesity effects, hypoglycemic effects, hyperlipidic effects (Abdelkareem et al., 2015; Mohamed et al., 2015), antidiabetic effects (Ahmed et al., 2015), prebiotic effects (Calame et al., 2008), and antioxidant effects (Abdelkareem et al., 2015), together with a protective role against cardiac toxicity (Abd-Allah et al., 2002), hepatic and nephritic syndrome (Al-Majed et al., 2003).

2.2.1.2. Applications

GA is a key ingredient in traditional lithography and is used in printing, paint production, glue, cosmetics and various industrial applications, including viscosity control in inks and textile industries; although there are other less costly materials to compete with it for many of these roles (Smolinske, 1992). The main application of GA is in the food industry as a stabilizer. It is an important ingredient in soft drink syrups, gummies, marshmallows, chocolate candies and edible glitter. In addition, GA is used as an emulsifier and a thickening agent in the formulations of ice cream, fillings, chewing gum, and other confectionery treats (Baughman, 2008). The characteristics of GA demonstrated by its acid stability, emulsifying ability, low viscosity at high concentration, and others led to the wide utilization of GA in pharmaceuticals (Karama, 2002).

GA has a long tradition of use in wine making, where it produces a clarity that is higher than that can be obtained with other hydrocolloids (Viinanen et al., 2011). GA delays or prevents the crystallization of sucrose in wine. It also emulsifies and distributes fatty components to slow their migration and accumulation on the surface of a product. GA and octenylsuccinate starch products are the hydrocolloids of choice for the emulsification of citrus oils, essential oils, imitation flavors and bakery concentrates for soft drinks (BeMiller, 2019). In addition, GA contains 80% fiber for its low consistency and high solvency in water; therefore, it is very easy to incorporate into food products in high amounts (Ross et al., 1983).

2.2.2. Alginate

Alginate is a natural polysaccharide derived from brown algae as a structural component in the cell walls of *Macrocystis pyrifera*, *Ascophyllum nodosum,* and *Laminaria hyperborea*, and bacterial cells, such as *Pseudomonas aeruginosa* and *Azobacter vinelandii* (Draget and Taylor, 2011). The characteristics of alginate vary from species to species, resulting in the variability of

its composition due to environmental and seasonal changes (Remminghorst and Rehm, 2006). The main commercially employed algae species are *Lamaria, Macrocyst, Ascophyllum, Durvillaea, Ecklonia, Lessonia, Sargasso* and *Turbinari* (George and Abraham, 2006).

Alginate is a linear copolymer composed of (1,4)-linked β-D-mannuronate (M) and α-L-guluronate (G) residues that are composed of consecutive M residues, alternating M and G residues, and consecutive G residues (Skaugrud et al., 1999). The chemical structure of alginate and its elements are shown in Figure 2.4. The composition of SA extracted from *Pseudomonas aeruginosa* bacteria was reported as 100% mannuronic acid (Skaugrud et al., 1999).

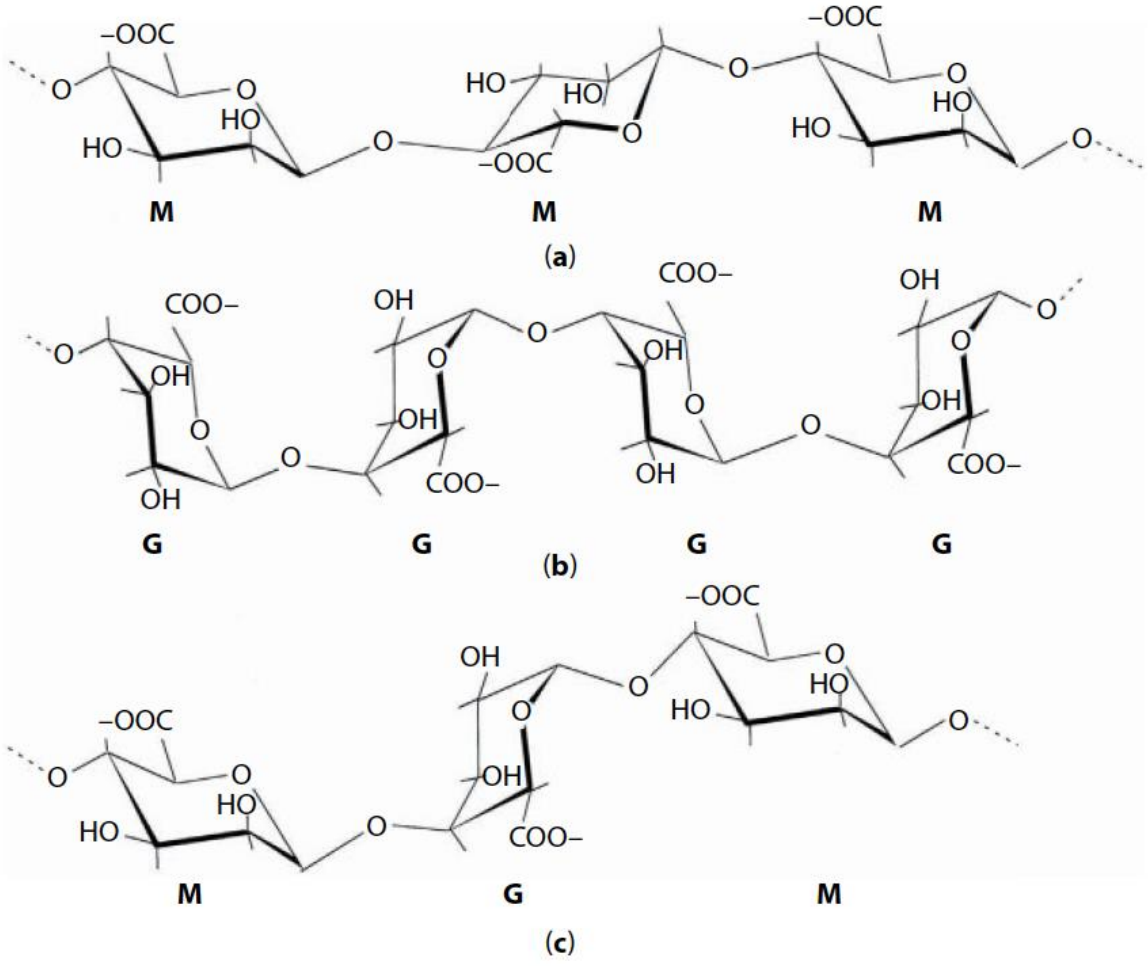

Figure 2. 4. Molecular structure of alginate and its constituent (1,4)-linked β-D-mannuronate (MM blocks) and α-L-guluronate (GG blocks) and blocks of MG random monomers (Source: Ahmed (2019)).

The molecular weight of SA ranges from 32,000 to 400,000 g/mol (Lee and Mooney, 2012); they are polydisperse similar to other polysaccharides and their polydispersity index ranges from 1.5 to 3.0 (Skaugrud et al., 1999).

At the time of polymer extraction, processing conditions can be altered by manufacturers to control the molecular weight and in turn the viscosity of the SA extract obtained, since viscosity is strongly dependent on the molecular weight. This way, an extract with viscosity ranging from 10 to 1000 mPa-s and a polymerization degree of 100 to 1000 units for a 1% solution can be obtained. These properties are of great interest in the production of alginate fibers where the extrusion of the alginate solution by spinning is involved (Qin, 2008).

2.2.2.1. Benefits

A review of the literature has indicated that alginate has several health benefits and utilized especially in the following application areas: wound dressing (Walker et al., 2003; Dutra et al., 2016; Lawrence, 1994), hemostasis (Boon, 1993; Xu et al., 2016), burns (Risbud et al., 2000; Bahemia et al., 2015; Chen et al., 2016), skin graft (Ratner, 2003; Miyanaga et al., 2016), and cartilage regeneration (Vunjak-Novakovic and Freed, 1998; Oliveira and Reis, 2011).

2.2.2.2. Applications

Alginate has various biomedical applications as mentioned in the above section, and alginate-based biomaterials can be used in regenerative medicine, such as a drug delivery system and cell transporter. Biodegradability, biocompatibility, mechanical strength and exceptional chelating properties of matrices derived from alginate make them useful for the human body (Petzold et al., 2019).

On the other hand, food applications of alginate include the use of its gels in various types of food structures, as well as its incorporation for greater viscosity and consistency. Alginate is

consumed directly in the form of an ingredient in various food products or as an encapsulating agent to deliver different ingredients or micronutrients for health and wellness. Alginate has been used for the microencapsulation of micronutrients and microorganisms such as polyphenols, vitamin C, and probiotics (Petzold et al., 2019).

Alginate is an important food ingredient that is used at very low concentrations to perform a technological function. In this sense, alginates in foods are used as emulsifiers, encapsulation and stabilization agents. Alginate is also used for its gelling characteristics in fruit gels, puddings, onion rings, dessert gels, and beer foam (Belitz et al., 2004). Calcium chloride can be used to form hydrogels, where the divalent Ca^{2+} acts as a cross-linking agent between the negatively charged carboxyl groups on the biopolymer (Draget, 2009).

2.3. Preparation of delivery systems

2.3.1. Conventional methods for vitamin encapsulation

Encapsulation is a process that entraps one substance into another wall material, producing particles with morphologies in nanometer, micrometer or millimeter scale. This is a favorable technique to protect bioactive molecules in food against light, moisture and oxygen as well as increase their solubility and dissolution rate (Turchiuli et al., 2014). Technologies used to accomplish this task are spray drying, lyophilization, solvent evaporation, gelation and fluidized bed (Nesterenko et al., 2013). Spray drying (SD) is an established technique for producing free-flowing encapsulated powders (Anandharamakrishnan et al., 2007). However, high temperatures employed in the spray drying operation are not favorable for heat-sensitive bioactive compounds, such as VitE. On the other hand, freeze-drying (FD) operates at low temperatures, which is the best for VitE encapsulation, but its main drawback is high capital and operating cost (Anandharamakrishnan et al., 2010).

VitE is lipophilic and cannot be dispersed into aqueous-based food matrices as previously mentioned. It is also susceptible to oxidation and may deteriorate during processing and storage. One approach to overcome these challenges is to incorporate VitE into colloidal dispersions, consisting of small lipophilic particles suspended within an aqueous medium, for example, an oil-in-water emulsion (Piorkowski and McClements, 2014). Indeed, different studies suggest emulsion-based systems for encapsulation, chemical degradation protection and VitE supply (Wagner, 2004). Emulsion-based systems have additional advantages for the encapsulation of lipid-soluble bioactive compounds (Huang, et al., 2010). Another encapsulation was based on orange oil emulsion beverages in water using food-grade ingredients (Raikos, 2017).

Nanoencapsulation allows the protection of bioactive ingredients in nanoparticles against harsh conditions and increases their dispersion in an aqueous system. Also, encapsulation techniques provide controlled release as well as proper dosing that helps prevent hypervitaminosis syndrome and its possible side effects. Fat-soluble vitamins (such as $VitD_3$ and VitE) are usually absorbed at specific sites in the small intestine through passive and active transport along with fats and fatty acids (Goncalves et al., 2015). Therefore, $VitD_3$ encapsulated within lipid-based delivery systems generally result in improved bioavailability (Porter et al., 2007; Reboul et al., 2011). Nanoemulsions are generally manufactured with generally recognized as safe (GRAS) ingredients using simple preparation methods, can be manipulated to improve oral bioavailability and water dispersibility, and are considered to be more suitable for lipophilic compounds such as $VitD_3$ (Maurya and Aggarwal, 2019).

Maurya and Aggarwal (2019) developed a nanoemulsion manufacturing process to encapsulate $VitD_3$ by combining caprylic/capric triglycerides (Leciva S70 and Kolliphor HS 15), $VitD_3$ and aqueous phase (sodium chloride solution) and demonstrated the formation of

nanoparticles. Similarly, nanofibrillated cellulose can form and stabilize oil emulsions in water through a "Pickering mechanism" (Winuprasith and Suphantharika, 2015). This involves adsorption of solid particles on oil droplet surfaces, where barriers are formed that block the coalescence of droplets (Chevalier and Bolzinger, 2013). A large number of Pickering emulsion studies have been performed with a view to food structuring to delay intestinal lipolysis and also to design physiologically relevant emulsions for the targeted supply and sustained release of hydrophobic bioactive components (Tzoumaki et al., 2011). Winuprasith et al. (2018) studied $VitD_3$ encapsulation in Pickering emulsions stabilized by nanofibrillated mangosteen cellulose and its impact on *in vitro* digestion and bioaccessibility.

Similarly, the application of colloidal supply systems for the encapsulation, protection and increased bioavailability of bioactive ingredients received increasing interest, and nanocomplex preparation of $VitD_3$ based on corn protein hydrolysate was reported (Yuan et al., 2016). Biopolymer nanogels (also referred to as polymer particles, nanogels, hydrogel beads or microsphere) are also receiving attention as oral administration agents of bioactives. Nanogels are relatively small (≤100 nm) and these particles are composed of biopolymer molecules that trap a large amount of solvent (usually water) in its interior (Dickinson, 2015).

2.3.2. Supercritical fluid technology

Supercritical fluids (SCF) are pure substances at pressure and temperature conditions beyond their critical pressure and temperature (Brunner, 2004). This is achieved by increasing the pressure and temperature of the gas above its critical values, where the supercritical condition is achieved, and the existing phase boundary between the liquid and gaseous states can no longer be distinguished. A significant increase in the system's dielectric constant gives dissolution

capabilities to a system that probably had none under normal conditions of pressure and temperature (Saus et al, 1993).

SCF has properties in between those of liquid phase and gaseous phase; the diffusivity of SCF is higher than that of liquids but similar to that of gas, which helps with better mass transfer, while its density is closer to that of liquids, giving it solvent power (Cooper and DeSimone, 1996). The physical or chemical characteristics of SCF differ from solvents at ambient temperature and pressure (Skouta, 2009).

Supercritical carbon dioxide (SC-CO_2) is CO_2 under pressure and temperature conditions beyond its critical point (31.1 °C, 73.8 bar) (Yeo and Kiran, 2005). From the outset it has been stated that SC-CO_2 is a "green" solvent (Zhang et al., 2014), and the fact that SC-CO_2 is inert, non-toxic, non-flammable and environmentally friendly (Boyére et al., 2014) allows it to be called "green" solvent. Also, the use of SC-CO_2 offers economic benefits, as it is an economical solvent with recovery processes that do not require high-energy consumption (Perrut and Perrut, 2019).

Properties of SC-CO_2 such as solvent density can be adjusted by means of minor variations in pressure and temperature (Boyére et al., 2014). SC-CO_2 shows selective solubility towards compounds of low molecular weight and nonpolar molecules, which are easily solubilized in SC-CO_2 (Kendall et al., 1999; Boyére et al., 2014). It is also used as an antisolvent in polar organic solvents, which leads to a significant decrease in its polar character, causing precipitation of the previously dissolved compounds in these solvents (Perrut and Perrut, 2019).

In addition, SC-CO_2 is very favorable as a solvent in reactions involved in fuel processing, biocatalysis, biomass conversion, homogeneous and heterogeneous catalysis, environmental control, polymerization, material synthesis, chemical synthesis, etc. (Knez et al., 2014; Brunner, 2010; Brunner, 2005). The enzymatic acceleration in SCF has gained considerable attention as an

effective process for the synthesis of natural products, pharmaceuticals, fine chemicals and food ingredients (Knez et al., 2019).

Applications of supercritical particle formation techniques have mostly been performed in pharmaceuticals, food-related and natural material-based ingredients, such as health products, cosmetics and personal hygiene products. Moreover, applications linked to food ingredients of SC-CO_2-based technologies can be classified as ingredients based on lipids, proteins, carbohydrates and minor components. The vast majority of studies are based on protein-based ingredients in pharmaceutical applications and more studies are required for food ingredients. As well, carbohydrate particles have been made using sugars, oligo and polysaccharides (Temelli, 2018).

The most common applications of natural product processing using SC-CO_2 can be classified into the following areas:

- Extraction: large-scale units operate around the world for the extraction of solid natural materials, mainly for food and phytopharmaceutical/nutraceutical ingredients (Perrut and Perrut, 2019).
- Fractionation: industrial applications are developed to use the selectivity of SCF including aroma production from fermented and distilled beverages, lipid fractionation (especially polyunsaturated fatty acids and polar lipid compounds), active compounds of the fermentation broth, etc (Perrut and Perrut, 2019).
- Reactions: SCF are very conducive to many chemical and biochemical reactions that lead to greater selectivity and reaction speed than in liquid solvents (Perrut and Perrut, 2019).
- Formulation: drying and formulating ingredients by vehicle impregnation and particle "engineering" have been performed, mainly to design drug supply systems, as well as to prepare new food, cosmetic and nutraceutical products (Perrut and Perrut, 2019).

- Sterilization and biological applications: biocidal properties are specific for SC-CO_2 with the addition of various additives, which lead to opportunities for pest elimination, sterilization and virus inactivation under "mild" conditions (near room temperature), preserving substrate quality (Perrut and Perrut, 2019).

The application of SC-CO_2 techniques for the encapsulation of vitamins has been limited. As mentioned above, the encapsulation of $VitD_3$ can be done in various ways, and the encapsulation of $VitD_3$ using alginate aerogels with the supercritical impregnation technique was developed by Pantić et al. (2016a; 2016b). They studied supercritical impregnation as a feasible technique for trapping fat-soluble vitamins in alginate aerogels, as well as high-pressure and low-pressure impregnation of $VitD_3$ into polysaccharide aerogels using moderate and low temperatures.

2.3.2.1. Pressurized Gas eXpanded (PGX) liquid process to produce the particles

Pressurized Gas eXpanded (PGX) liquid technology is a recently developed technology as a drying method for high molecular weight water-soluble biopolymers that operate at moderate temperatures (40 °C) and low pressures (100–200 bar), resulting in the control of the type of structures and particles formed by the control of conditions, which is not possible to achieve by conventional techniques (Temelli and Seifried, 2016; Seifried, 2010).

This technology was based on the use of pressurized carbon dioxide (CO_2), anhydrous ethanol (EtOH) and an aqueous biopolymer solution. After the pressure is stabilized in a high-pressure vessel, the aqueous biopolymer solution is pumped in together with SC-CO_2 and EtOH and mixed at the tip of a co-axial nozzle, resulting in the precipitation of the biopolymer where CO_2 + EtOH acts as an antisolvent. After a certain period of time, the water is removed by pumping in SC-CO_2 + EtOH, and then just SC-CO_2 is pumped in to remove the EtOH from the system,

followed by the final step of depressurization and collecting the dried powder product. This leads to the generation of nano and microscale structures, agglomerates and fibrils with a large specific surface area and very low apparent density. Then, biopolymer powders with large surface area can be loaded with different bioactives to develop improved delivery systems (Temelli and Seifried, 2016; Seifried, 2010). Previous studies from our group have employed the PGX technology for the drying of high molecular weight biopolymers, such as β-glucan (Liu et al., 2018), GA (Couto et al., 2018), and SA (Liu, 2019).

2.3.2.2. Adsorptive precipitation to incorporate the bioactives into the biopolymers

In the adsorptive precipitation, a porous matrix is first immersed in a supercritical solution of a bioactive or drug and then a slow or rapid expansion is performed. Various adsorbents (polymers, plant derivatives and others) have been used for adsorptive precipitation employing SC-CO_2. This process is performed in two steps. CO_2 solubilized the bioactive compound and carrier to the biopolymer vessel when the molecular interactions between them happened this first step is called adsorption of the bioactive compound on the surface of the carrier system based on its affinity, and the second step is the precipitation of the bioactive compound out of the solvent stream based on the loss of solubility upon depressurization at the same time forced the interactions between bioactive (Gurikov and Smirnova, 2018).

During the adsorptive precipitation process, a bioactive in solid crystalline form under ambient conditions prior to processing can be transformed into amorphous form in two ways: direct conversion or transformation into a thermodynamically stable form after the processing, which improves their bioavailability. The crystalline compound can be converted to non-crystalline form and solubilized into the solvent stream. Generally, a solid porous biopolymer is used as a carrier and the matrix is loaded with a hydrophobic bioactive; therefore, a high surface

area is preferred because a high amount of bioactive or drug can be loaded on it. SC-CO_2 has many advantages to serve as a solvent since it has moderate processing conditions to reach the SCF region. Although not all drugs and bioactive compounds are soluble or highly soluble in SC-CO_2, some co-solvents, such as anhydrous ethanol, are generally used to increase potency towards polar compounds. On the other hand, organic solvents can be involved in the adsorptive precipitation process, where a bioactive product can be used and washed during depressurization (Gurikov and Smirnova, 2018).

Some studies focused on the adsorptive precipitation of co-enzyme Q10 (CoQ10) on PGX-processed β-glucan, a biopolymer derived from oats. CoQ10 is first solubilized in SC-CO_2, which is then contacted with PGX-processed β-glucan, resulting in adsorptive precipitation (Couto et al., 2018). Then, the physicochemical properties of oat β-glucan powder (BG) and BG powder loaded with CoQ10 (L-BG) produced by the PGX technology were characterized (Liu et al., 2018). Additionally, Couto et al. (2020) investigated the PGX technology to simultaneously dry and purify high molecular weight biopolymers, resulting in nano/micro sized powders with large surface areas that can be loaded with the bioactive. The preparation of the dried GA particles with PGX and its loading with CoQ10 by adsorption precipitation was investigated in a two-step process. Finally, Liu (2019) investigated adsorptive precipitation of CoQ10 on PGX-processed SA. The interest in the loading of fat-soluble bioactive compounds on biopolymer carriers using the adsorptive precipitation method has been growing. However, there is a lack of information on the adsorptive precipitation of $VitD_3$ and VitE on biopolymers, which is the focus of this MSc thesis.

Chapter 3. Adsorptive precipitation of vitamin D_3 ($VitD_3$) on gum arabic and alginate dried using Pressurized Gas eXpanded (PGX) liquid technology

3.1. Introduction

Vitamin D_3 ($VitD_3$) is a fat-soluble compound responsible for increasing intestinal absorption of calcium and phosphorus. Some health benefits related to the consumption of $VitD_3$ were previously described in Chapter 2 (Section 2.1.1.1) (Health Canada, 2010). According to Health Canada, a daily dose of 600 IU (15 μg) is recommended for people of 1-70 years of age. The main challenge of handling $VitD_3$ during processing is its high tendency to be degraded or oxidized by heat, light and presence of oxygen. In addition, its hydrophobicity limits its utilization in aqueous-based products.

In order to improve the dispersion of hydrophobic vitamins, including $VitD_3$, in aqueous systems, biopolymers such as gum arabic and sodium alginate have been used as carrier materials in an effort to incorporate this type of vitamin into various food products. Structure and properties of gum arabic (GA) and sodium alginate (SA) were described in Chapter 2 (Sections 2.2.1 and 2.2.2, respectively). Current technologies such as encapsulation and nanoencapsulation through spray drying, lyophilization, solvent evaporation, gelation, and emulsions have been used for the incorporation of $VitD_3$ into various delivery systems but many of these approaches involve the use of organic solvents (Chapter 2, Section 2.3.1).

The Pressurized Gas eXpanded (PGX) liquid technology, which is an anti-solvent method, is used to dry high molecular weight biopolymers such as GA and SA from aqueous solution, resulting in increased surface area, reduced bulk density and unique morphologies (Temelli and Seifried, 2016). In this method, the aqueous biopolymer solution is sprayed together with a mixture

of ethanol and CO_2 into a pressurized chamber through a co-axial nozzle, resulting in dried biopolymer particles. Few examples of the application of PGX technology for drying of biopolymers include β-glucan extracted from oat (Liu, et al., 2018), gum arabic from acacia tree (Couto et al., 2020), and sodium alginate extracted from brown algae (Liu, 2019). In this study, the PGX-processed GA and SA were used as carries for $VitD_3$.

Supercritical carbon dioxide (SC-CO_2) can be used for the preparation of delivery systems and solubilizing the bioactive compounds while avoiding the use of toxic organic solvents. The adsorptive precipitation technology has two main steps: first, the bioactive solubilized in SC-CO_2 is adsorbed by the porous carrier biopolymer, and then precipitation of the bioactive occurs at the time of depressurization (Gurikov and Smirnova, 2018). This technology has been used to prepare drug delivery systems using silica aerogels as the carrier for drugs such as, ketoprofen, miconazol, menthol, benzoic acid, nimesulide, and domperidone (Gurikov and Smirnova, 2018). However, the use of adsorptive precipitation is limited for the loading of bioactive compounds on food-grade biopolymers, and there is a lack of information on such delivery systems for $VitD_3$, and their food applications. In addition, the effect of processing parameters employed during adsorptive precipitation on the properties of the products obtained is not well known. Therefore, the objective of this study was to investigate the effect of adsorptive precipitation processing parameters (recirculation flow rate and time) on the $VitD_3$ loading on PGX-processed GA and SA and to characterize the physicochemical properties ($VitD_3$ loading, particle morphology, molecular interactions, crystallinity, storage stability, and release kinetics) of the loaded particles obtained.

3.2. Materials and Methods

3.2.1. Materials

Vitamin D_3 (cholecalciferol) (≥98% purity) was purchased from Enzo Life Sciences, Inc. (Burlington, ON, Canada). Gum arabic from acacia tree was purchased from Fisher Scientific (Ottawa, ON, Canada). PGX-processed gum arabic was provided by Ceapro Inc. (Edmonton, AB, Canada) (July 2018 batch, obtained at 100 bar, 40 ^{o}C, 20% w/w aqueous solution, and flow rates of 22.5 g/min for aqueous solution, 45 g/min ethanol and 15 g/min for CO_2). Alginic acid sodium salt powder extracted from brown algae was purchased from Sigma-Aldrich (Oakville, ON, Canada). PGX-processed sodium alginate was provided by Ceapro Inc. (Edmonton, AB, Canada) (March 1, 2019 batch, obtained at 100 bar, 40 ºC, 1.0% w/w aqueous solution, and flow rates of 40 g/min aqueous solution, 150 g/min ethanol, and 50 g/min CO_2). CO_2 (99.9% purity) was purchased from Praxair Canada Inc. (Mississauga, ON, Canada). For the *in vitro* release kinetics analysis, sodium hydroxide (≥98% purity), potassium phosphate monobasic (ACS reagent grade, ≥99% purity), bile salts for microbiology and pancreatin from porcine pancreas were purchased from Sigma-Aldrich (Oakville, ON, Canada).

3.2.2. Adsorptive precipitation unit

The adsorptive precipitation unit was described in detail previously by Couto et al. (2018). However, the original unit was modified for this study in order to simplify the operation. The total internal volume of the modified unit was 190 mL, which was determined by pressurizing the system with CO_2 at 300 bar, and then slowly depressurizing and measuring the CO_2 volume at the exit with a gas meter (Canadian Meter Company Limited, Type AL225, Cambridge, ON, Canada). Finally, the volume of CO_2 measured at ambient conditions was multiplied with the ratio of CO_2 densities (NIST Chemistry WebBook) at ambient pressure to that at 300 bar to calculate the

volume of the unit. The flow chart of the modified unit was presented in Figure 3.1. The unit was composed of two high-pressure vessels, containing the biopolymer (42.5 mL volume) and $VitD_3$ (6.2 mL volume), which were located inside an oven (Fisher, Econotemp 15F, Pittsburgh, PA, USA) in order to control the temperature. A syringe pump (Teledyne ISCO, model 260D, Lincoln, NE, USA) was used to pressurize the unit, and CO_2 was recirculated with a magnetic drive gear pump (Micropump, GAH−T23.J9FS.Z−N1CH50, Vancouver, WA, USA). A micrometering valve (Parker Autoclave Engineers, 10VRMM2812, Erie, PA, USA) was placed at the exit of the unit, to release the CO_2 and depressurize the system in a manually controlled manner.

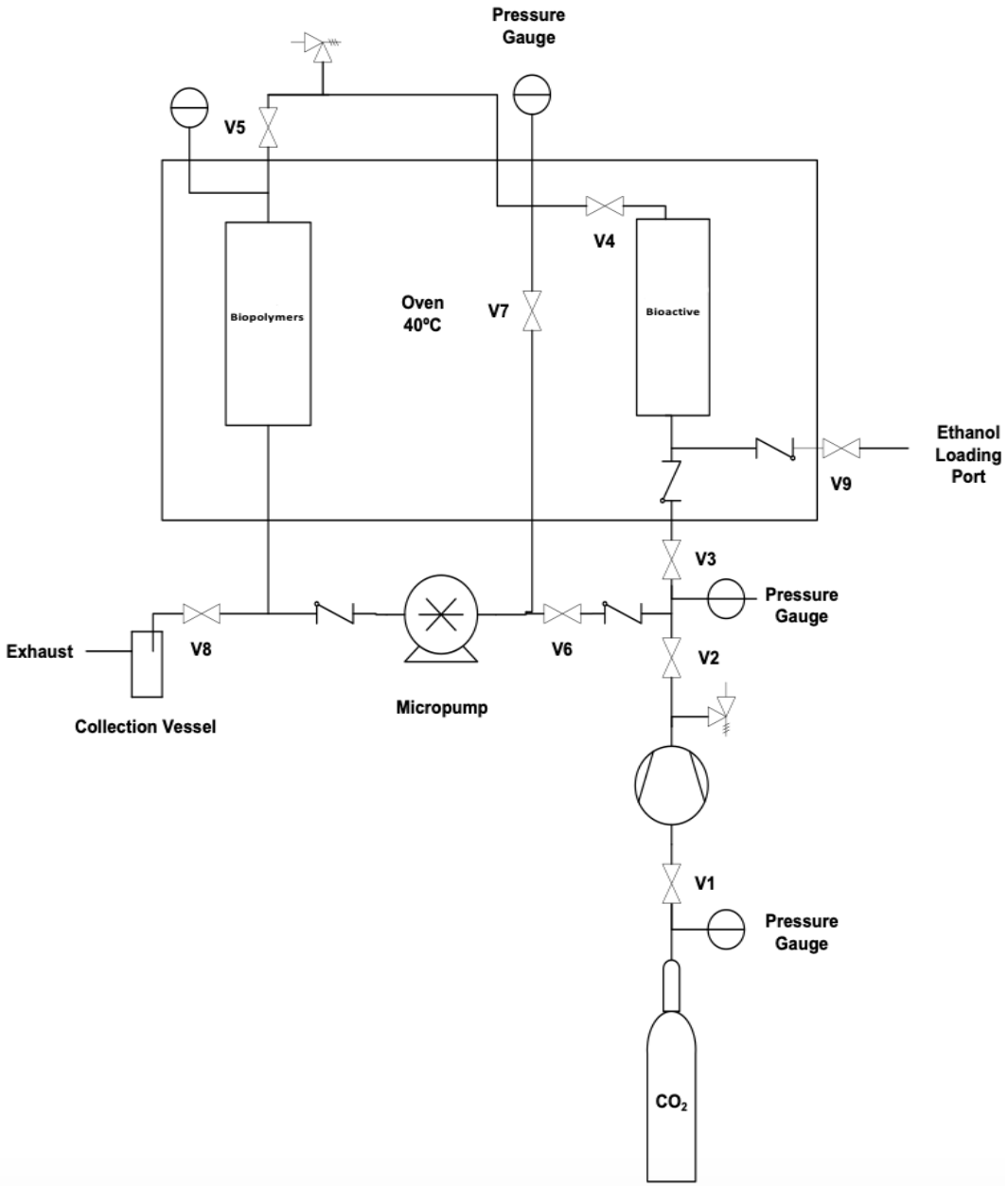

Figure 3. 1. Flow chart of the adsorptive precipitation unit.

3.2.3. Adsorptive precipitation protocol

The VitD3 sample (0.5 g) was loosely packed between felt filters (polyester felt, pore size 2.5 μm, McMaster-Carr, Aurora, OH, USA) in the bioactive vessel; whereas, the PGX-processed GA (0.5 g) was loosely packed in a glass tube (11 mm diameter, 2.5 mm wall thickness, and 110

length) with felt filters on the top and bottom of the glass tube. An o-ring was placed outside the top of the glass tube to ensure that the CO_2 would flow through the glass tube once it is placed inside the vessel. The PGX-processed SA was ground by using an herb grinder (zinc alloy designed with 4 pieces and 3 chambers with a mesh screen for fine filtering, and 24 diamond-shaped teeth, Ohuhu, CA, USA) to break up its long strands because it was difficult to pack into the biopolymer vessel in a uniform manner. Finally, the same procedure was followed for PGX-processed GA.

The unit was operated following the one-step mode according to Couto et al. (2018). Briefly, after the temperature was stabilized, the $VitD_3$ vessel was isolated from the rest of the system by closing the valves V3 and V4, and a syringe pump pressurized CO_2 until the system reached the targeted pressure. CO_2 was recirculated with the micropump for 20 min to achieve thermal equilibrium. The valves used to isolate the $VitD_3$ vessel were opened, and the unit was allowed to reach the target pressure value again. Then, V7 was closed to allow CO_2 to be recirculated from top to bottom in the $VitD_3$ vessel for CO_2 to be loaded with $VitD_3$ and passing from bottom to top in the biopolymer vessel for the adsorption of $VitD_3$ onto the biopolymer. At the end of the targeted adsorption time, the micropump was turned off, the biopolymer vessel was isolated by closing valves V5, V6 and V8, and then depressurized through the micrometering valve, resulting in the precipitation of $VitD_3$ solubilized in SC-CO_2 onto the biopolymer.

3.2.4. Experimental design

According to Johannsen and Brunner (1997), the solubility of $VitD_3$ in SC-CO_2 was in the range of 4.0 to 44 g/kg, corresponding to 0.46×10^{-3} to 5.2×10^{-3} mole fraction within the temperature and pressure ranges tested, 40-80 ^{o}C and 200-350 bar, respectively. Considering the limitations of the unit, all experiments were performed at 50 ºC and 300 bar to maximize the solubility of $VitD_3$ in SC-CO_2, based on the results obtained by Johannsen and Brunner (1997).

Under these selected conditions, VitD$_3$ solubility in SC-CO$_2$ was 9.1 g/kg (Johannsen and Brunner, 1997). The CO$_2$ flow rate used to pressurize the system initially was kept constant to achieve a pressurization rate of 15 bar/min to minimize compaction of the of PGX-processed biopolymer powder bed, and the final depressurization rate was maintained between 130 to 150 bar/min (resulting in a total depressurization time of 1 to 2 min), according to Couto et al. (2018), to improve the precipitation step and increase loading. The parameters tested in this study were different recirculation times (30, 45, and 60 min) and recirculation flow rates (135, 190, 250 mL/min) for both biopolymers. Micropump calibration was performed using ethanol to achieve targeted flow rates. Each experiment was performed in duplicate.

3.2.5. Sample characterization

The VitD$_3$ content loaded onto PGX-GA or PGX-SA was measured by UV spectrometry (FLAME-S-XR1-ES Assembly from 200-1050 nm, Ocean Optics, Dunedin, FL, USA) at the wavelength of 265 nm. A sample of PGX-GA or PGX-SA (20 mg) loaded with VitD$_3$ (L-GA or L-SA) was dissolved in hexane (10 mL) by manual agitation and soaked at ambient conditions for 10 min to solubilize the vitamin. Then, the mixture was filtered using a 0.45 μm pore size syringe (Whatman, Mississauga, ON, Canada) and the supernatant was used for the UV measurement with additional dilutions performed as necessary for each sample. Calibration curve was established by preparing a stock solution with further dilutions of known concentrations in order to have 10 points within the range of 0.02 - 0.23 mg/mL. The calibration curve was prepared in duplicate with R^2 values of 0.997 and 0.995. The VitD$_3$ loading was calculated, according to Eq. (3.1).

$$VitD_3\ loading\ (\%) = \frac{Mass\ of\ VD_3}{Mass\ of\ L{-}GA\ or\ L{-}SA} \times 100 \qquad (3.1)$$

The morphology of PGX-GA and PGX-SA, L-GA and L-SA, a physical mixture (PM) of VitD$_3$ and biopolymer at 50% (w/w) and pure VitD$_3$ were analyzed by using Zeiss Orion Helium

Ion Microscope (Ostalbkreis, BW, Germany), located at NanoFab, University of Alberta. Secondary electrons were collected at 30 kV accelerating voltage and 1.5 pA beam current. Moreover, an electron flood gun was used to neutralize positive charges on the surface of the samples that made it possible to directly take images of insulating materials without coating.

Fourier-transform infrared (FTIR**)** analysis of PGX-GA and PGX-SA, L-GA and L-SA, PM of $VitD_3$ and biopolymer at 50% (w/w) and pure $VitD_3$ were performed by using Nicolet iS50 spectrometer (ThermoFisher Scientific, Waltham, MA, USA) equipped with a built-in Attenuated Total Reflection (ATR) crystal. The analysis of each sample was performed in duplicate with 64 scans per sample (Data analysis software).

X-ray diffraction (XRD) of PGX-GA and PGX-SA, L-GA and L-SA, PM of $VitD_3$ and biopolymer at 50% (w/w) and pure $VitD_3$ were examined by using Bruker D8 Discover diffraction system (Bruker, Billerica, MA, USA), located at NanoFab, University of Alberta, and equipped with Cu-source and high throughput LynxEYE 1-dimensional detector. A voltage of 40 kV and 30 mA scanned from 5 to 80° at 5° 2θ per min were employed for the measurements. Data were analyzed by using JADE 9.6 software.

Differential scanning calorimetry (DSC) was employed to evaluate the thermal behaviors of PGX-GA and PGX-SA, L-GA and L-SA, PM of $VitD_3$ and biopolymer at 50% (w/w) and pure $VitD_3$ by using a DSC Q2000 system (TA Instruments, Mississauga, ON, Canada) calibrated with indium standards. An empty aluminum pan was used as the blank and each sample (5 mg) was placed into an aluminum pan for measurement. The measurements were performed at the heating rate of 5 °C/min from 5 to 160 °C, with a modulation of +/-1.00 °C every 60 s^{-1}. Data were interpreted by using Advantage software.

Storage stability of the samples obtained at the best experimental conditions was performed by storing the samples at 4 °C for one month. Every 6 to 7 days, a sample of 20 mg was soaked in 10 mL hexane to extract $VitD_3$ for 10 min. Then, the supernatant was analyzed by UV spectrometry as described above for the determination of $VitD_3$ loading content.

In vitro release of $VitD_3$ was studied by placing the vitamin-loaded biopolymers in simulated intestinal fluid (SIF) (pH 6.8) according to Zhao et al. (2017) with some modification. SIF was prepared with sodium hydroxide (44.8 mg/mL), potassium dihydrogen phosphate (340 mg/mL), pancreatin (238 mg/mL), and bile salts (258 mg/mL). Digestion was performed in duplicate, and the samples were taken every 30 min for 4 h intestinal digestion. GA and SA loaded with $VitD_3$ with a loading content of 10% for L-GA, and 13.8% for L-SA (15 mg) was mixed with 2 mL of release medium in individual tubes (separate tubes prepared, corresponding to each sampling time), and incubated at 37 °C while continuously being stirred at 150 rpm in a shaker bath. At each set time point, tubes in duplicate were placed in a 95 °C water bath for 3 min to inactivate the enzymes completely. All samples were transferred to specific centrifuge tubes. Ultracentrifugation at 50,000x*g* for 30 min was applied to maximize the phase separation and the supernatant was collected. Pure biopolymers were used as control to minimize the interference on the absorbance readings. Hexane extraction was performed to analyze the bioactive release, where the supernatant was mixed with 3 mL hexane for 30 min, which was then analyzed by UV spectrometry at 265 nm and absorbance was recorded with additional dilutions performed as necessary for each sample. The results were reported as percentage of the vitamin present in the starting sample that is released into the SIF at each time point.

3.2.6. Statistical analysis

All experiments and measurements at each condition were performed at least in duplicate. Two-way analysis of variance (ANOVA) was performed on loading content results to determine the effects of type of biopolymer and recirculation flow rate or time followed by comparison of the means by Tukey's multiple range test. Both analyses were performed using Minitab software package v. 17 (Minitab Inc., State College, PA, USA) at a level of significance at $p < 0.05$.

3.3. Results and discussion

3.3.1. Vitamin D_3 loading

The $VitD_3$ loading on PGX-GA and PGX-SA (provided by Ceapro Inc.) by adsorptive precipitation was obtained in two sets of experiments. In the first set, three different recirculation flow rates were tested at 300 bar, 50 ^{o}C and fast depressurization, and the results are presented in Figure 3.2. Temperature and pressure levels were selected to maximize the solubility of the $VitD_3$ in SC-CO_2. According to the two-way ANOVA results, recirculation flow rate did not have a significant effect ($p>0.05$) on $VitD_3$ loading but the effects of the type of biopolymer and the flow rate*type of polymer interaction were significant ($p<0.05$) (Fig. 3.2). The $VitD_3$ loading levels on SA were similar at all three flow rates, but the loading on GA obtained at 190 mL/min of recirculation flow rate during the adsorptive precipitation process was significantly higher ($p<0.05$) than those obtained at the other flow rates tested. At the higher recirculation flow rate, more CO_2 is passing through the bioactive vessel, dissolving and carrying more of the vitamin to the biopolymer vessel. However, the different effects of the recirculation flow rate for the two biopolymers could be related to the possibly different interactions between the $VitD_3$ and the PGX-processed biopolymers. Except for the recirculation flow rate of 190 mL/min, the loading amount on SA was significantly higher ($p<0.05$) than that on GA (overall mean of 13.8% vs 10.1%), which

can be associated with the difference in the surface areas of the biopolymers. The surface area was determined as 65 m_2/g for GA and 164.5 m_2/g for SA in other parallel studies using the same lots of biopolymers by Couto et al. (2020) and Liu (2019), respectively. According to Couto et al. (2020), who loaded PGX-GA with co-enzyme Q10 (CoQ10) by adsorptive precipitation, the recirculation flow rate applied was 85 mL/min in order to reduce clumping of particles; however, clumping of GA or SA particles was not observed in this study.

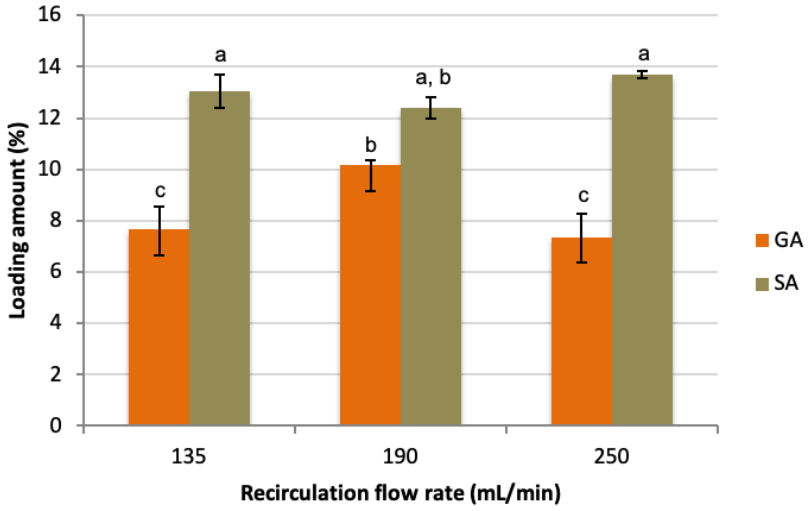

Figure 3. 2. $VitD_3$ loading on PGX-GA and PGX-SA obtained at different recirculation flow rates at 300 bar, 50 ^oC, and fast depressurization.
a, b, c Different letters for loading amounts indicate a significant difference between the mean values ($p < 0.05$).

In the second set of experiments, the recirculation flow rate was kept constant at 190 mL/min for GA, and 250 mL/min for SA, considering the slightly higher loading obtained at this flow rate for SA, in addition to the other parameters mentioned in the first set of experiments, and three different recirculation times were tested as shown in Figure 3.3. The loading of $VitD_3$ on GA increased significantly ($p<0.05$) from 5.2 ± 0.4 to 10.1 ± 0.2% with an increase in recirculation time from 30 to 45 min but did not change with a further increase to 60 min. For SA, the loading of 13.8 ± 0.1% at 45 min was slightly higher than those at other recirculation times. GA processed

by PGX and adsorptive precipitation in this study showed 60% higher loading of $VitD_3$ compared with the GA processed by spray drying as reported by Jafari et al. (2019). Again, the $VitD_3$ loading on SA was significantly ($p<0.05$) higher than that on GA (overall mean of 13.8% vs 10.1%), and the higher loading of $VitD_3$ on SA could be associated with the increased surface area due to the grinding of the original structure of the particles. Based on two-way ANOVA results, both recirculation time and type of biopolymer as well as their interaction (time*type of polymer) had significant effects ($p<0.05$) on $VitD_3$ loading. Overall, loading increased significantly ($p<0.05$) with an increase in time from 30 to 45 min but loadings obtained at 45 and 60 min were similar.

Couto et al. (2017), who investigated the adsorptive precipitation of CoQ10 on PGX-processed β-glucan, also reported a similar trend with 45 min recirculation time being the best time to maximize loading, which indicated that SC-CO_2 carried the $VitD_3$ during the recirculation step with good access to the pores of the biopolymer powder until the biopolymer reached the highest level of adsorption and saturation. At the end of each experiment, there was residual $VitD_3$ in the bioactive vessel, confirming that there was excess bioactive in the system throughout the run time. It was demonstrated that at the levels tested the recirculation flow rate was not a significant parameter for vitamin loading content; however, time had a significant effect on loading.

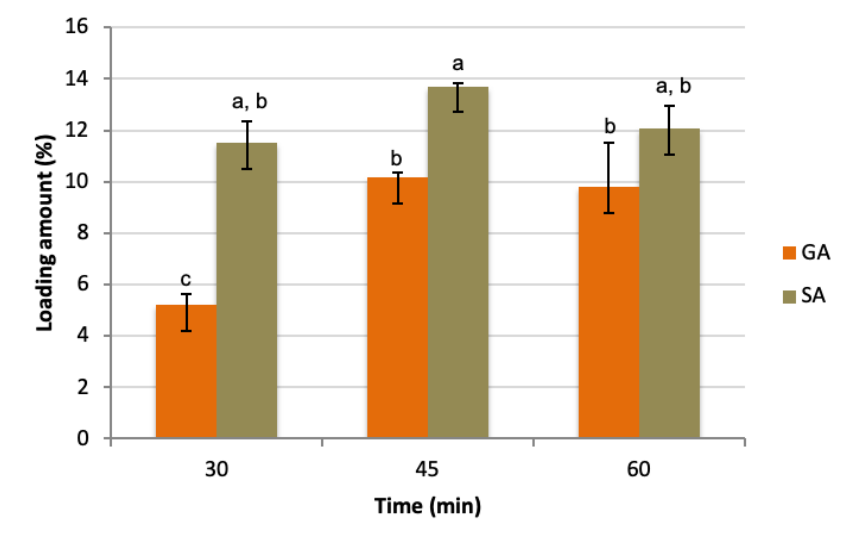

Figure 3. 3. VitD3 loading on PGX-GA and PGX-SA obtained at different recirculation times at 300 bar, 50 oC, fast depressurization, and recirculation flow rate of 190 mL/min for GA, and 250 mL/min for SA.
a, b, c Different letters for loading amounts indicate a significant difference between the mean values ($p < 0.05$).

For comparison, Bostan and Ghaitaranpour (2019) reported co-encapsulation of VitD3 and calcium for food fortification using sonication, emulsions and spray-drying technologies and obtained an encapsulation efficiency (EE), as the percentage of drug that is successfully entrapped into the micelle or nanoparticle and EE% is calculated as (total drug added – free non-entrapped drug)/total drug added) between 79-90% based on 0.2% of VitD3 loading, which was low VitD3 used than this study. Pantić et al. (2016a) reported alginate aerogels impregnated with 0.052 g VitD3/g aerogel that was 60% less than the loading of VitD3 on SA obtained in this study by the adsorption precipitation process. Pantić et al. (2016b) used low and moderate temperatures (subcritical and supercritical regions) to impregnate VitD3 onto alginate aerogels with a concentration ratio of 1:10 and the highest loading was obtained under subcritical region at 25 oC (0.069 VitD3/g aerogel), which was less than 50% of the loading obtained in this study. Moreover, Luo et al. (2012) reported an encapsulation efficiency of 52.2% for zein as a single encapsulant, and 87.9% for zein nanoparticles coated with carboxymethyl chitosan. They used 1 mg/mL VitD3

content for particle formation, resulting in a low loading of 1.7% to 3.9%. In addition, the loading encapsulated $VitD_3$ on oleoyl alginate ester nanoparticles were between 45.8±1.55 to 67.6±2.76%, using vitamin concentration of 5 to 20 μg/mL to produce the nanoparticles; however, low $VitD_3$ loading capacity was achieved at 0.33 ± 0.02 to 0.91 ± 0.03% (Li et al., 2011). Based on the comparison with these previous studies employing other techniques, the adsorptive precipitation technique used in this study resulted in high loading content of $VitD_3$.

The loading content of $VitD_3$ can also be reported by considering the amount of $VitD_3$ per unit surface area of the biopolymer powders, considering the different surface areas for GA and SA as previously mentioned. At the best processing conditions, 3.23 mg $VitD_3/m_2$ PGX-GA and 4.38 mg $VitD_3/m_2$ PGX-SA could be loaded, highlighting the differences in the level of interactions between $VitD_3$ and the two biopolymers.

3.3.2. Morphology

The morphology of the loaded L-GA and L-SA particles were assessed using helium ion microscopy and the HIM images are presented in Figure 3.4. The image of the pure $VitD_3$ (Fig. 3.4 (a)) showed large clusters due to its crystalline nature and the image of the physical mixtures (Figs. 3.4 (b, c)) showed no distribution of the $VitD_3$ on the surface of the biopolymers and distinct $VitD_3$ clusters were apparent. There was no major difference in the images between the analyzed samples, regardless of the different processing parameters applied. Similar to the previous reports, the morphology of PGX-GA (Fig. 3.4 (d)) was agglomerated spherical nanoparticles (Couto et al., 2018) as opposed to the fibrous form of PGX-SA (Fig. 3.4 (g)) (Liu, 2019). Comparison of PGX-GA (Fig. 3.4 (d)) to the L-GA (Fig. 3.4 (e, f)) showed that the L-GA had a homogeneous distribution of $VitD_3$ on the surface of GA, without distinct $VitD_3$ clusters even though there was some agglomeration of the $VitD_3$ in specific areas, which could be related to the precipitation step.

Similar uniform distribution of VitD3 throughout the surface of L-SA was also apparent in Figs. 3.4 (h, i). Based on the loading results (Figs. 3.2, 3.3), SA showed higher loading and therefore more intense distribution throughout its larger surface area. There are no similar results to compare in the literature with VitD3 and the biopolymers used in this study. However, loading of CoQ10 using adsorptive precipitation on the same PGX-dried biopolymers was reported by Couto et al. (2018) for GA, and by Liu (2019) for SA. Even though they used similar biopolymers but loaded with different bioactives, their HiM results also presented uniform distribution on the surface of particles.

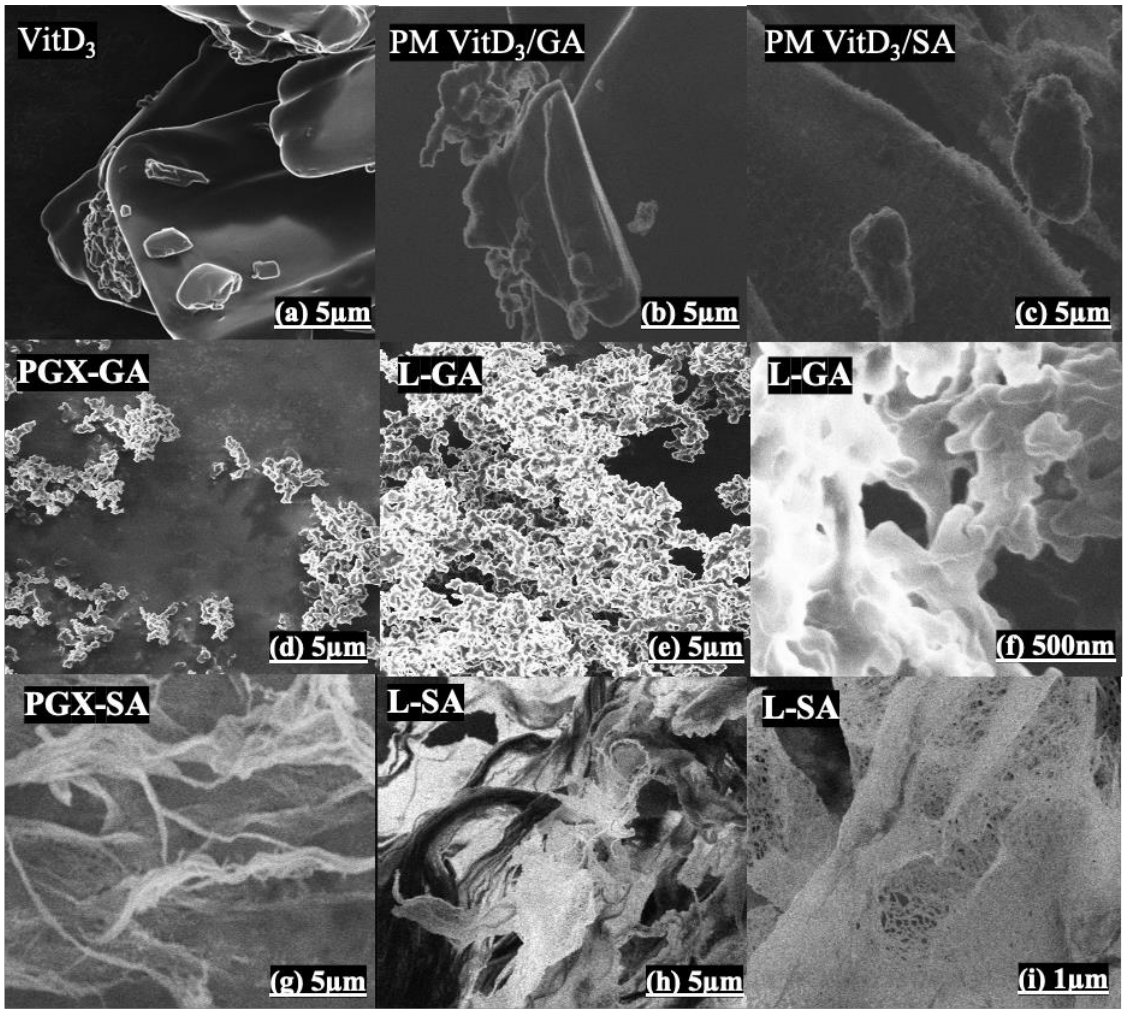

Figure 3. 4. HIM images (a) VitD3, (b) PM of VitD3 and GA at 50% (w/w), (c) PM of VitD3 and SA at 50% (w/w), (d) PGX-GA, (e) L-GA (at 190 mL/min), (f) L-GA (at 190 mL/min), (g) PGX-SA, (h) L-SA (at 250 mL/min) and (i) L-SA (at 250 mL/min) during 45 min.

3.3.3. Fourier-transform infrared (FTIR)

ATR-FTIR analysis was performed to evaluate the interactions between the $VitD_3$ and the biopolymers. Figure 3.5 showed the spectra of the pure $VitD_3$, PGX-GA, PM, and L-GA while Figure 3.6 displayed the spectra of pure $VitD_3$, PGX-SA, PM, and L-SA. The loaded samples processed at 30, 45, and 60 min recirculation time and recirculation flow rates of 135, 190, 250 mL/min for both biopolymers showed no significant differences and therefore a representative spectrum is presented for the samples obtained at the best conditions. The infrared spectra of pure $VitD_3$ (Figs. 3.5 and 3.6) displayed a multitude of bands that were generally present in the loaded samples for both biopolymers.

The broad peak at 3300 cm^{-1} corresponds to hydroxyl group (O-H) stretching vibrations. The next small peak around 3100 cm^{-1} could be the -C-H stretching from the $=CH_2$ group. The four peaks between 3000-2800 cm^{-1} represent the C-H stretching vibration due to the aliphatic chain and these could be methyl symmetric stretching at 2960 cm^{-1}, methylene asymmetric stretching at 2930 cm^{-1}, methyl asymmetric stretching at 2870 cm^{-1}, and methylene symmetric stretching at 2850 cm^{-1}. The higher level of the presence of methyl groups resulted in strong peaks due to the symmetric and asymmetric stretching than the methylene groups. In addition, C=C stretching from the double bonds is visible in the region 2000-1500 cm^{-1}. The presence of a weak peak at 1650 cm^{-1} corresponds to the alkene double bond (C=C) stretching vibrations of the unsaturated bonds of the $VitD_3$ molecule. The peaks between 1500-1400 cm^{-1} show the C-C stretches. The peak close to 1000 cm^{-1} is typical of C-O stretching (Stuart, 2004).

The spectra of PGX-GA (Fig. 3.5) and PGX-SA (Fig. 3.6) exhibited a broad band at 3400 cm^{-1} that indicates O-H vibrations related to intermolecular hydrogen bonds. The low intensity of this band could be associated with the low water content of the PGX-dried biopolymers. Similarly,

weak bands at frequencies of 1650-1510 and 1400-1280 cm^{-1} that correspond to the asymmetric and symmetric stretching vibrations of carboxyl groups (COO-) of the glucuronic acid backbone of GA and SA were identified (Espinosa et al., 2000). Peaks were found at frequencies between 1200-920 cm^{-1} associated with the vibration of glycosidic bonds (C-O-C) (Espinosa et al., 2010; Nikonenko et al., 2000).

The peak between 3500-3000 cm^{-1} for PM was higher than that for the L-GA, demonstrating the presence of $VitD_3$. This peak (3300 cm^{-1}) indicates O-H stretching vibration (Stuart, 2004). Furthermore, the peak at 2800 cm^{-1} could be related to the C-H stretching and the intensity was higher for the PM compared to L-GA. Another peak appeared in the fingerprint region corresponding to proteins (polypeptide backbone) (Couto et al., 2020a). This peak at 1645 cm^{-1} could be associated with the C=O stretching and the next close peak at 1450 cm^{-1} could be related to C-H bending from carbonyl groups (Stuart, 2004). Sharp and intense peaks start at 1200 cm^{-1} and finish at 800 cm^{-1} in the carbohydrate fingerprint region, which were related to C-O stretching as well as C-H out of plane bending vibrations in ethylenic systems. Similar results were obtained for PM and L-SA with low intensity peaks (Fig. 3.6).

Based on the information revealed in the FTIR spectra, it appears that there was no formation of new covalent bonds, and the processed samples loaded with $VitD_3$ displayed their characteristic peaks after the adsorptive precipitation process. Certain small peaks of the $VitD_3$ were covered by the broad peak of PGX-GA and PGX-SA, due to the lower concentration of $VitD_3$ relative to the biopolymer, which could also be hiding some other characteristic peaks formed between the PGX-GA, PGX-SA and $VitD_3$. Couto et al. (2020) also showed similar results in terms of the characteristic peaks of GA loaded with CoQ10 where the adsorptive precipitation processed

sample showed no new covalent bond formation. Similar findings were reported by Liu (2019) for CoQ10-loaded SA.

The SC-CO_2 adsorption step led to strong intermolecular interactions between $VitD_3$ and the two biopolymers studied, PGX-GA and PGX-SA; however, no new covalent bond formation was evidenced by FTIR analysis, suggesting dipole-dipole interactions between hydroxyl groups of the biopolymers and $VitD_3$. As reported by Liu (2019), during PGX-processing, carboxyl groups on the SA molecules would be neutralized due to the formation of carbonic acid upon high pressure CO_2 getting in contact with water. The double bonds present in pure $VitD_3$ could be prone to interact under SC-CO_2 conditions, which favored more $VitD_3$-SA molecular interactions, resulting in higher loading on this biopolymer.

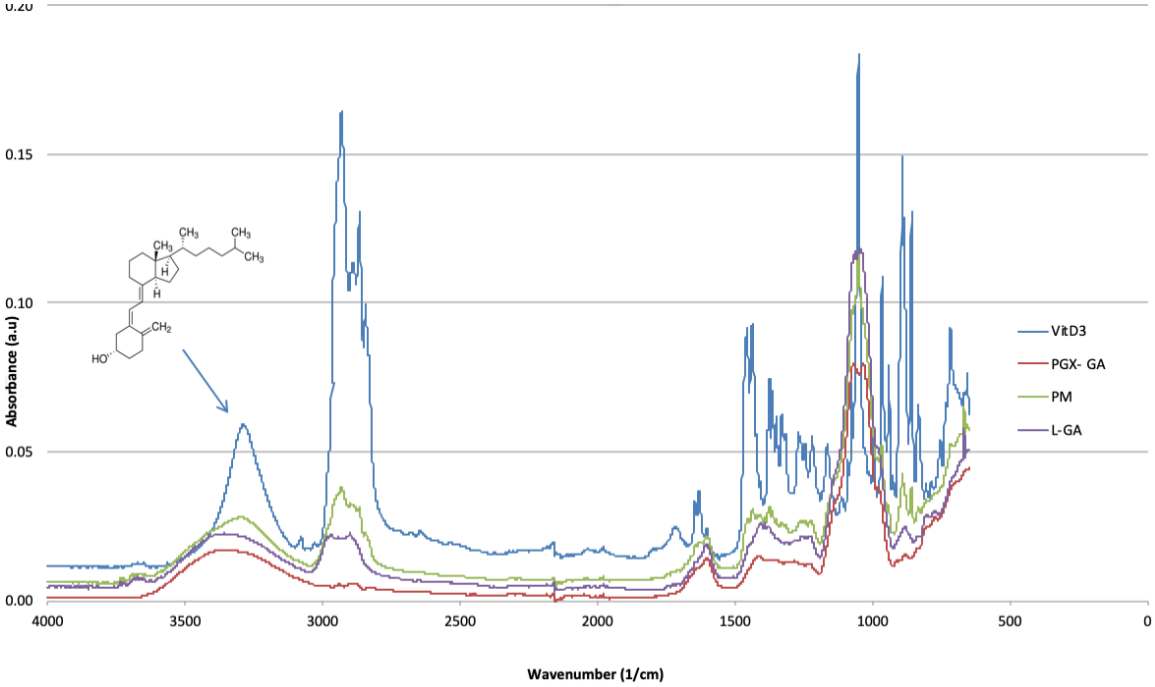

Figure 3. 5. ATR-FTIR spectra of $VitD_3$ (1,25-dihydroxycholecalciferol), PGX-GA, PM (PGX-GA and 50% of pure $VitD_3$), and L-GA (processed at 190 mL/min and 45 min).

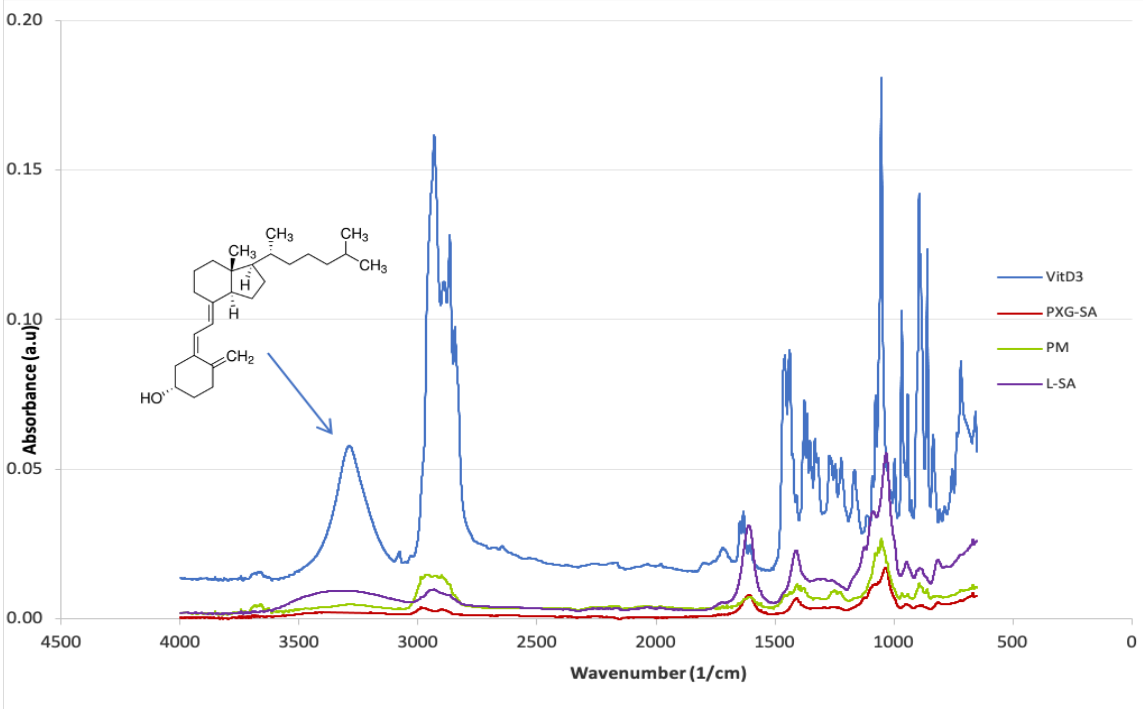

Figure 3. 6. ATR-FTIR spectra of VitD3 (1,25-dihydroxycholecalciferol), PGX-SA, PM (PGX-SA and 50% of pure VitD3), and L-SA (processed at 250 mL/min and 45 min).

3.3.4. X-ray diffraction analysis (XRD)

The crystallinity of the generated samples was assessed by XRD analysis and the spectra are presented in Figure 3.7 for GA and Figure 3.8 for SA. The XRD spectra demonstrated the crystalline nature of the pure VitD3. The L-GA sample presented a characteristic peak of VitD3 at 26.6o and the PM sample had similar peaks as the pure bioactive. This peak could indicate the presence of some level of crystallinity of VitD3 on L-GA, due to the lower surface area of GA compared to SA that allow the vitamin to interact more with itself, and it can also be related to the interactions between VitD3 and the biopolymer that does not allow crystallinity to develop on SA. However, it is also possible that some peaks may be hidden behind the broad peak of PGX-GA in between 10o -20o. On the other hand, the spectrum for L-SA (Fig. 3.8) did not show any characteristic peak that could be related with its crystalline form after the loading process. In this

study, the highest loading and surface area was associated with L-SA, which resulted in the elimination of the crystallinity of $VitD_3$, leading to its amorphous form in L-GA. Pantić et al. (2016) characterized the $VitD_3$ loaded on alginate aerogels processed by SC-CO_2 impregnation using XRD to examine the crystallinity of $VitD_3$. They found that the $VitD_3$ had a characteristic peak after the loading process. In general, the amorphous form of a bioactive compound is associated with fast dissolution, contributing to high bioavailability. Therefore, L-SA may be expected to have higher bioavailability, which needs to be demonstrated. Further research is needed to decrease the extent of crystallinity of $VitD_3$ on L-GA and obtain $VitD_3$ in its amorphous form, by possibly investigating low recirculation times to minimize the chance for crystal growth; however, this can also affect the loading content since recirculation time had a significant effect on loading of GA.

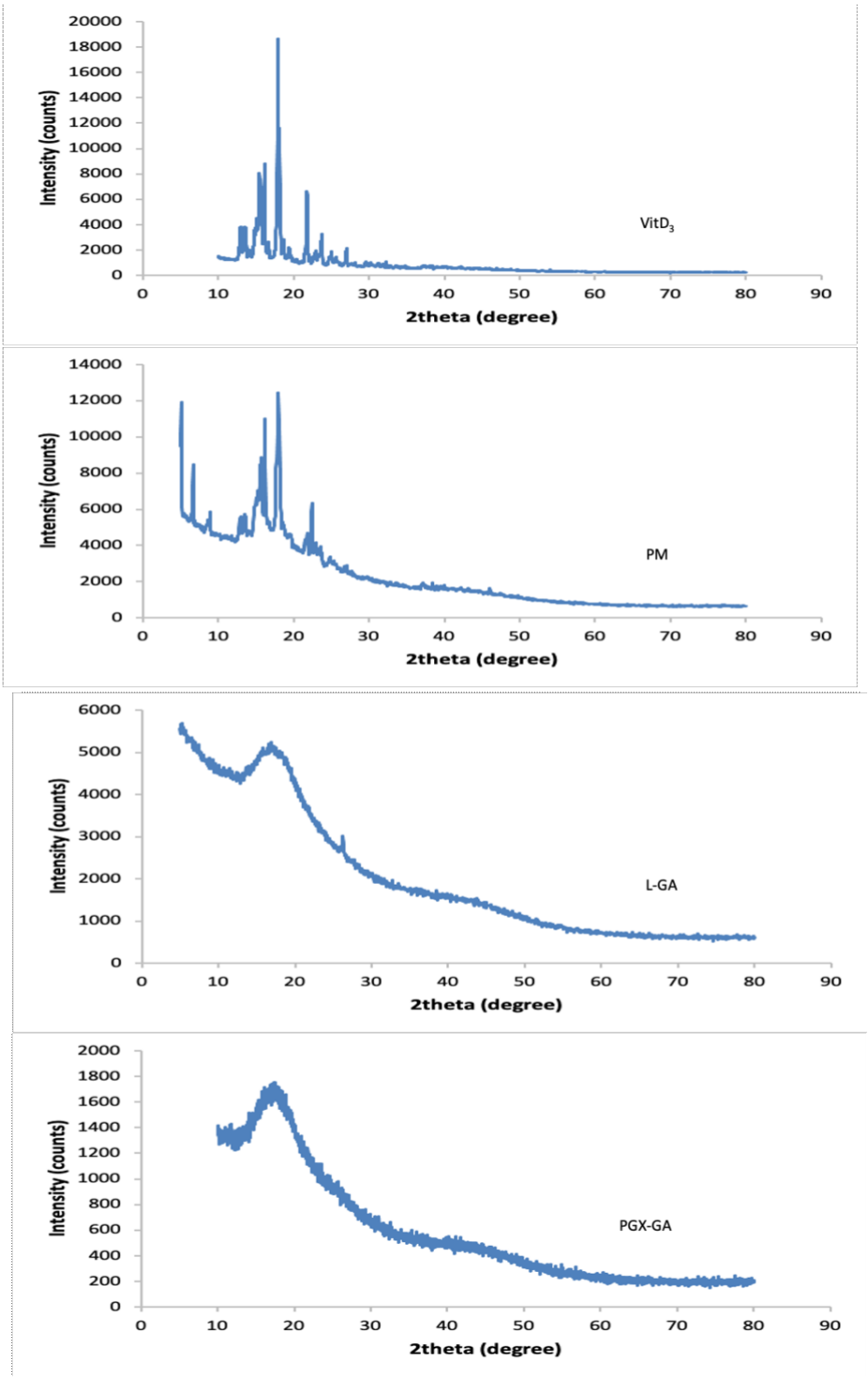

Figure 3. 7. XRD spectra (from top to bottom) of $VitD_3$, PM (PGX-GA and 50% of pure $VitD_3$), L-GA (processed at 190 mL/min and 45 min), and PGX-GA.

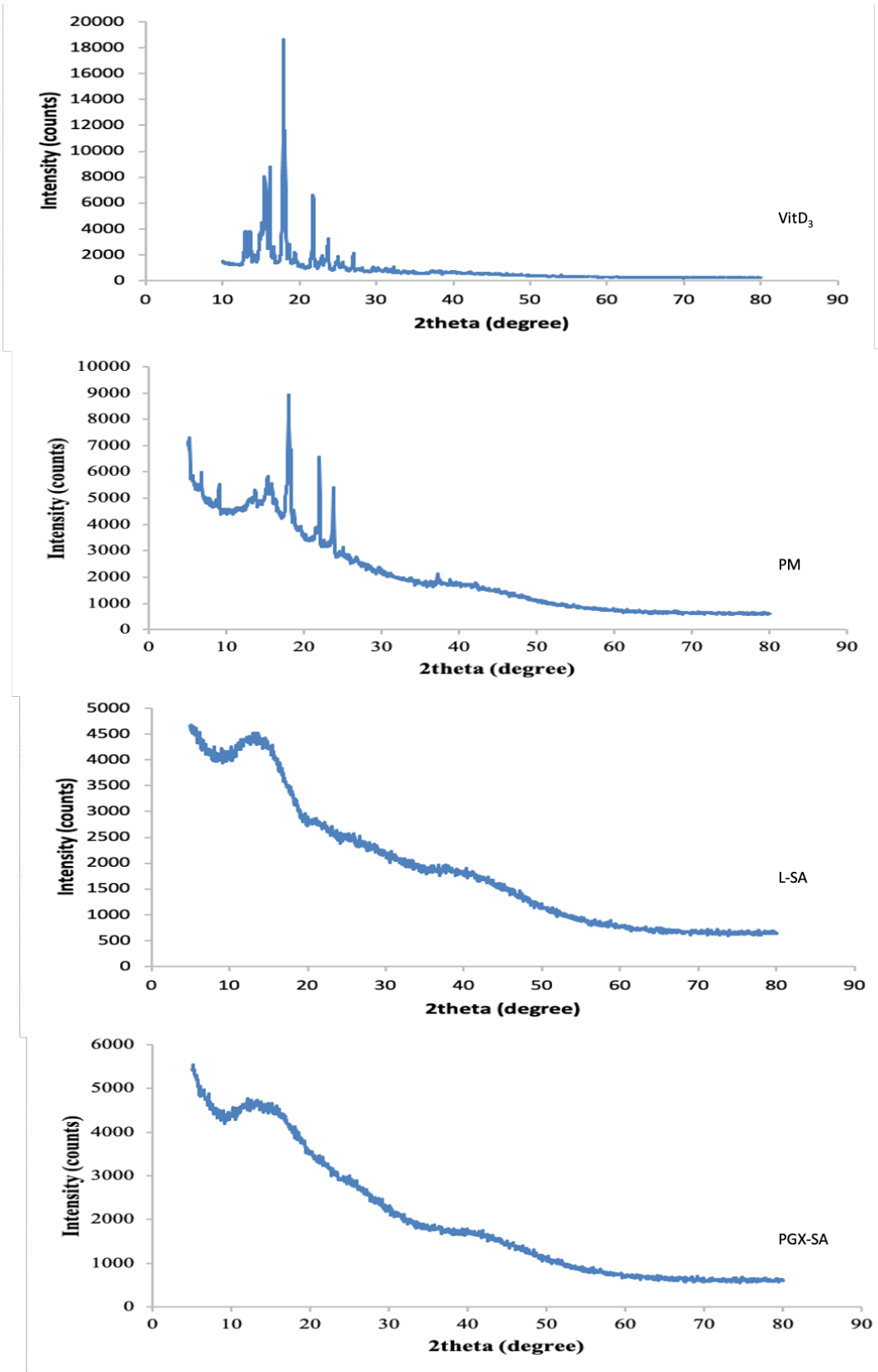

Figure 3. 8. XRD spectra (from top to bottom) of VitD3, PM (PGX-SA and 50% of pure VitD3), L-SA (processed at 250 mL/min and 45 min), and PGX-SA.

3.3.5. Differential scanning calorimetry (DSC)

The DSC analysis results were displayed in Figure 3.9 for GA and in Figure 3.10 for SA. The pure $VitD_3$ and the PM of GA and the bioactive at 50% had similar onset, offset and endothermic peak temperatures, indicating that physically mixing these two compounds did not lead to any no chemical interactions. The broader peaks of PGX-GA and L-GA were centered around the same temperature from 52 ^{o}C to 113 ^{o}C for L-GA and 52 ^{o}C to 129 ^{o}C (Fig. 3.9), which could be associated to the loss of water present in the biopolymers between 2-10 wt.% (Zohuriaan and Shokrolahi, 2004; Couto et al., 2020). However, the DSC analysis of SA demonstrated that in the case of L-SA (1) and L-SA (2), obtained at different conditions (Fig. 3.10), the peak temperatures of both loaded samples were around 90 ^{o}C. Thus, a higher amount of energy could be required to break the structure. Also, during the PGX drying process, the water is removed by using ethanol+CO_2 and the PGX-processed sample could have residual ethanol trapped in between the nanofiber particles (Couto et al., 2018). However, the sharp peak of the pure $VitD_3$ disappeared in the adsorption precipitation processed samples for both biopolymers (L-GA and L-SA), which indicated the loss of crystallinity, in agreement with the XRD results.

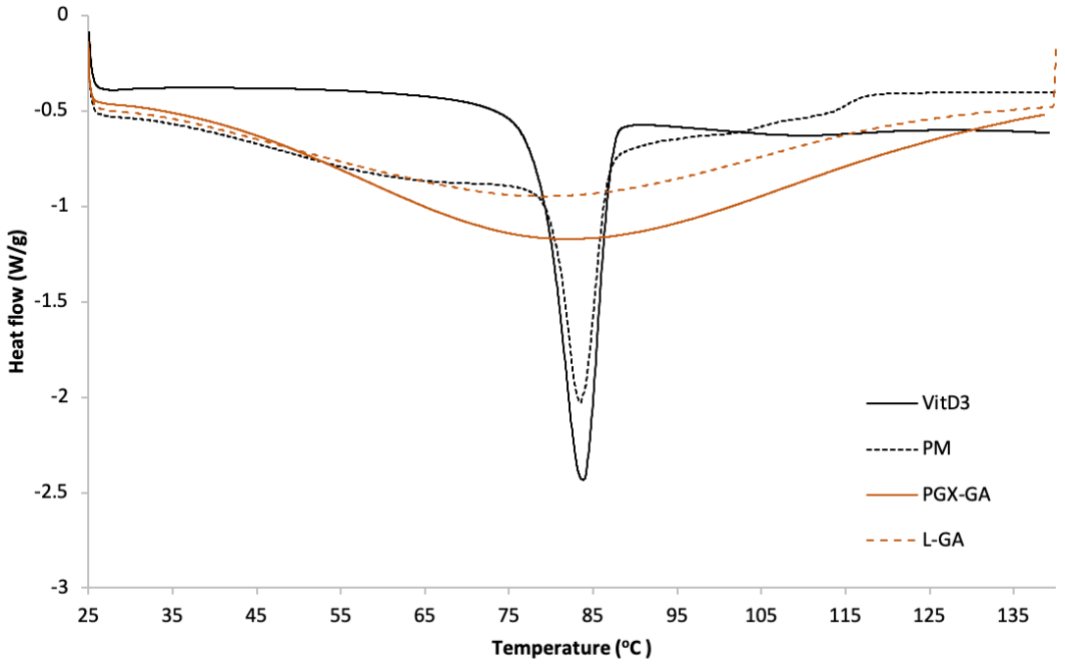

Figure 3. 9. DSC spectra of VitD$_3$, PM (PGX-GA and 50% of pure VitD$_3$), PGX-GA, and L-GA (processed at 190 mL/min and 45 min).

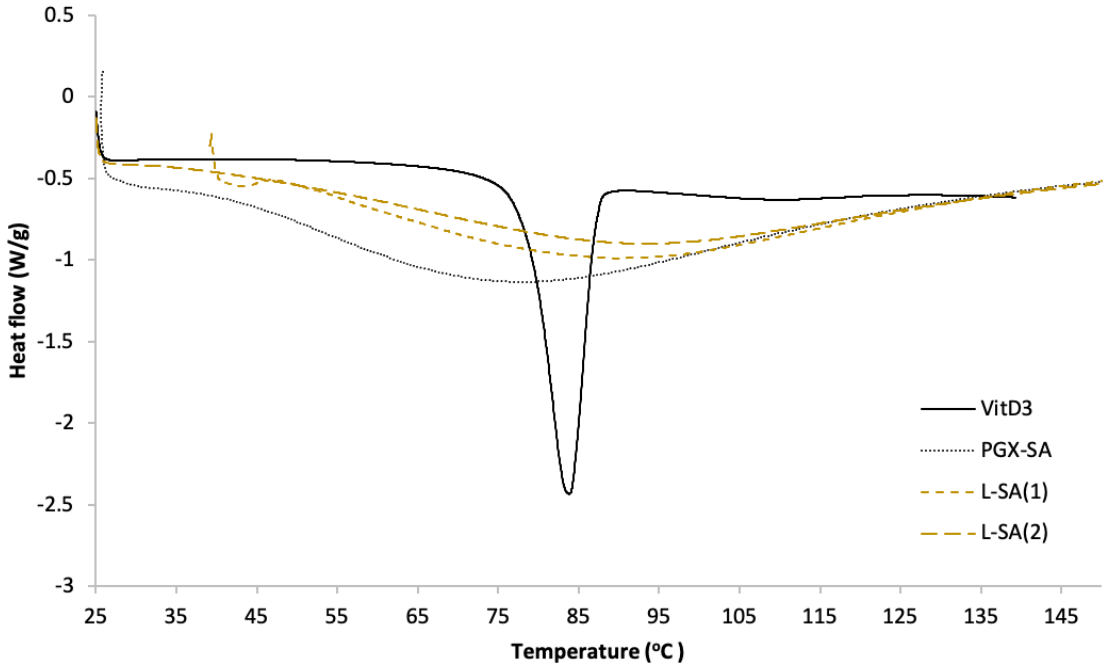

Figure 3. 10. DSC spectra of VitD$_3$, PGX-SA, L-SA (1) (processed at 250 mL/min and 45 min), and L-SA (2) (processed at 250 mL/min and 30 min).

3.3.6. Storage stability

Storage stability of VitD3-loaded L-GA and L-SA powders was tested at 4 oC for 60 days. As shown in Figure 3.11, the VitD3 content on both biopolymers showed a slight decrease after 7 days, from 100% to 93% for L-GA and to 95% for L-SA. The VitD3 content continued to decrease with time but L-SA stabilized after 21 days at 82%, and L-GA stabilized after 28 days at 80% with no further change up to 60 days. The decrease in VitD3 loading over time could be associated to the large surface area of the biopolymers, where the vitamin outside the pores of the biopolymer may start to degrade.

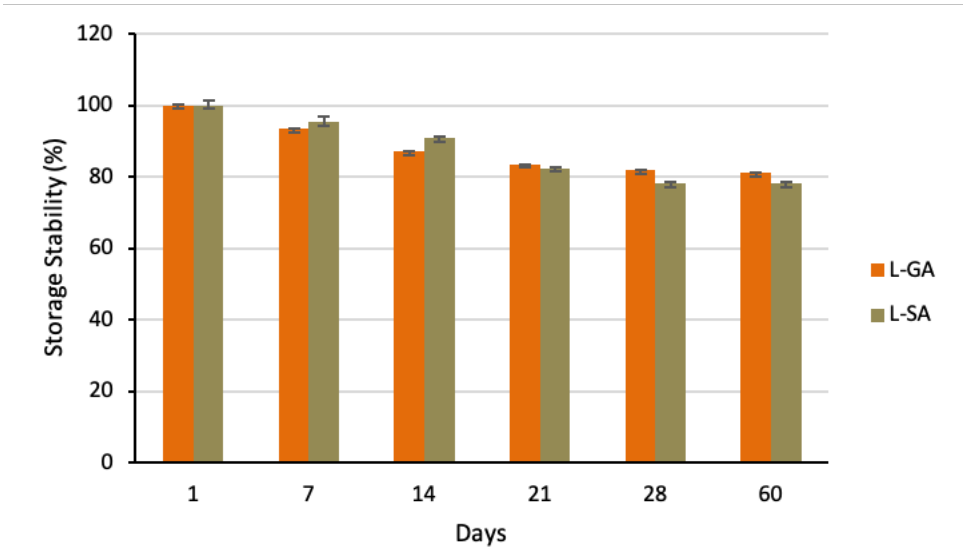

Figure 3. 11. Storage stability of L-GA processed at 190 mL/min and 45 min, and L-SA processed at 250 mL/min and 45 min.

3.3.7. Release kinetics

VitD3 release profiles from the L-GA and L-SA were analyzed using pancreatin (a mixture of amylase, lipases, trypsin and chymotrypsin) as the enzyme source for the hydrolysis of loaded samples and release in a simulated intestinal fluid (SIF) environment. The samples analyzed had a VitD3 loading content of 10.1% for L-GA and 13.8% for L-SA. The release profile of L-GA

showed sustained release of $VitD_3$ of up to 18.6% (percentage of total vitamin available on the sample used) in SIF (Fig. 3.12) from the first hour until the end of the 4 h intestinal digestion period. However, only 14% of the $VitD_3$ present in L-SA was released in the first 30 min, which was decreased to 8.7% after 120 min and then dramatically decreased to 3.6% by 240 min. The difference in the release profiles could be related to the nature of the biopolymers, the extent of interactions between the biopolymer and $VitD_3$ and degradation of the bioactive within the SIF environment.

For comparison, the same release kinetics test was also performed with the pure $VitD_3$ to demonstrate how much of the vitamin is dispersed in the SIF environment, considering its crystalline nature. After 4 h of incubation, the release of the pure bioactive was up to just 1%. With a sustained release of 18.6%, L-GA showed great potential as a delivery system for $VitD_3$, which is anticipated to increase its bioavailability. Several studies reported the release of $VitD_3$ from different carriers and with the use of the same enzymes in the SIF. Amphiphilic chitosan was described as a sustained release delivery system by Li et al. (2014), similar to the L-GA system observed in this study. The release of $VitD_3$ from zein (a maize prolamine protein) nanoparticles coated with carboxymethyl chitosan with a loading content of 1.7-3.9% showed an initial burst followed by the sustained release with a maximum value of 40% (Luo et al., 2012). Ovalbumin-pectin particles loaded with $VitD_3$ at a level of 1.93% resulted in a maximum release of 96.37% (Xiang et al., 2020). The maximum release values reported in all of these studies were dependent on the conditions of the medium employed.

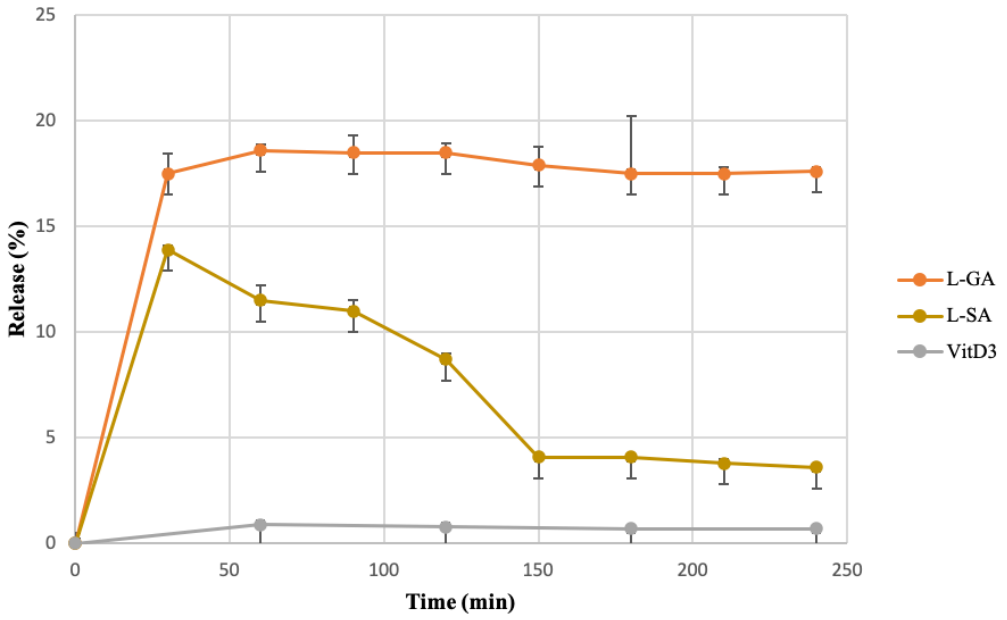

Figure 3. 12. Release kinetics of L-GA processed at 190 mL/min and 45 min, L-SA processed at 250 mL/min and 45 min, and pure $VitD_3$.

3.4. Conclusions

The adsorptive precipitation process was demonstrated to be a successful method to load $VitD_3$ on biopolymers. Even though recirculation flow rate did not have a significant effect, the type of biopolymer and flow rate*type of polymer interaction effects had a significant effect ($p<0.05$) on loading of $VitD_3$. In addition, loading of $VitD_3$ was significantly ($p<0.05$) affected by recirculation time, type of biopolymer and their interaction. The higher loading of 10.1 ± 0.2% was obtained at 190 mL/min and 45 min for GA, and for SA the loading was 13.8 ± 0.1% at 250 mL/min and 45 min. Helium ion microscopy demonstrated homogeneous coating on the surface of the biopolymer particles resulting from the solubilization of $VitD_3$ in SC-CO_2 first followed by adsorptive precipitation on the biopolymer during the process. The $VitD_3$ loaded onto GA maintained some crystalline form, whereas no crystallinity was observed when it was loaded onto SA. After an initial drop of $VitD_3$ loading content, both loaded biopolymers demonstrated storage

stability after 21 days for L-SA and after 28 days for L-GA samples for up to 60 days. Sustained release was demonstrated for L-GA sample, but the release of $VitD_3$ from L-SA was low, which can be associated to the nature of the biopolymers and the nature of interactions between $VitD_3$ and biopolymer. SA could have stronger interaction with the $VitD_3$ than GA due to more charged nature of the SA. The findings demonstrate that the adsorptive precipitation is a potential process for loading of $VitD_3$ on gum arabic and on sodium alginate as a delivery system, targeting different aqueous-based applications.

Chapter 4. Adsorptive precipitation of vitamin E on gum arabic and alginate dried using Pressurized Gas eXpanded (PGX) liquid technology

4.1 Introduction

Vitamins are necessary for the maintenance of biochemical reactions in the cells of the human body. Vitamins should generally be obtained from the diet. Although present in many foods, vitamin deficiencies still exist in many countries and population groups. The reason for this is not always insufficient food intake, but it can also be an unbalanced diet. Together, food processing and cooking can destroy or remove some of the vitamins normally present in a food (Walther and Schmid, 2017).

Vitamin E (VitE) plays a fundamental role in the normal metabolism of all cells. For this reason, their deficiency can affect different organ systems. Its function is related to those of several other nutrients and endogenous factors that collectively comprise a multi-component system, which provides protection against the potentially harmful effects of reactive oxygen species formed during metabolism or found in the environment (Combs and McClung, 2017). VitE is defined as the collective of tocopherol and tocotrienol isomers, which are fat-soluble vitamins and show powerful antioxidant activity through their lipoperoxyl radical removal properties (Ahsan et al., 2015). An important role of VitE focuses on its antioxidant properties (Zingg, 2007). Some additional benefits of VitE are related to fertility and the development of tissues and organs. The recommended dose of VitE is equivalent to 22 IU (international units) of natural source VitE per day, or 33 IU from synthetic sources (Health Canada, 2006).

The applications of VitE in aqueous-based food systems are limited, as it degrades rapidly in the presence of oxygen and oxidative processes by free radicals (Anandharamakrishnan and

Ishwarya, 2015). In order to improve the dispersion of hydrophobic vitamins in aqueous systems, such as VitE, biopolymers have been used as carrier materials, which represent a possible solution for incorporating vitamins into food products like the use of gum arabic (GA) and sodium alginate (SA) described in Chapter 2.

Pressurized gas expanded (PGX) liquid technology was used to process the biopolymers to be used as carriers for $VitD_3$ in the previous study described in Chapter 3. In this study, the same PGX-GA and PGX-SA are used as carriers for VitE in an effort to expand the knowledge on different bioactive-biopolymer combinations and understand differences in their behavior.

Adsorptive precipitation technology described in Chapter 2 was also implemented in this study to load the VitE on the biopolymer carriers. Even though this technology has been investigated to a greater extent for drug delivery systems, its use has been limited in the loading of bioactive compounds on food-grade biopolymers, and there is a lack of information for the loading of VitE on delivery systems targeting food applications. Therefore, the main objective of this study was to determine the effect of processing parameters such as recirculation time (30, 45 and 60 min) and recirculation flow rate (135, 190 and 250 mL/min) on the loading of VitE on PGX-GA and PGX-SA by the adsorptive precipitation process and to characterize the particles obtained in terms of their VitE loading content, particle morphology, molecular interactions, thermal behaviours, storage stability, release kinetics, and adsorption kinetics.

4.2. Materials and Methods

4.2.1. Materials

Vitamin E (±-α-tocopherol synthetic) (≥96% purity) (HPLC) was purchased from Sigma-Aldrich (Oakville, ON, Canada)**.** Gum arabic from acacia tree was purchased from Fisher Scientific (Ottawa, ON, Canada). PGX-GA was supplied by Ceapro Inc. (Edmonton, AB, Canada)

(July 2018 batch, obtained at 100 bar, 40 ^{o}C, 20% w/w aqueous solution, and flow rates of 22.5 g/min for aqueous solution, 45 g/min ethanol and 15 g/min for CO_2. Alginic acid sodium salt powder extracted from brown algae was purchased from Sigma-Aldrich (Oakville, ON, Canada). PGX-SA was provided by Ceapro Inc. (Edmonton, AB, Canada) (March 1, 2019 and January 31, 2020 batches obtained at 100 bar, 40 ^{o}C, 1.0% w/w aqueous solution, and flow rates of 40 g/min aqueous solution, 150 g/min ethanol, and 50 g/min CO_2). CO_2 (99.9% purity) was purchased from Praxair Canada Inc. (Mississauga, ON, Canada). For the release kinetics test, sodium hydroxide (≥98% purity), potassium phosphate monobasic (ACS reagent grade, ≥99% purity), bile salts for microbiology, and pancreatin from porcine pancreas were purchased from Sigma-Aldrich (Oakville, ON, Canada).

4.2.2. Adsorptive precipitation protocol

The adsorptive precipitation unit was previously described in Chapter 3. However, the bioactive vessel was modified for VitE because it was in liquid state as opposed to the powder form of $VitD_3$. The new vessel was a high-pressure vessel closed at the bottom with a small inlet tube inside, extending to the bottom that allowed the passage of CO_2 from bottom to the exit on top. Approximately 1 g of VitE was placed on five felt filters (polyester felt, pore size 5 μm, McMaster-Carr, Aurora, OH, USA) to hold the liquid VitE and another three clean filters were placed on top to avoid any carry over of the vitamin without being solubilized. A whole was punched in the middle of the filters so that they could be stacked around the CO_2 inlet line inside the vessel. The sample preparation and placement of the biopolymers in the vessel were similar to that described in Chapter 3. The same operational protocol described in Chapter 3 (Section 3.2.3) for $VitD_3$ was also followed in this study for VitE.

4.2.3. Experimental design

Based on the results obtained by Johannsen and Brunner (1997), the maximum solubility of VitE in SC-CO_2 was 33.9 g/kg at 60 ^oC and 350 bar. The solubilities measured were in the range of 6.2 to 33.9 g/kg, corresponding to 0.64×10^{-3} to 3.57×10^{-3} mole fraction within the temperature range of 40-80 ^oC and pressure range of 200-350 bar. In this study, all experiments were performed at 50 ºC and 300 bar in order to maximize the solubility of the VitE in SC-CO_2 (25.3 g/kg) within the maximum operating limits of the unit. The parameters examined in this study were recirculation time (30, 45, and 60 min) and recirculation flow rate (135, 190, 250 mL/min) for both biopolymers (PGX-GA and PGX-SA). Each experiment was performed in duplicate.

4.2.4. Sample characterization

The determination of VitE loading by UV spectrometry at the wavelength of 297 nm, analysis of morphology by Zeiss Orion Helium Ion Microscope (HiM), molecular interactions by Fourier-transform infrared (FTIR) spectroscopy, thermal behavior by differential scanning calorimetry (DSC), storage stability, and release kinetics of VitE were performed following the same protocols described in Chapter 3 (Section 3.2.5) for the PGX-GA and PGX-SA as well as the VitE loaded samples of L-GA and L-SA.

4.2.4.1. Adsorption kinetics

Adsorption kinetics of VitE on the two biopolymers (PGX-GA and PGX-SA) were studied using the same adsorptive precipitation unit; however, the system was operated in one-way flow rather than recirculation mode. Sample preparation was the same as that described in Section 4.2.2, where 0.5 g PGX-GA or PGX-SA was loosely packed in a glass tube, but the amount of VitE placed in the vessel was increased to 4 g to ensure having sufficient VitE during the whole

experiment. The unit operation was modified to one-way flow at constant pressure and temperature (300 bar and 50 ^{o}C). The initial steps for pressurization of the unit was the same as those described in Chapter 3, but the valves V6 and V7 remained closed throughout the run, and the check valve located between valve V3 and the bottom connection of the bioactive vessel was reversed to allow flow directly from the pump into the bioactive vessel. Thus, CO_2 flowed into the bioactive vessel, solubilized VitE and carried it through the biopolymer vessel. A portion of VitE was adsorbed on the biopolymer and the rest was carried out with the SC-CO_2, which was collected in glass vials sitting in an ice bath upon depressurization. A gas meter (Canadian Meter Company Limited, Type AL225, Cambridge, ON, Canada) was added to the exit line to record the volume of CO_2 passing through the system. During the experiment, CO_2 flow rate was kept constant, which was controlled manually by the micrometering valve on the exit line and recorded through the gas meter as a function of time. The CO_2 flow rate was set at 1 L/min (measured at ambient conditions) to allow sufficient residence time for CO_2 to solubilize and get saturated with VitE. The samples were collected in glass vials every 10 min between 10 to 40 min, every 5 min between 45 to 70 min, and back to every to 10 min until 120 min and their weight was determined after allowing them to stabilize at room temperature (23 ^{o}C).

4.2.5. Statistical analysis

All experiments and measurements at each condition were performed in duplicate and two-way analysis of variance (ANOVA) was carried out on loading content results to determine the effects of type of biopolymer and recirculation flow rate or time followed by comparison of the means by using Tukey's multiple range test. Both were performed using Minitab software package v.17 (Minitab Inc., State College, PA, USA) at a level of significance of $p < 0.05$.

4.3. Results and discussion

4.3.1. Vitamin E loading

Two sets experiments were performed for the VitE loading on PGX-GA and PGX-SA by adsorptive precipitation technology. In the first set, three recirculation flow rates were evaluated at 300 bar, 50 ^{o}C and fast depressurization, and the results are presented in Figure 4.1. Based on the ANOVA results, recirculation flow rate and type of biopolymer had a significant ($p<0.05$) effect on VitE loading, but their interaction effect was not significant ($p>0.05$). The higher loading for both biopolymers were obtained at 135 mL/min (14.95% for GA and 22.35% for SA), then the loading showed a significant decrease ($p<0.05$) at 190 mL/min, which remained similar for GA but increased for SA at 250 mL/min. The VitE loading on L-SA was significantly higher ($p<0.05$) than that on L-GA, which could be associated with the different interactions between the VitE and the biopolymers. The double bonds present in the structure of VitE (Fig. 2.2) allow dipole-dipole interactions, which can lead to more VitE being loaded onto the biopolymers. The anionic charges of SA were partly neutralized after PGX processing in the presence of SC-CO_2 and water, leading to low pH due to carbonic acid formation, which could favor more interaction with VitE. However, the loading of $VitD_3$ (5.2 ± 0.4 to 10.1 ± 0.2% for GA, and from 11.5 ± 0.8 to 13.8 ± 0.1% for SA, Chapter 3) was lower than that for VitE on the same biopolymers. VitE has a higher molecular weight but higher solubility in SC-CO_2 (16 g/kg) compared to $VitD_3$ (9.1 g/kg), and it seems to be more feasible for it to be physically trapped or retained inside the porous SA matrix, perhaps due to its long hydrophobic tail that facilitate its adsorption onto the SA matrix.

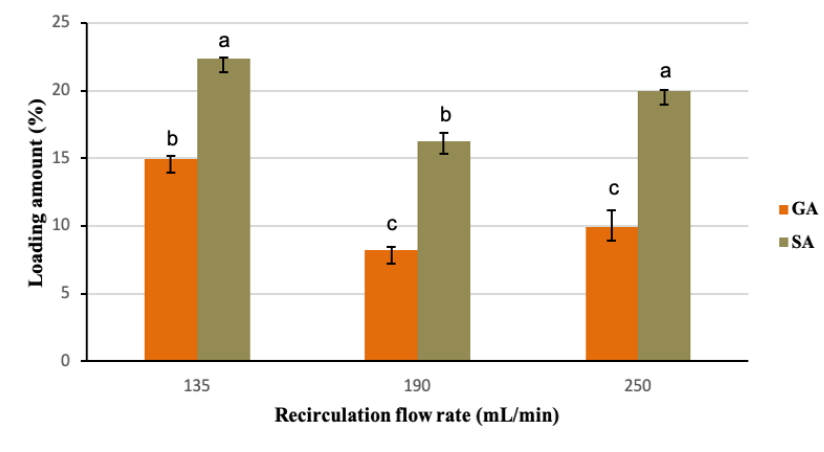

Figure 4. 1. VitE loading in L-GA and L-SA obtained at different recirculation flow rates at 300 bar, 50 $_{o}$C, and fast depressurization.
a, b, c Different letters for loading amounts indicate a significant difference between the mean values ($p < 0.05$).

In the second set of experiments, the recirculation flow rate of 135 mL/min was kept constant as well as the other parameters mentioned in the first set experiments, while the recirculation time was varied. Based on the ANOVA results, recirculation time, type of biopolymer and their interaction (time*type of polymer) had significant effects ($p<0.05$) on the VitE loading. Overall, the VitE loading increased significantly ($p<0.05$) when the recirculation time was increased from 30 to 45 min but then decreased ($p<0.05$) at 60 min. For SA, the loading at 45 min was the highest at 22.35 ± 0.1%; whereas the loading on GA of 14.95 ± 0.2%obtained at 45 was similar to those at 30 and 60 min, as shown in Figure 4.2. The SA loading decreased after 45 min, which was similar to the trend reported for CoQ10 by Couto et al. (2020). This trend is related to the high access to the pores of the particles during the initial period, but after 45 min the biopolymers could reach the maximum adsorption and saturation of the surface. After 45 min, some of the bioactive could be washed away from the biopolymer. The time required to reach saturation was confirmed with the results of the adsorption kinetics curve, as discussed later. Once

again, the loading on SA was significantly ($p<0.05$) higher than that on GA (overall mean 17.1% vs 13.1%).

There are no other similar studies for comparison with the same biopolymers and VitE, but according to Liu (2019) and the results reported for $VitD_3$ in the previous study (Chapter 3), the surface area of the biopolymer is an important parameter related to the level of loading. Based on the loading data, in order to achieve the highest loading with VitE, experiments will be performed on SA at 135 mL/min and 45 min. However, other studies performed with the same bioactive compound showed less loading than those obtained in this study. For example, spray drying technology was applied to encapsulate vitamin E into a mixture of maltodextrin in combination with Capsul® or sodium caseinate and Tween 80, resulting in an encapsulation efficiency of 48 ± 3% with Capsul® and 29 ± 5% with sodium caseinate using a vitamin ratio of 1:6 (w:w) (Mujica et al., 2020). Yokozaki and Shimoyama (2018) reported the loading of vitamin E into silicon hydrogels obtained through supercritical impregnation as 0.4 g VitE/g hydrogel at the concentration of 1 g/L.

The loading content of VitE can also be reported as the amount of VitE per square meter of the surface of the biopolymer. At the best processing conditions, 4.77 mg VitE/m_2 PGX-GA and 7.14 mg VitE/m_2 PGX-SA could be loaded. The $VitD_3$ loadings per unit area reported in the previous study (Chapter 3) were similar for VitE in this study (3.23 mg $VitD_3$/m_2 PGX-GA and 4.38 mg $VitD_3$/m_2 PGX-SA) where the loading on SA was higher; however, the loading levels of VitE were higher than those of $VitD_3$. On the other hand, VitE loading on PGX-SA was similar to the highest loading result obtained by Liu (2019) for CoQ10 on PGX-SA (7.5 mg/m_2) and by Couto et al. (2018) for CoQ10 on β-glucan (7.2 mg/m_2) using the same adsorptive precipitation process.

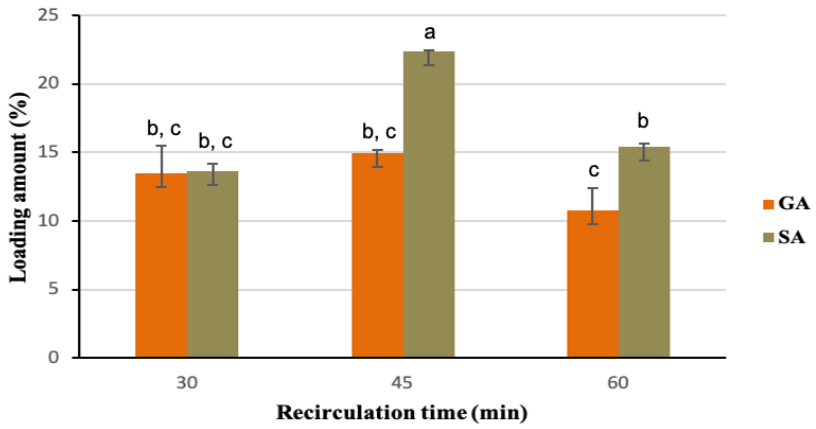

Figure 4. 2. VitE loading in L-GA and L-SA obtained at different recirculation times at 300 bar, 50 $_{o}$C, and fast depressurization, and recirculation flow rate of 135 mL/min for both biopolymers. $_{a, b, c}$ Different letters for loading amount indicate a significant difference between the mean values ($p < 0.05$).

4.3.2. Morphology

The morphology of L-GA and L-SA particles processed at 135 mL/min and 45 min were displayed in Figure 4.3 for both biopolymers. Samples obtained at other processing conditions were also analyzed by HIM, but there was no major difference between the analyzed samples and therefore these representative samples are presented in Figure 4.3. Comparison of PGX-processed biopolymers (Fig. 4.3 (a, d)) to the L-GA and L-SA showed that the L-GA and L-SA had a homogeneous distribution of VitE on the surface of L-GA, but some agglomeration of the VitE in specific areas was observed in the L-SA. This could be associated to the precipitation step. There are no similar studies to compare in the literature with VitE and the same biopolymers. However, similar biopolymers were used at the same operational conditions with a different bioactive ($VitD_3$, Chapter 3) and similar morphologies were observed. Even though, based on the loading content results, L-SA with VitE showed higher loading, no visually distinguishable differences were apparent on the HIM images.

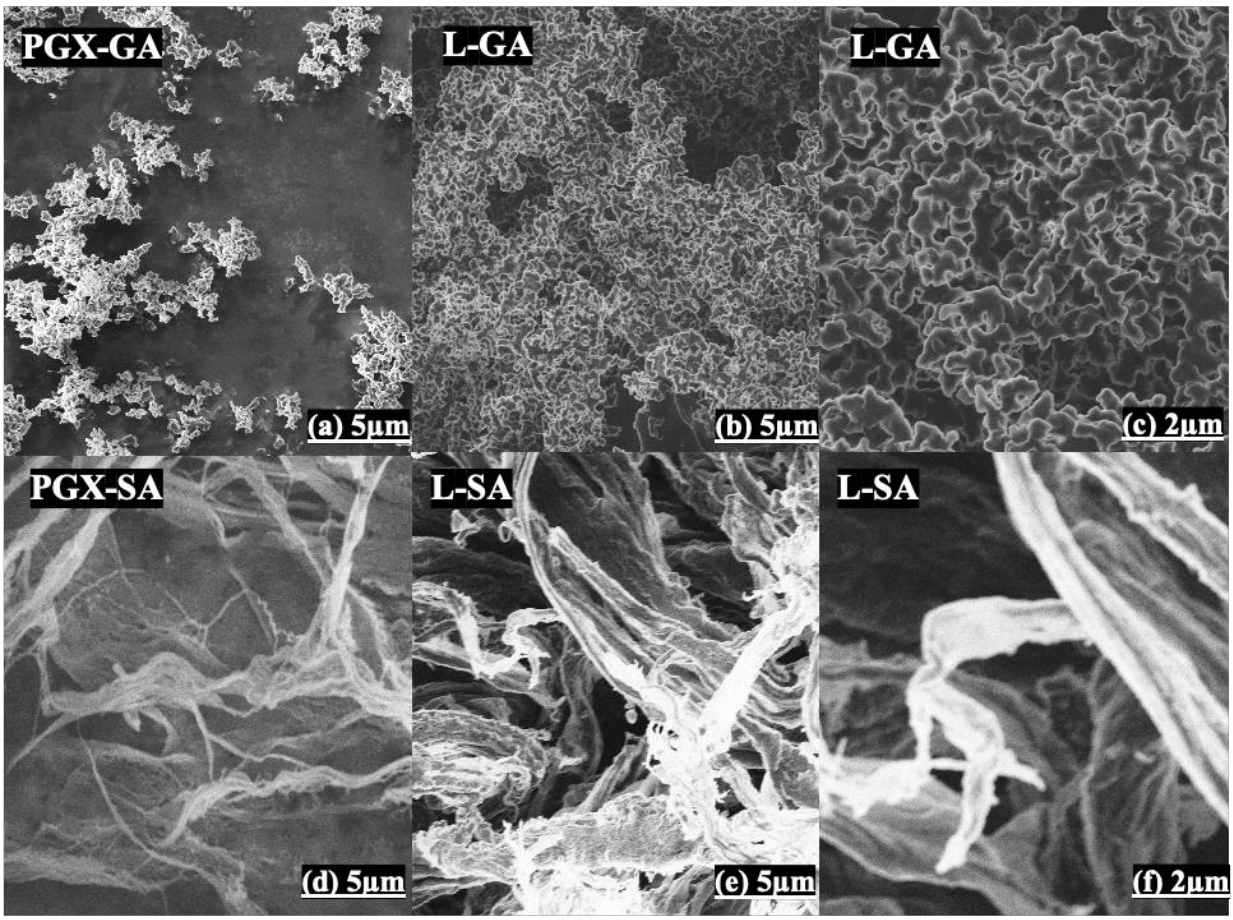

Figure 4. 3. HIM images of (a) PGX-GA, (b) L-GA at 5µm, (c) L-GA at 2µm, (d) PGX-SA (e) L-SA at 5µm, (f) L-SA at 2µm (biopolymers processed at135 mL/min and 45 min and the images of PGX-GA and PGX-SA are the same as in Chapter 3).

4.3.3. Fourier-transform infrared (FTIR)

ATR-FTIR analysis was performed to study the interactions between VitE and the biopolymers. There was no difference in the spectra of the different loaded samples obtained at different processing parameters and representative spectra for the samples with the highest loading are presented in Figures 4.4-4.7.

The VitE spectrum (Fig. 4.5 and 4.7) showed a multitude of bands that are generally present in compounds with aromatic groups. The peak located at 3456 cm^{-1} correspond to OH stretching vibrations when hydrogen bonds are formed. The peaks at 2925 and 2887 cm^{-1} represent

asymmetric and symmetric stretching vibration of the CH_2 and CH_3 vibrations, respectively. The peak in the region 1650-1430 cm^{-1} could be associated with C=C stretching. Also, the bands from C-H bending show at 1275-1000 cm^{-1} for in-plane bending and at 900-690 cm^{-1} for out-of-plane bending. The peak close to 1000 cm^{-1} is typical of C-O stretching. The consecutive peaks at 1460 and 1450 cm^{-1} correspond to phenyl skeletal and methyl asymmetric bending, at 1378 cm^{-1} to methyl symmetric bending, at 1262 cm^{-1} to CH_2 vibration, at 1086 cm^{-1} to in-plane bending vibrations of phenyl, and at 919 cm^{-1} for trans $=CH_2$ stretching vibrations (Silva et al., 2009). The spectra of PGX-GA and PGX-SA were described in Chapter 3 (section 3.3.3), but also included here for comparison purposes.

The spectra of L-GA and PGX-GA (Fig. 4.4) showed that the L-GA presented all the peaks of the PGX-GA spectra. The comparison of FTIR spectra for pure VitE and L-GA, shown in Figure 4.5, demonstrated that some characteristic peaks of the VitE were also present in the L-GA spectra, such as the peaks at 3371-2959-1462-1429-1278 cm^{-1}. There were no new peaks in the L-GA spectra, indicating that there was no new covalent bond formation between the bioactive and the biopolymer after processing. In addition, the spectra of L-SA (Fig. 4.6) displayed the same peaks present on the PGX-SA.

The spectra for the L-GA and L-SA showed the appearance of new peaks compared to PGX-GA and PGX-SA, respectively, and a change in the intensity of others, but those peaks corresponded with the peaks found in the spectrum for VitE, which confirms the loading of the PGX-processed samples and reflects the high level of loading.

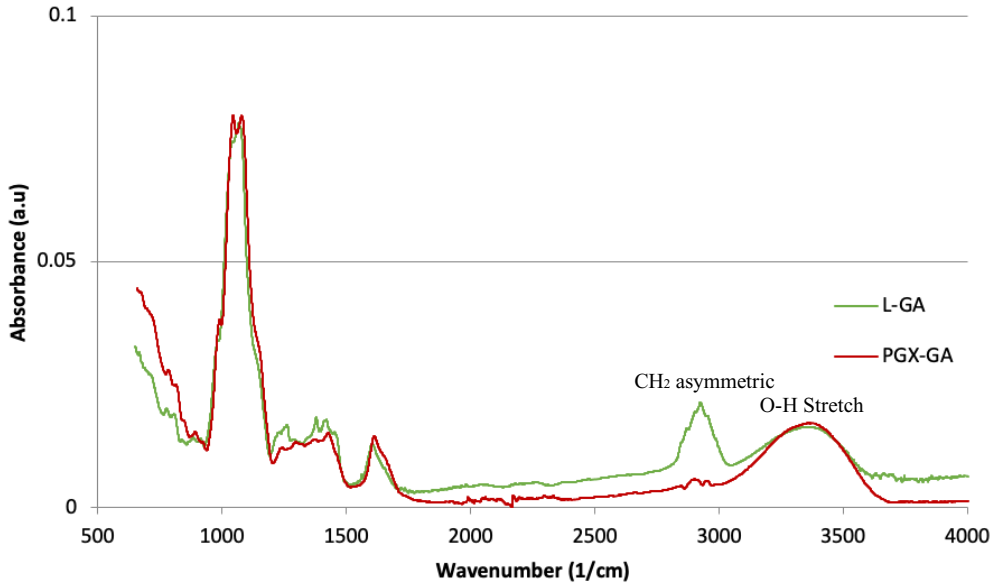

Figure 4. 4. ATR-FTIR spectra of L-GA processed at 135 mL/min and 45 min, and PGX-GA.

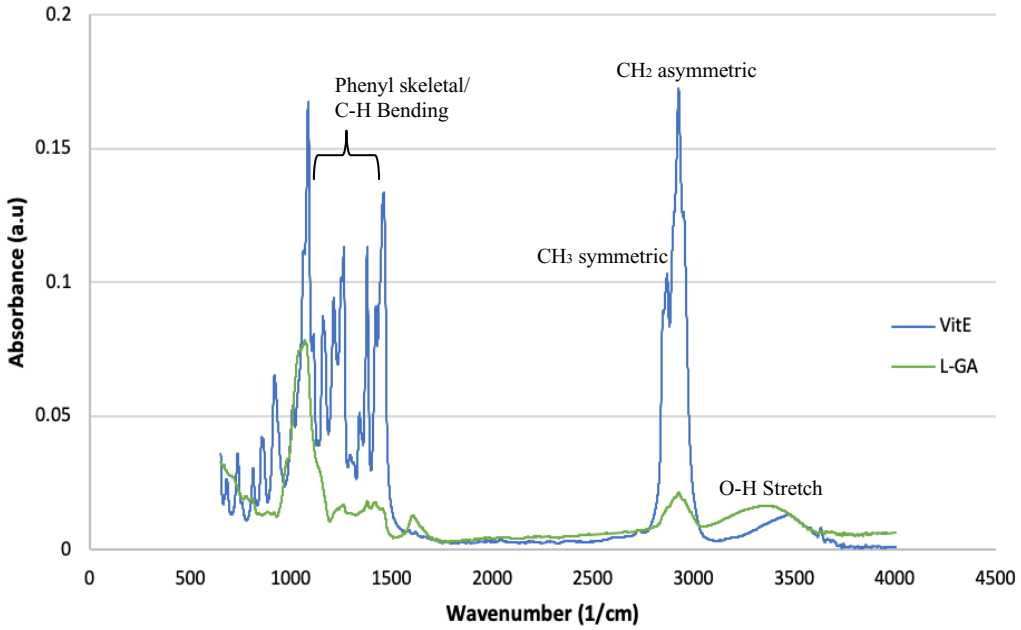

Figure 4. 5. ATR-FTIR spectra of VitE (±-α-tocopherol), and L-GA processed at 135 mL/min and 45 min.

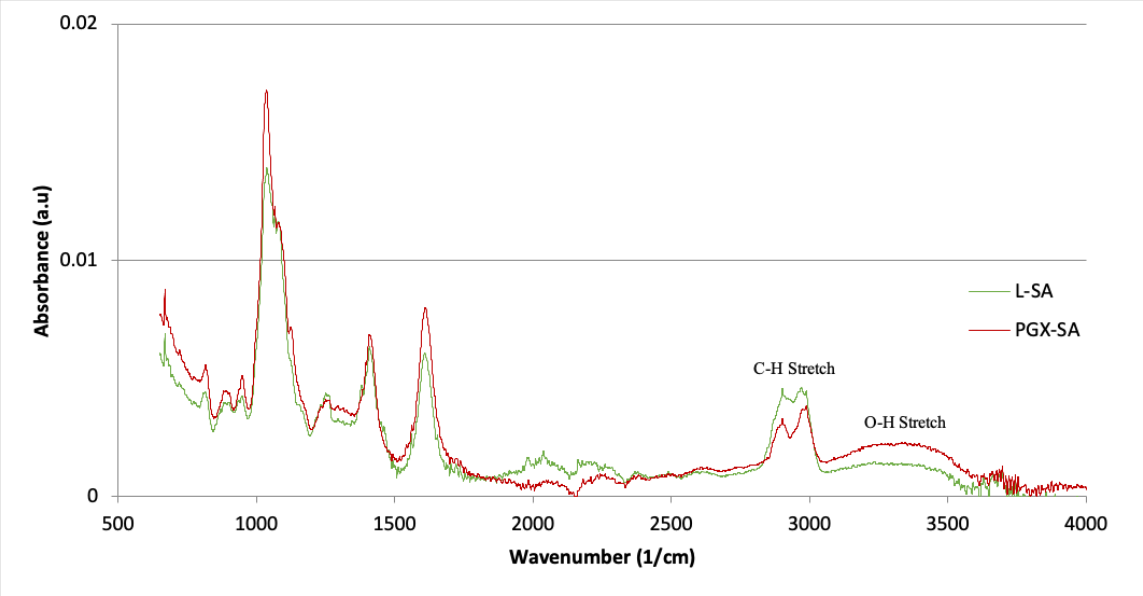

Figure 4. 6. ATR-FTIR spectra L-SA (processed at 135 mL/min and 45 min), and PGX-SA.

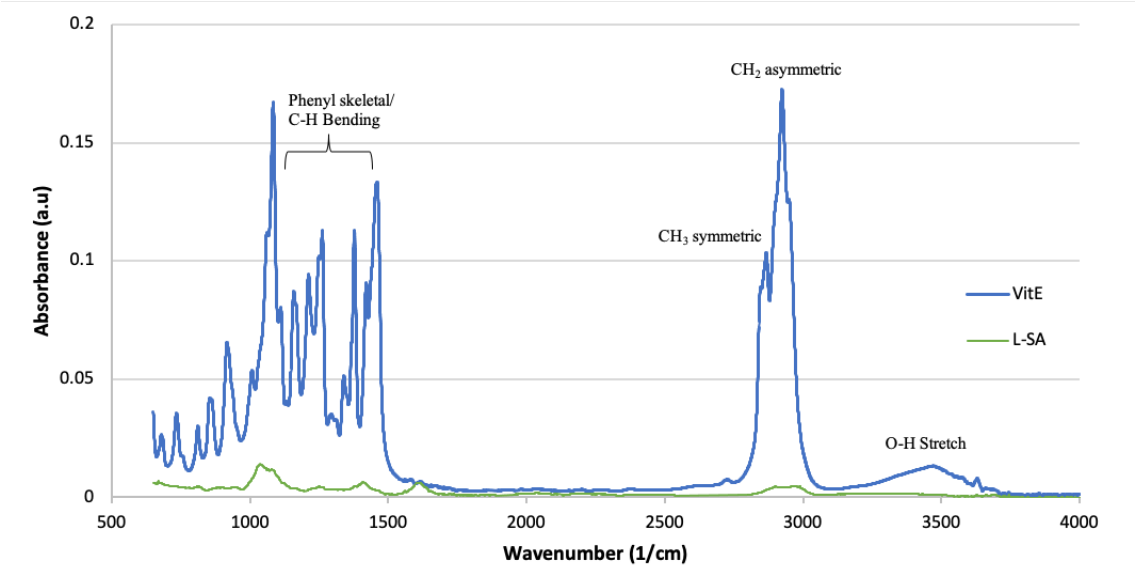

Figure 4. 7. ATR-FTIR spectra of VitE (±-α-tocopherol), and L-SA (processed at 135 mL/min and 45 min).

4.3.4. Differential scanning calorimetry (DSC)

The DSC spectra were shown in Figure 4.8 for GA (L-GA and PGX-GA) and Figure 4.9 for SA (L-SA and PGX-SA). All samples presented one broad endothermic peak. The peaks for PGX-GA and L-GA were approximately from 45 ^{o}C to 132 ^{o}C, and from 45 ^{o}C to 113 ^{o}C,

respectively. Those peaks were centered approximately at similar temperatures of 83.5 ₒC for PGX-GA and 80.5 ₒC for L-GA, which could be related to evaporation of residual ethanol from the powder (Couto et al., 2018). PGX-SA and L-SA peaks were about from 38 ₒC to 132 ₒC and 34 ₒC to 144 ₒC, respectively. Moreover, similar center peaks were present in the spectra for PGX-SA (78 ₒC) and L-SA (80.3 ₒC), which could be associated with the interaction of the biopolymers with the VitE. The area under the endothermic peaks correspond to enthalpy and it is apparent that L-GA and L-SA had different peak sizes, resulting in 287 J/g and 354.5 J/g, respectively, which may be an indication of the stronger molecular interactions between VitE and SA within L-SA.

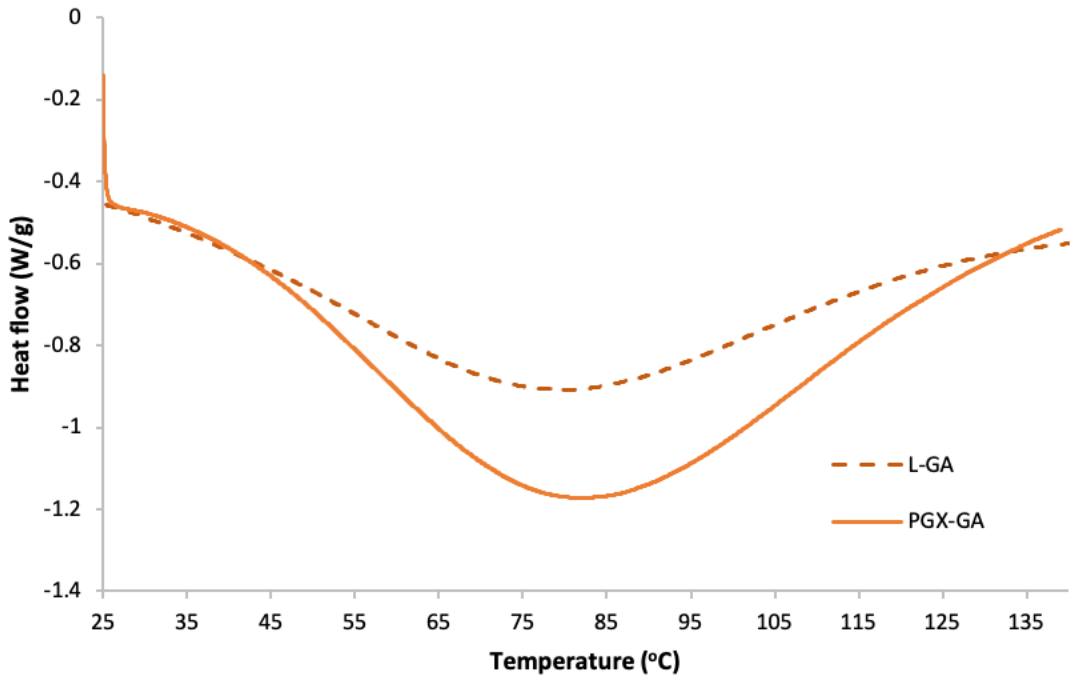

Figure 4. 8. DSC spectra of L-GA (processed at 135 mL/min and 45 min) and PGX-GA.

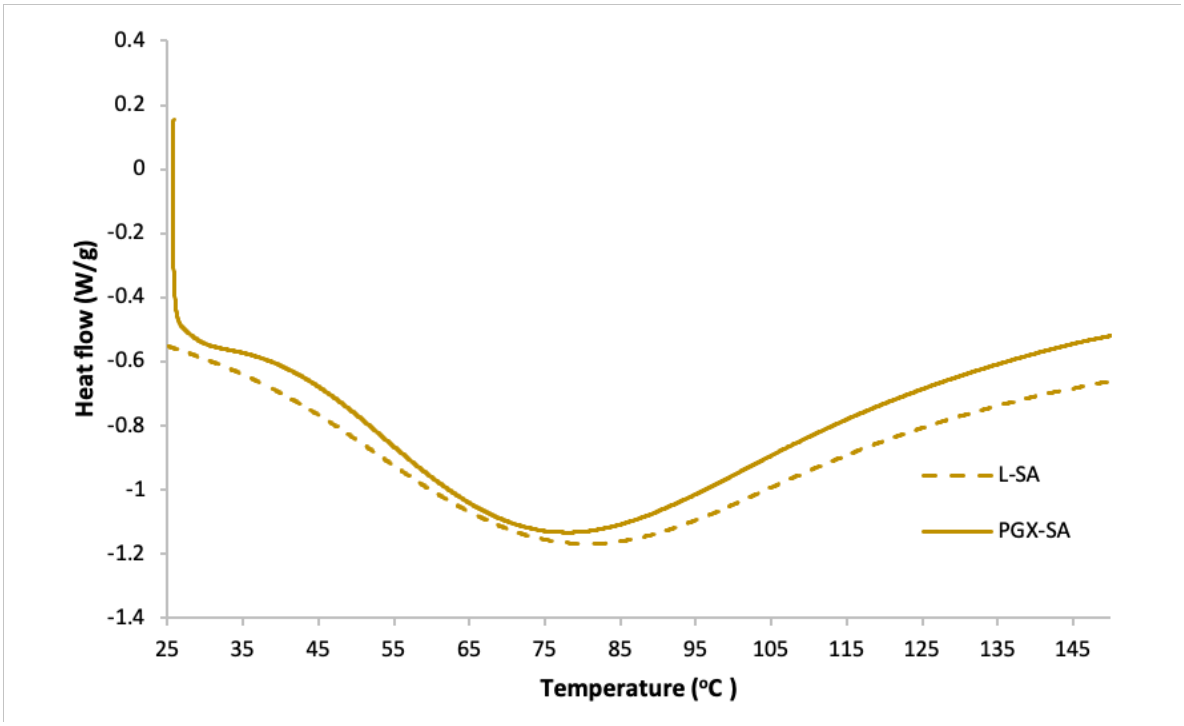

Figure 4. 9. DSC spectra of L-SA (processed at 135 mL/min and 45 min) and PGX-SA.

4.3.5. Storage stability

As previously mentioned in Chapter 2, the stability of VitE during storage depends on environmental factors such as, light, oxygen, heat, moisture/humidity, and pH. Therefore, a question that needs to be addressed is the stability of VitE adsorbed on the large surface of biopolymer particles over storage, and thus, the storage stability of loaded powders was tested in terms of the change in VitE loading over time. In this study, VitE-loaded biopolymer samples processed at 135 mL/min recirculation flow rate for 45 min for both biopolymers were packed in glass containers with plastic lids and stored for up to 28 days at 4 ^{o}C in a refrigerator, but the containers were not covered with aluminum foil to allow exposure to light.

As displayed in Figure 4.10, the VitE content on both biopolymers started to decrease from day 1 to day 14 from 100% to 92% for L-GA and from 100% to 97% for L-SA and but then remained stable at 28 days at 91% for L-GA and 96% for L-SA. The vitamin adsorbed on the large

surface area of the biopolymers being exposed to oxygen and light could be the reason for the small extent of degradation. In contrast, zein nanoparticles encapsulating VitE showed 58% storage stability after 28 days (Zhang et al., 2019). Encapsulation of lycopene with lecithin and VitE showed 24.3% degradation after 28 days of storage (Cheng et al., 2017). In comparison, the degradation of VitE in L-SA over 28 days storage was minimal in this study, demonstrating the protection provided by PGX-SA particles, despite its large surface area.

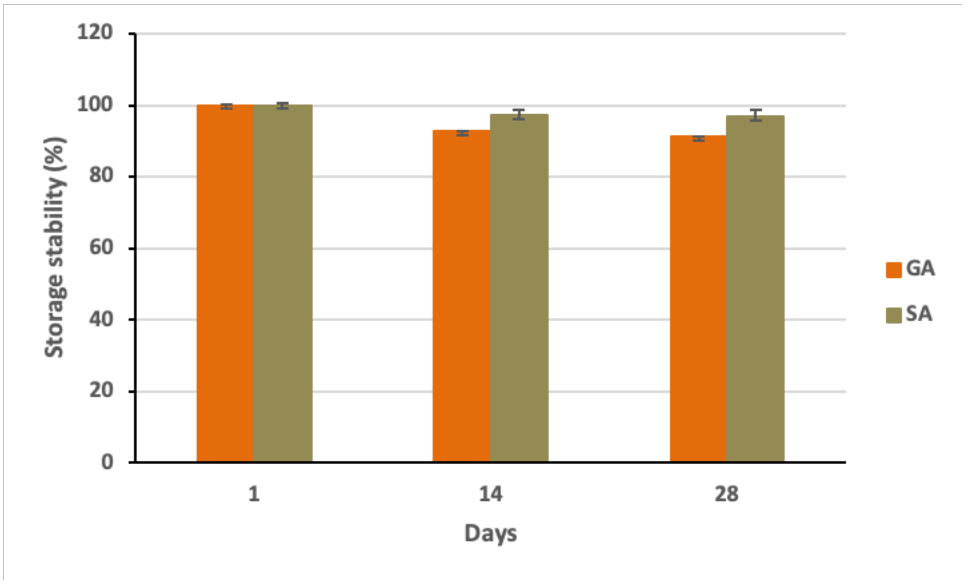

Figure 4. 10. Storage stability of L-GA and L-SA processed at 135 mL/min and 45 min.

4.3.6. Release kinetics

VitE release profiles from L-GA and L-SA were studied using pancreatin as the enzyme to achieve the hydrolysis of loaded samples and release in a simulated intestinal fluid (SIF) environment. The loading contents of the samples analyzed were 15% for L-GA and 22% for L-SA. The release profile of L-GA showed an increasing release of VitE over time of up to 20.1% (percentage of the initial amount of VitE in the sample that is released into the SIF) (Fig. 4.11) at the end of the intestinal digestion time of 240 min. However, only 7.4% of VitE was released from L-SA at 30 min, which decreased to 4.8% at 60 min with a further decrease to 4% at 240 min.

Lower release could be related with the DSC results and storage stability that stronger interaction between VitE and PGX-SA could be also related with reduced dissolution in the SIF medium. The variance in the release profiles can be associated to the nature of the biopolymers, the extent of interactions between biopolymers and VitE, and possible degradation of the VitE within the SIF environment (Padro et al., 2012; Xi et al., 2019).

The release of the pure VitE was less than 1% after 4 h of simulated intestinal digestion. Considering the substantial increase in the release of VitE within the SIF media, L-GA showed great potential as a delivery system for VitE, which would contribute to enhanced bioavailability of this important vitamin. Even though no studies employing similar compounds were found in the literature, some studies reported release of VitE from different carriers using the same enzyme in SIF media. For example, the cumulative VitE release obtained from chitosan microspheres increased up to 12.8% from particles containing 13.4 mg of VitE per gram of microspheres (Padro et al., 2012). The release of VitE from an assembly of β-cyclodextrin and octadecenyl anhydride with a loading of 75 mg/g showed a cumulative release of up to 66% (Xi et al., 2019).

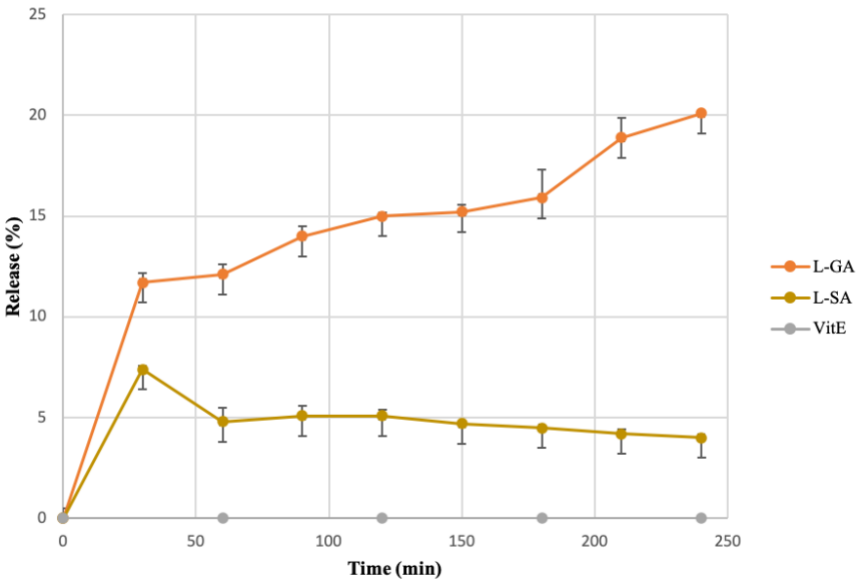

Figure 4. 11. Release kinetics of L-GA, L-SA processed at 135 mL/min and 45 min, and pure VitE.

4.3.7. Adsorption kinetics

In this study, the adsorption kinetics of VitE on PGX-GA and PGX-SA within SC-CO_2 environment were investigated. One-way flow allowed the bioactive to be solubilized in SC-CO_2 first and then carried to the bed of biopolymer from the top. The bioactive not adsorbed by the biopolymer came out of the bottom of the biopolymer vessel together with SC-CO_2, which was collected in vials upon depressurization and separation of CO_2. Low CO_2 flow rate (1 L/min, measured at ambient conditions) was implemented to ensure sufficient contact time for solubilization of VitE in CO_2. Also, a sufficient amount of VitE was placed on the bioactive vessel to keep CO_2 saturated throughout the run and there was excess left over on the felt filters at the end of each experiment. The adsorption kinetics curve was plotted as solute concentration in the exit stream (C, mg VitE/g CO_2, using CO_2 density value obtained from the NIST Chemistry WebBook (NIST SRD 69, 2018)), as a function of time (min) and the curve had the expected shape, demonstrating the time required for the biopolymer to adsorb the bioactive and reach saturation. Figure 4.12 showed the adsorption of VitE on PGX-GA, where the vitamin started to come out in the exit stream after 30 min (5.95 mg/g), then around double that amount came out at 40 min (10.49 mg/g) and increased further until 50 min (16 mg/g). The PGX-SA displayed around 1.4 mg/g coming out at 30 min, then gently increased from 4.8 to 8.4 mg/g between 30 and 40 min, followed by a sharp increase up to the maximum point at 16.3 mg/g. The VitE concentration in the exit stream reached up to around 16 mg/g at 50 min for both biopolymers; however, there was a difference in how the VitE reached the maximum point. This difference was related to the higher level of adsorption occurring on SA compared to GA based on the loading results, due to the difference in the level of interactions between the vitamin and biopolymers, and also to the difference in the surface area of the biopolymers.

The setup used in this study was a dynamic system and the final concentration in SC-CO_2 is expected to correspond to the solubility limit. The solubility of VitE in SC-CO_2 was reported by Johannsen and Brunner (1997) as 25.3 mg/g at 300 bar and 50 ^{o}C based on a static system. However, there are differences in the literature regarding the solubility values reported, due to differences in the techniques and purity of the samples used, since Del Valle et al. (2020) and Güçlü-Üstündağ and Temelli (2003) reported the solubility of VitE at 300 bar and 50 ^{o}C as 16 mg/g. Similar solubility results were obtained in this study as 16.3 mg VitE/g CO_2 when saturation was reached at 50 min.

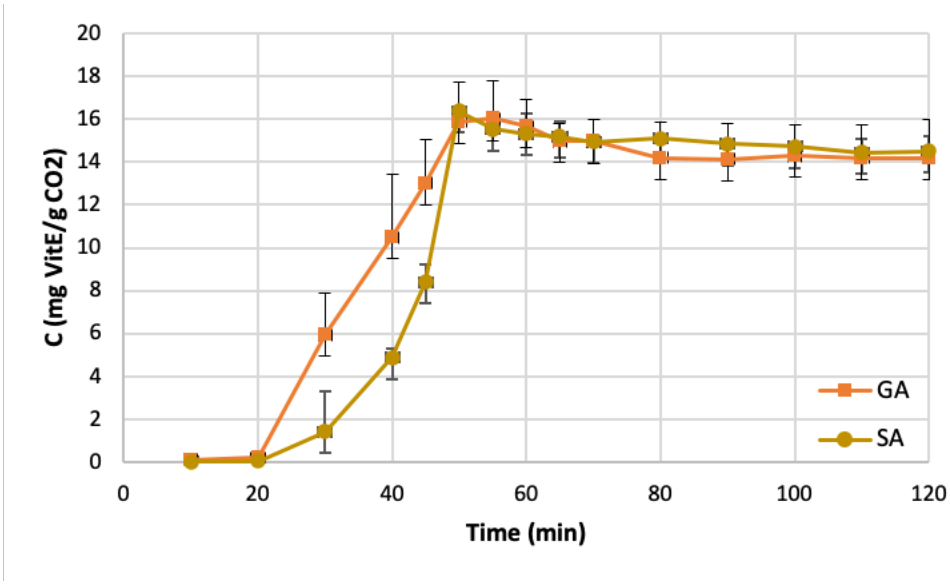

Figure 4. 12. Adsorption kinetics curve of L-GA and L-SA (processed at 135 mL/min and 45 min) preformed in one-way flow for 120 min at 50 ^{o}C and 300 bar, showing the concentration of VitE in the exit CO_2 stream as a function of time.

4.4. Conclusions

The adsorptive precipitation process is an effective method to load VitE on gum arabic and sodium alginate. Recirculation flow rate, time and type of biopolymer were significant ($p<0.05$) parameters impacting VitE loading. The highest loading content for both biopolymers were

achieved at the same conditions of 135 mL/min recirculation flow rate for 45 min. The VitE loading content varied from 10.75 ± 1.6 to 14.95 ± 0.2% for GA, and from 13.65 ± 0.5 to 22.35 ± 0.1% for SA. Homogeneous coating of VitE on the surface of the biopolymers was observed based on HIM images after the adsorptive precipitation process. Based on the analytical tests conducted, it was apparent that there was no new covalent bond formation between the biopolymers and VitE during the adsorptive precipitation process. Both loaded biopolymers were stored for 28 days at 4 ^{o}C and showed a small drop in VitE loading content from 100% to 91% for L-GA and to 96% for L-SA. Release from L-GA in SIF increased slowly during the 240 min digestion time up to 20.1%. However, L-SA showed a much lower release that can be associated to the difference in the nature of biopolymers, possible degradation of the bioactive in the intestinal medium, and due to the large surface area and fibrous nature of SA where VitE could be trapped in during the adsorption step. Adsorption kinetics were different for the two biopolymers over 50 min, where both biopolymers reached the same saturation limit at 50 min but the amount adsorbed on L-SA was higher because of the large surface area and higher level of interactions. This study confirmed that adsorptive precipitation using SC-CO_2 shows great potential for VitE loading on water-soluble biopolymers as delivery systems, which would open new opportunities for developing different aqueous-based applications for this fat-soluble vitamin.

Chapter 5: Conclusions and recommendations

5.1. Summary of key findings

Gum arabic and sodium alginate are high molecular weight polysaccharides with potential for use as carriers after being dried by Pressurized Gas eXpanded (PGX) liquid technology and loaded with fat-soluble bioactive components by adsorptive precipitation technique as delivery systems. In this MSc thesis research, the effect of adsorptive precipitation process parameters on the loading of two fat-soluble vitamins, vitamin D_3 ($VitD_3$) and vitamin E (VitE), onto the PGX-dried high-surface-area biopolymers (gum arabic (GA) and sodium alginate (SA)) were studied to characterize the powders obtained in an effort to assess their potential for further product applications. $VitD_3$ and VitE were selected for this purpose because they have many health benefits, but their bioavailability in the human body is low, and developing aqueous-based applications is challenging due to their hydrophobic nature. Even though adsorptive precipitation of different drugs on various polymeric carriers has been reported previously, there are no reports on the adsorptive precipitation of $VitD_3$ and VitE on PGX-GA and PGX-SA using supercritical carbon dioxide (SC-CO_2). In addition, having different vitamins in solid ($VitD_3$) and liquid (VitE) form at ambient conditions required some modification of the processing unit.

The first study was focused on how different processing parameters (recirculation flow rate and recirculation time) affect the loading of $VitD_3$ and the physicochemical properties of the loaded particles obtained. Recirculation time and type of biopolymer had a significant ($p<0.05$) effect on $VitD_3$ loading, but recirculation flow rate did not. The highest $VitD_3$ loading levels obtained were $10.1 \pm 0.2\%$ for GA and $13.7 \pm 0.1\%$ for SA. In addition, based on helium ion microscopy imaging, uniform coating of $VitD_3$ on the surface of the biopolymers after processing by adsorptive precipitation was observed. Based on XRD results, the loaded $VitD_3$ on PGX-GA maintained its

crystalline form to a certain extent. The non-crystalline portion released into the simulated intestinal fluid was 18.6% of the $VitD_3$ present in the starting sample, which was sustained over the 240 min of digestion. The pure $VitD_3$ release was just 1% over the 240 min. Even though the release for L-SA was low, it showed an improvement compared to the pure bioactive release. Storage stability was demonstrated with an extent of degradation of 20% over the first 28 days for L-GA and 18% for L-SA over the first 21 days, but there was no further degradation after that time over the total storage time of 60 days.

The second study of this thesis research was to investigate the effects of recirculation flow rate and recirculation time applied during the adsorptive precipitation process of VitE on PGX-processed GA and SA. Similar conditions (135 mL/min and 45 min) resulted in the highest loading content for both biopolymers. Loaded samples showed maximum values of 14.95 ± 0.2% for GA, and 22.35 ± 0.1% for SA, which were higher than those obtained for $VitD_3$. HIM images demonstrated homogeneous coating of VitE on the biopolymer surface. Over refrigerated storage, stability of VitE on both biopolymers was high such that after 28 days storage, L-GA had 91% and L-SA had 96% of the initial amount of vitamin loaded. The release of VitE from L-GA (20.1%) was higher than that from L-SA, which could be associated with the higher level of interaction between SA and the bioactive during the adsorption step. Adsorption kinetics test showed a difference in the rate of concentration increase in the exit CO_2 stream over the first 50 min for both biopolymers and that difference can be related to the higher level of adsorption occurring on PGX-SA compared to PGX-GA based on the loading results until saturation of the biopolymer is reached, as well as the difference in the surface area of the biopolymers.

The combination of two vitamins and two biopolymers with different properties used in this research provided interesting results in terms of their behavior during the adsorptive

precipitation process using SC-CO_2. The appearance of $VitD_3$ was in crystalline form (solid) but VitE was a highly viscous liquid under ambient conditions. Even though the molecular weight of VitE (430.71 g/mol) was slightly higher than that of $VitD_3$ (384.64 g/mol), the solubility in SC-CO_2 was higher for VitE (16 mg VitE/g CO_2 vs 9.1 mg $VitD_3$/g CO_2) probably due to the long hydrophobic tail in its structure, which contributed to the higher loading of VitE on both biopolymers. For the biopolymers, GA was a neutral polymer in the form of spherical aggregates whereas SA was negatively charged fibrous particles. In addition to having a higher surface area after PGX processing (164.5 m_2/g SA vs 65 m_2/g GA), the loading of both vitamins per unit area was higher for SA due to the strong interactions. This led to higher stability of vitamins over refrigerated storage with SA. On the other hand, the release of both vitamins in simulated intestinal fluid was higher with GA even though both biopolymers led to substantially higher release compared to the pure vitamin (<1%), which would contribute to higher bioavailability of these hydrophobic vitamins.

Overall, this MSc research provided findings on a novel delivery system for fat-soluble vitamins even though there are other conventional delivery systems available. PGX-drying of biopolymers followed by loading them with fat-soluble vitamins using adsorptive precipitation provides a novel approach that may offer some advantages in terms of stability and enhanced bioavailability, leading to new opportunities for aqueous-based applications of hydrophobic vitamins in various food and natural health products as well as pharmaceutical and cosmetics products. The preparation of vitamin-loaded samples using the adsorption precipitation process did not affect the properties of the bioactive compounds. In addition, fundamental characterization of the loaded samples provided useful information not only for optimizing the processing conditions but also developing novel combinations of different bioactives and biopolymers as

delivery systems in order to increase the release and bioavailability of fat-soluble vitamins in aqueous environment.

5.2. Recommendations for future work

Based on the findings of the two studies, the following aspects are recommended for future investigations:

- The optimal amount of bioactive loading on both biopolymers can be investigated in order to obtain more efficient aqueous-based delivery systems, maximize the stability during storage, and release of the bioactive from the final powder, in addition to cost analysis to minimize processing cost.
- Release kinetics were studied under simulated intestinal conditions only and it is recommended to assess the release kinetics also under the simulated gastric conditions.
- The bioavailability of the bioactive compounds on gum arabic and sodium alginate loaded samples can be investigated further, in order to better understand how it can be improved after adsorptive precipitation process. This would require testing in animals while delivering the recommended daily dose of the bioactive with appropriate amount of the powder.
- Adsorption kinetics testing should also be performed for $VitD_3$ on L-GA and L-SA, for a better understanding of the interactions between the biopolymers and $VitD_3$.
- The degree of crystallinity of the loaded $VitD_3$ on L-GA can be determined.
- Zeta potential and thermal gravimetric analysis should be performed for better understanding of the surface charges on each of the components and the interactions between vitamins and both biopolymers.

- New functional food products can be formulated with the loaded samples studied in this research to demonstrate their performance in a complex food matrix.
- Other bioactive-biopolymer combinations need to be studied separately to assess their potential unique properties.
- A systematic study of biopolymer type is recommended for a better understanding of the relationship between biopolymers and bioactives.

Bibliography

Abd-Allah, A., Al-Majed, A., Mostafa, A. M., Al-Shabanah, O., Din, A. G. E., & Nagi, M. N. (2002). Protective effect of arabic gum against cardiotoxicity induced by doxorubicin in mice: A possible mechanism of protection. Journal of Biochemical and Molecular Toxicology, 16(5), 254-259.

Abdelkareem A. Ahmed, Jaafar S. Fedail, Hassan H. Musa, & Amal Z. Sifaldin. (2015). Gum arabic supplementation improved antioxidant status and alters expression of oxidative stress gene in ovary of mice fed high fat diet. Middle East Fertility Society Journal, 21(2), 101-108.

Abuasal, B. S., Lucas, C., Peyton, B., Alayoubi, A., Nazzal, S., Sylvester, P. W., & Kaddoumi, A. (2012). Enhancement of intestinal permeability utilizing solid lipid nanoparticles increases γ-tocotrienol oral bioavailability. Lipids, 47(5), 461-469.

Ahmed, A. A., Fedail, J. S., Musa, H. H., Kamboh, A. A., Sifaldin, A. Z., & Musa, T. H. (2015). Gum arabic extracts protect against hepatic oxidative stress in alloxan induced diabetes in rats. Pathophysiology, 22(4), 189-194.

Ahmed, S. (2019). "AlginateBbased Biomaterials for Bio-Medical Applications in the Biomedical and Food Industries". (Chapter 10), (pp. 174-204). Scrivener Publishing LLC.

Ahsan, H., Ahad, A., & Siddiqui, W. (2015). A review of characterization of tocotrienols from plant oils and foods. Journal of Chemistry Biology, 8(2), 45-59.

Ali, B. H., Ziada, A., & Blunden, G. (2009). Biological effects of gum arabic: A review of some recent research. Food and Chemical Toxicology, 47(1), 1-8.

Al-Majed, A., Abd-Allah, A., Al-Rikabi, A., Al-Shabanah, O., & Mostafa, A. M. (2003). Effect of oral administration of arabic gum on cisplatin-induced nephrotoxicity in rats. Journal of Biochemical and Molecular Toxicology, 17(3), 146-153.

Almarri, F., Haq, N., Alanazi, F. K., Mohsin, K., Alsarra, I. A., Aleanizy, F. S., & Shakeel, F. (2017). Solubility and thermodynamic function of vitamin D3 in different mono solvents. Journal of Molecular Liquids, 229, 477-481.

Anandharamakrishnan, C., & Ishwarya, S. P. (2015). “Spray Drying Technique for Food Ingredient Encapsulation”. (pp. 65-74) Published by John Wiley & Sons, Ltd. West Sussex, England.

Aslam, A., Misbah, S. A., Talbot, K., & Chapel, H. (2004). Vitamin E deficiency induced neurological disease in common variable immunodeficiency: Two cases and a review of the literature of vitamin E deficiency. Clinical Immunology, 112(1), 24-29.

Ballard, J. M., Zhu, L., Nelson, E. D., & Seburg, R. A. (2007). Degradation of vitamin D3 in a stressed formulation: The identification of esters of vitamin D3 formed by a transesterification with triglycerides. Journal of Pharmaceutical and Biomedical Analysis, 43(1) 142-150.

BeMiller, J. N. (2019). “Carbohydrate Chemistry for Food Scientists (3rd Edition)”. Gum arabic and other exudate gums. (pp. 313-321). Publishing by Elsevier Inc.

Birringer, M. (2010). Analysis of vitamin E metabolites in biological specimen. Molecular Nutrition & Food Research, 54(5), 588-598.

Bostan, A., & Ghaitaranpour, A. (2019). Co- encapsulation of vitamin D and calcium for food fortification. Journal of Fasting and Health, 7(4), 229-239.

Boyère, C., Jérôme, C., & Debuigne, A. (2014). Input of supercritical carbon dioxide to polymer synthesis: An overview. European Polymer Journal, 61, 45-63.

Calame, W., Weseler, A. R., Viebke, C., Flynn, C., & Siemensma, A. D. (2008). Gum arabic establishes prebiotic functionality in healthy human volunteers in a dose-dependent manner. British Journal of Nutrition, 100(6), 1269-1275.

Cheng, Y., Lu, P., Huang, C., & Wu, J. (2017). Encapsulation of lycopene with lecithin and α-tocopherol by supercritical antisolvent process for stability enhancement. The Journal of Supercritical Fluids. 130, 246-252.

Combs, G. F., & McClung, J. P. (2017a). “Chapter 7 - Vitamin D. The Vitamins (Fifth edition) Fundamental Aspects in Nutrition and Health”. Academic Press (pp 161-206). Publishing by Elsevier Inc.

Combs, G. F., & McClung, J. P. (2017b). “Chapter 8 - Vitamin E. The Vitamins (Fifth edition) Fundamental Aspects in Nutrition and Health”. Academic Press (pp 207-242). Publishing by Elsevier Inc.

Coulter, L. A., & Amadò, R. (1993). Review of proceedings of the penn state ice cream centennial conference, by M. kroger; controlling dietary fiber in food products, by leon prosky and jonathan de vries and the technology of vitamins in food. Food Science and Technology, 26(3), 281-283.

Couto, R., Seifried, B., Yépez, B., Moquin, P., & Temelli, F. (2018). Adsorptive precipitation of co-enzyme Q10 on PGX-processed β-glucan powder. The Journal of Supercritical Fluids, 141, 157-165.

Couto, R., Wong, E., Seifried, B., Yépez, B., Moquin, P., & Temelli, F. (2020). Preparation of PGX-dried gum arabic and its loading with coQ10 by adsorptive precipitation. The Journal of Supercritical Fluids. 156, 104-662.

Cui S. W. (2001). “Polysaccharides Gums from Agricultural Products: Processing, Structure and Functionality”. Technomic Publishing Company Inc, Lancaster, USA.

Deeb, K. K., Johnson, C. S., & Trump, D. L. (2007). Vitamin D signalling pathways in cancer: Potential for anticancer therapeutics. Nature Reviews Cancer, 7(9), 684-700.

Del Valle, J. M., Reveco-Chilla, A. G., Valenzuela, L. M., & de la Fuente, Juan C. (2020). Estimation of the solubility in supercritical CO_2 of α- and δ-tocopherol using Chrastil’ model. The Journal of Supercritical Fluids, 157, 104688.

Delgado, D. R., Almanza, O. A., Martínez, F., Peña, M. A., Jouyban, A., & Acree, W. E. (2016). Solution thermodynamics and preferential solvation of sulfamethazine in (methanol+water) mixtures. The Journal of Chemical Thermodynamics, 97, 264-276.

Draget, K. I. (2009). Alginates. In “Handbook of Hydrocolloids” (pp. 807-828). Woodhead Publishing. Cambridge, U.K.

Draget, K. I., & Taylor, C. (2011). Chemical, physical and biological properties of alginates and their biomedical implications. Dietary Fibre and Bioactive Polysaccharides Food Hydrocolloids. 25(2), 251-256.

Espinosa-Andrews, H., Sandoval-Castilla, O., Vázquez-Torres, H., Vernon-Carter, E. J., & Lobato-Calleros, C. (2010). Determination of the gum arabic–chitosan interactions by fourier transform infrared spectroscopy and characterization of the microstructure and rheological features of their coacervates. Carbohydrate Polymers, 79(3), 541-546.

Eyles, D. W., Burne, T. H. J., & McGrath, J. J. (2013). Vitamin D, effects on brain development, adult brain function and the links between low levels of vitamin D and neuropsychiatric disease. Organizational Actions of Hormones in the Brain, Frontiers in Neuriendocrinology. 34 (1), 47-62.

Galli, F., Azzi, A., Birringer, M., Cook-Mills, J. M., Eggersdorfer, M., Frank, J., Cruciani, G., Lorkowski, S., Özer, N. K. (2017). Vitamin E: Emerging aspects and new directions. Radical Biology and Medicine. 102, 16-36.

Garland, C. F., Garland, F. C., Gorham, E. D., Lipkin, M., Newmark, H., Mohr, S. B., & Holick, M. F. (2006). The role of vitamin D in cancer prevention. American Journal of Public Health, 96(2), 252-261.

George, M., & Abraham, T. E. (2006). Polyionic hydrocolloids for the intestinal delivery of protein drugs: Alginate and chitosan - a review. Journal of Controlled Release. 114(1), 1-14.

Gibson, G. R., & Williams, C. M. (2000). Functional foods. (pp. 9-206) Woodhead Publishing.

Glover, D. A., Ushida, K., Phillips, A. O., & Riley, S. G. (2009). Acacia(sen) SUPERGUM™ (gum arabic): An evaluation of potential health benefits in human subjects. Food Hydrocolloids, 23(8), 2410-2415.

Goncalves, A., Roi, S., Nowicki, M., Dhaussy, A., Huertas, A., Amiot, M., & Reboul, E. (2015a). Fat-soluble vitamin intestinal absorption: Absorption sites in the intestine and interactions for absorption. Food Chemistry, 172, 155-160.

Gong, X., Dang, G., Guo, J., Liu, Y., & Gong, Y. (2020). A sodium alginate/feather keratin composite fiber with skin-core structure as the carrier for sustained drug release. International Journal of Biological Macromolecules, 155, 386-392.

Gonnet, M., Lethuaut, L., & Boury, F. (2010). New trends in encapsulation of liposoluble vitamins. Journal of Controlled Release. 146(3), 276-290.

Güçlü-Üstündağ, Ö, & Temelli, F. (2004). Correlating the solubility behavior of minor lipid components in supercritical carbon dioxide. The Journal of Supercritical Fluids, 31(3), 235-253.

Gurikov, P., & Smirnova, I. (2018). Amorphization of drugs by adsorptive precipitation from supercritical solutions: A review. The Journal of Supercritical Fluids, 132, 105-125.

Health Canada. (2006). The safety of vitamin E supplements. Ottawa, ON: Health Canada. https://www.canada.ca/en/health-canada/services/healthy-living/your-health/food-nutrition/safety-vitamin-supplements.html (accessed on January 22th, 2020)

Health Canada. (2010). Vitamin D and calcium: Updated dietary reference intakes. Ottawa, ON: Health Canada. https://www.canada.ca/en/health-canada/services/food-nutrition/healthy-eating/vitamins-minerals/vitamin-calcium-updated-dietary-reference-intakes-nutrition.html (accessed on February 19th, 2020).

Henry, P., & Kathryn, M. (2014). Commentary on fatty acid wars. Arteriosclerosis, Thrombosis, and Vascular Biology, 34(5), e8-e9.

Holick, M. F. (2010). Vitamin D and health: Evolution, biologic functions, and recommended dietary intakes for vitamin D. Clinical Reviews in Bone and Mineral Metabolism. 7(1), 2-19.

Holick, M. F. (2011), Vitamin D: Physiology, molecular biology, and clinical applications. Nutrition & Food Science, 41(1), 81-82

Holick, M. F. (2017). The vitamin D deficiency pandemic: Approaches for diagnosis, treatment and prevention. Reviews in Endocrine and Metabolic Disorders. 18(2), 153-165.

Jaafar, N. (2019). Clinical effects of gum arabic (acacia): A mini review. Iraqi Journal of Pharmaceutical Sciences, 28, 9-16.

Javiera Mujica-Álvarez, Gil-Castell, O., Barra, P. A., Ribes-Greus, A., Rubén Bustos, Faccini, M., & Matiacevich, S. (2020). Encapsulation of vitamins A and E as spray-dried additives for the feed industry. Molecules, 25(6), 1357.

Johannsen, M., & Brunner, G. (1997). Solubilities of the fat-soluble vitamins A, D, E, and K in supercritical carbon dioxide. Journal of Chemical & Engineering Data, 42(1), 106-111.

Kannappan, R., Gupta, S. C., Kim, J. H., & Aggarwal, B. B. (2012). Tocotrienols fight cancer by targeting multiple cell signaling pathways. BioMed Central, 7(1) 43-52.

Kanno, C., Kobayashi, H., Tsugo, T., & Yamauchi, K. (1999). Identification of alpha -, beta -, gamma - and delta -tocopherols and their contents in human milk. Biochimica et Biophysica Acta, 380(2), 282-290.

Karama, M. (2002), Gum arabic marketing issues: Marketing model, buffer- stocking, processing and finance. Presented by the international workshop on gum Arabic production, processing and marketing. Khartoum, Sudan.

Korkmaz, O., Girgin, B., Sunna, Ç, Yavaşer, R., & Karagözler, A. A. (2016). Production and investigation of controlled drug release properties of tamoxifen loaded alginate-gum arabic microbeads. Journal of the Turkish Chemical Society, Section A: Chemistry, 3(3), 47-58.

Krisanova, N., Pozdnyakova, N., Pastukhov, A., Dudarenko, M., Maksymchuk, O., Parkhomets, P., Sivko, R., Borisova, T. (2019). Vitamin D3 deficiency in puberty rats causes presynaptic malfunctioning through alterations in exocytotic release and uptake of glutamate/GABA and expression of EAAC-1/GAT-3 transporters. Food and Chemical Toxicology. 123, 142-150.

Lee, K. Y., & Mooney, D. J. (2012). Alginate: Properties and biomedical applications. Polymers in Polymer Science, 37(1), 106-126.

Li, Q., Liu, C., Huang, Z., & Xue, F. (2011). Preparation and characterization of nanoparticles based on hydrophobic alginate derivative as carriers for sustained release of vitamin D3. Journal of Agricultural and Food Chemistry, 59(5), 1962-1967

Li, W., Peng, H., Ning, F., Yao, L., Luo, M., Zhao, Q., Zhu, X., Xiong, H. (2014). Amphiphilic chitosan derivative-based core–shell micelles: Synthesis, characterisation and properties for sustained release of vitamin D3. Food Chemistry, 152, 307-315.

Lips, P., & van Schoor, N. M. (2011). The effect of vitamin D on bone and osteoporosis. Best Practice & Research Clinical Endocrinology & Metabolism, 25(4) 585-591.

Liu, N., Couto, R., Seifried, B., Moquin, P., Delgado, L., & Temelli, F. (2018). Characterization of oat beta-glucan and coenzyme Q10-loaded beta-glucan powders generated by the pressurized gas-expanded liquid (PGX) technology. Food Research International, 106, 354-362.

Liu, Z. (2019). Pressurized gas eXpanded (PGX) liquid drying of sodium alginate and its loading with coenzyme Q10 by adsorptive precipitation. MSc. thesis. University of Alberta, Edmonton, Canada.

Lobo, L. M. C., Schincaglia, R. M., Peixoto, M. d. R., & Hadler, M. C. C. M. (2019). Multiple micronutrient powder reduces vitamin E deficiency in Brazilian children: A pragmatic, controlled clinical trial. Nutrients, 11(11), 2730.

Luo, Y., Teng, Z., & Wang, Q. (2012). Development of zein nanoparticles coated with carboxymethyl chitosan for encapsulation and controlled release of vitamin D3. Journal of Agricultural and Food Chemistry, 60(3), 836-843.

Luo, Y., Wang, T. T. Y., Teng, Z., Chen, P., Sun, J., & Wang, Q. (2013). Encapsulation of indole-3-carbinol and 3,3′-diindolylmethane in zein/carboxymethyl chitosan nanoparticles with controlled release property and improved stability. Food Chemistry, 139(1-4), 224-230.

Mahdi Jafari, S., Masoudi, S., & Bahrami, A. (2019). A taguchi approach production of spray-dried whey powder enriched with nanoencapsulated vitamin D3. Drying Technology, 37(16), 2059-2071.

Marcel C, B. S. (2017), “Vitamin E Deficiency”. CINAHL Nursing Guide EBSCO Publishing, (Ipswich, Massachusetts).

Masuelli, Martin & Illanes, Cristian. (2014). Review of the characterization of sodium alginate by intrinsic viscosity measurements. comparative analysis between conventional and single point methods. International Journal of BioMaterials Science and Engineering, 1(1), 1-11.

Mujica-Álvarez, J., Gil-Castell, O., Barra, P. A., Ribes-Greus, A., Rubén Bustos, Faccini, M., & Matiacevich, S. (2020). Encapsulation of vitamins A and E as spray-dried additives for the feed industry. Molecules, 25(6), 1357.

Maurya, V. K., Bashir, K., & Aggarwal, M. (2020). Vitamin D microencapsulation and fortification: Trends and technologies. Journal of Steroid Biochemistry and Molecular Biology, 196,105489.

McClements, D. J., Decker, E. A., Park, Y., & Weiss, J. (2009). Structural design principles for delivery of bioactive components in nutraceuticals and functional foods. Critical Reviews in Food Science and Nutrition, 49(6), 577-606.

Mocchegiani, E., Costarelli, L., Giacconi, R., Malavolta, M., Basso, A., Piacenza, F., . . . Monti, D. (2014). Vitamin E–gene interactions in aging and inflammatory age-related diseases: Implications for treatment. A systematic review. Ageing Research Reviews, 14, 81-101.

Mohamed, R. E., Gadour, M. O., & Adam, I. (2015). The lowering effect of gum arabic on hyperlipidemia in Sudanese patients. Frontiers in Physiology, 6.

Montenegro, M., Boiero, L., Valle, L., & Borsarelli, C. (2012). Gum arabic: More than an edible emulsifier. Intechopen, 1-26

Nehdi, I., Omri, S., Khalil, M. I., & Al-Resayes, S. (2010). Characteristics and chemical composition of date palm (*Phoenix canariensis*) seeds and seed oil. Industrial Crops & Products. 32(3), 360-365.

Ness, R. A., Miller, D. D., & LI, W. (2015). The role of vitamin D in cancer prevention. Chinese Journal of Natural Medicines, 13(7), 481-497.

Nesterenko, A., Alric, I., Silvestre, F., & Durrieu, V. (2013). Vegetable proteins in microencapsulation: A review of recent interventions and their effectiveness. Industrial Crops and Products, 42, 469-479.

Niki, E., & Abe, K. (2019). Vitamin E: Structure, properties and functions. Ch. 1 in "Vitamin E: Chemistry and nutritional benefits" (pp. 1-11) The Royal Society of Chemistry.

Nikonenko, N. A., Buslov, D. K., Sushko, N. I., & Zhbankov, R. G. (2000). Investigation of stretching vibrations of glycosidic linkages in disaccharides and polysaccharides with use of IR spectra deconvolution. Biopolymers, 57(4), 257-262.

Öztürk, B. (2017). Nanoemulsions for food fortification with lipophilic vitamins: Production challenges, stability, and bioavailability. European Journal of Lipid Science and Technology, 119(7), 1500539.

Ozturk, B., Argin, S., Ozilgen, M., & McClements, D. J. (2015). Formation and stabilization of nanoemulsion-based vitamin E delivery systems using natural biopolymers: Whey protein isolate and gum arabic. Food Chemistry, 188, 256-263.

Pantić, M., Knez, Ž, & Novak, Z. (2016a). Supercritical impregnation as a feasible technique for entrapment of fat-soluble vitamins into alginate aerogels. Journal of Non-Crystalline Solids, 432, 519-526.

Pantić, M., Kotnik, P., Knez, Ž, & Novak, Z. (2016b). High pressure impregnation of vitamin D3 into polysaccharide aerogels using moderate and low temperatures. Journal of Supercritical Fluids, 118, 171-177.

Park, E. Y., Murakami, H., & Matsumura, Y. (2005). Effects of the addition of amino acids and peptides on lipid oxidation in a powdery model system. Journal of Agricultural and Food Chemistry, 53(21), 8334-8341.

Peh, H. Y., Tan, W. S., Liao, W., & Wong, W. S. (2016). Vitamin E therapy beyond cancer: Tocopherol versus tocotrienol. Pharmacology & Therapeutics, 162, 152-169.

Perrut, M., & Perrut, V. (2019). Supercritical Fluid Applications in the Food Industry. Ch. 7.7 in "Gases in Agro-food Processes" (pp. 483-509) Academic Press.

Petzold, G., Rodríguez, A., Valenzuela, R., Moreno, J., & Mella, K. (2019). Alginate as a versatile polymer matrix with biomedical and food applications. Materials for Biomedical Engineering, 323-350.

Phillips, A. O., & Phillips, G. O. (2011). Biofunctional behaviour and health benefits of a specific gum arabic. Food Hydrocolloids, 25(2) 165-169.

Phillips, G. O., & Williams, P. A. (2000). Alginates, Ch. 29 in "Handbook of hydrocolloids". (pp. 807-829). Woodhead Publishing Series in Food Science, Technology and Nutrition.

Phillips, G. O., & Williams, P. A. (2009). Gum Arabic, Ch. 11 in "Handbook of hydrocolloids". (pp. 252-273). Woodhead Publishing Series in Food Science, Technology and Nutrition.

Pike, J. W. (1991). Vitamin D3 receptors: Structure and function in transcription. Annual Review of Nutrition, 11(1), 189-216.

Prado, A. G. S., Santos, A. L. F., Nunes, A. R., Tavares, G. W., & de Almeida, C. M. (2012). Designed formulation based on α-tocopherol anchored on chitosan microspheres for pH-controlled gastrointestinal controlled release. Colloids and Surfaces B: Biointerfaces, 96, 8-13.

Qin, Y. (2008). Alginate fibres: An overview of the production processes and applications in wound management. Polymer International, 57(2), 171-180.

Remminghorst, U., & Rehm, B. (2006a). Bacterial alginates: From biosynthesis to applications. Biotechnology Letters, 28(21), 1701-1712.

Renard, D., Robert, P., Lavenant, L., Melcion, D., Popineau, Y., Guéguen, J., Duclairoir, C., Nakache, E., Schmitt, C. (2002). Biopolymeric colloidal carriers for encapsulation or controlled release applications. France International Journal of Pharmaceutics. 242(1-2), 163,166.

Ross, A. H., Eastw. Drug Desigood, M. A., Brydon, W. G., Anderson, J. R., & Anderson, D. M. (1983). A study of the effects of dietary gum arabic in humans. The American Journal of Clinical Nutrition, 37(3), 368-375.

Sanchez, B., Relova, J. L., Gallego, R., Ben-Batalla, I., & Perez-Fernandez, R. (2009). 1,25-Dihydroxyvitamin D3 administration to 6-hydroxydopamine-lesioned rats increases glial cell line-derived neurotrophic factor and partially restores tyrosine hydroxylase expression in substantia nigra and striatum. Journal Neuroscience Research, 87(3), 723-732.

Sanchez, C., Nigen, M., Mejia Tamayo, V., Doco, T., Williams, P., Amine, C., & Renard, D. (2018). Acacia gum: History of the future. Food Hydrocolloids, 78, 140-160.

Seifried, B. (2010). Physicochemical properties and microencapsulation process development for fish oil using supercritical carbon dioxide. PhD thesis. University of Alberta, Edmonton, Canada.

Shakeel, F., Alanazi, F. K., Alsarra, I. A., & Haq, N. (2014). Solubility of antipsychotic drug risperidone in transcutol+water co-solvent mixtures at 298.15 to 333.15K. Journal of Molecular Liquids, 191, 68-72.

Sheppard, A. J., Pennington, J. A., & Weihrauch, J. L. (1993). Analysis and Distribution of Vitamin E in Vegetable Oils and Foods (pp 195-239) in "Bioavailability and Analysis of Vitamins in Foods", Springer. Boston, MA.

Silva, S., Rosa, N., Ferreira, A., Boas, L., & Bronze, M. (2009). Rapid determination of alpha tocopherol in vegetable oils by fourier transform infrared spectroscopy. Food Analytical Methods, 2, 120-127.

Siró, I., Kápolna, E., Kápolna, B., & Lugasi, A. (2008). Functional food. product development, marketing and consumer acceptance—A review. Appetite, 51(3), 456-467.

Skaugrud, Ø, Hagen, A., Borgersen, B., & Dornish, M. (1999). Biomedical and pharmaceutical applications of alginate and chitosan Intercept. Biotechnology & Genetic Engineering Reviews, 16, 23-40.

Slavin, J. (2003). Why whole grains are protective: Biological mechanisms. Proceedings of the Nutrition Society, 62(1), 129-134.

Smolinske, S. C. (1992). "Handbook of Food, Drug, and Cosmetic Excipients" (pp 439) CRC Press. Boca Raton.

Stuart, B. (2004). "Infrared spectroscopy: Fundamentals and Applications" J. Wiley. Chichester, West Sussex, England.

Szymańska, R., Nowicka, B., & Kruk, J. (2017). Vitamin E - occurrence, biosynthesis by plants and functions in human nutrition. Mini Reviews in Medicinal Chemistry, 17(12), 1039-1052.

Temelli, F., & Seifried, B. (2016). Supercritical fluid treatment of high molecular weight biopolymers. U.S. Patent No. 9,249,266. Washington, DC: U.S. Patent and Trademark Office.

Temelli, F. (2018). Perspectives on the use of supercritical particle formation technologies for food ingredients. The Journal of Supercritical Fluids, 134, 244-251.

Tippetts, M., Martini, S., Brothersen, C., & McMahon, D. J. (2012). Fortification of cheese with vitamin D3 using dairy protein emulsions as delivery systems. Journal of Dairy Science, 95(9), 4768-4774.

Traber, M. G. (2013). Mechanisms for the prevention of vitamin E excess. Journal of Lipid Research, 54(9), 2295-2306.

Viinanen, A., Salokannel, M., & Lammintausta, K. (2011). Gum arabic as a cause of occupational allergy. Journal of Allergy, 2011.

Wagner, D., Sidhom, G., Whiting, S. J., Rousseau, D., & Vieth, R. (2008). The bioavailability of vitamin D from fortified cheeses and supplements is equivalent in adults. The Journal of Nutrition, 138(7), 1365-1371.

Walther, B., & Schmid, A. (2017). Effect of fermentation on vitamin content in food. Ch. 7 in "Fermented Foods in Health and Disease Prevention", Academic Press (pp 131-157). Publishing by Elsevier Inc.

Wessels, I., & Rink, L. (2020). Micronutrients in autoimmune diseases: Possible therapeutic benefits of zinc and vitamin D. The Journal of Nutritional Biochemistry, 77.

Xi, Y., Zou, Y., Luo, Z., Qi, L., & Lu, X. (2019). pH-responsive emulsions with β-cyclodextrin/vitamin E assembled shells for controlled delivery of polyunsaturated fatty acids. Journal of Agricultural and Food Chemistry, 67(43), 11931-11941.

Xiang, C., Gao, J., Ye, H., Ren, G., Ma, X., Xie, H., Fang, S., Lei, Q., Fang, W. (2020). Development of ovalbumin-pectin nanocomplexes for vitamin D3 encapsulation: Enhanced storage stability and sustained release in simulated gastrointestinal digestion. Food Hydrocolloids, 106.

Yan, R., Chuang, H. C., Kapuriya, N., Chou, C. C., Lai, P. T., Chang, H. W., Yang C. N., Kulp S. K., Chen, C. S. (2015). Exploitation of the ability of γ-tocopherol to facilitate membrane co-localization of akt and PHLPP1 to develop PHLPP1-targeted akt inhibitors. Journal of Medicinal Chemistry, 58(5), 2290-2298.

Yeh, E. B., Barbano, D. M., & Drake, M. (2017). Vitamin fortification of fluid milk. Journal of Food Science, 82(4), 856-864.

Yeo, S., & Kiran, E. (2005). Formation of polymer particles with supercritical fluids: A review. The Journal of Supercritical Fluids, 34(3), 287-308.

Yokozaki, Y., & Shimoyama, Y. (2018). Loading of vitamin E into silicone hydrogel by supercritical carbon dioxide impregnation toward controlled release of timolol maleate. The Journal of Supercritical Fluids, 131, 11-18.

Zhang, F., Khan, M. A., Cheng, H., & Liang, L. (2019). Co-encapsulation of α-tocopherol and resveratrol within zein nanoparticles: Impact on antioxidant activity and stability. Journal of Food Engineering, 247, 9-18.

Zhang, X., Heinonen, S., & Levänen, E. (2014). Applications of supercritical carbon dioxide in materials processing and synthesis. Royal Society of Chemistry Advances, 4(105), 61137-61152.

Zhao, Y., Lee, M., Cheung, C., Ju, J., Chen, Y., Liu, B., Long-Qin H., Yang, C. S. (2010). Analysis of multiple metabolites of tocopherols and tocotrienols in mice and humans. Journal of Agricultural and Food Chemistry, 58(8), 4844-4852.

Zingg, J. M. (2007). Vitamin E: An overview of major research directions. Molecular Aspects of Medicine, 28(5), 400-422.

Zohuriaan, M. J., & Shokrolahi, F. (2004). Thermal studies on natural and modified gums. Polymer Testing, 23(5), 575-579.